UNIVERSITÀ DEGLI STUDI DI MILANO

Dottorato di Ricerca in Scienze Biochimiche
XXXIII ciclo

Dipartimento di Biotecnologie Mediche
e Medicina Traslazionale

GM1 oligosaccharide modulation of calcium signalling in neuronal functions

Giulia Lunghi
Matricola n. R12092

Docente guida 2017/2019:
Prof. Sandro Sonnino

Docente guida 2019/2020:
Prof. Alessandro Prinetti

Tutor:
Dott.ssa Elena Chiricozzi

Coordinatore del Dottorato:
Prof. Alessandro Prinetti

Anno Accademico 2019/2020

This thesis was conducted under the guidance of Prof Sonnino and Dr. Chiricozzi. Even if Prof Sonnino retired in November 2019, he still actively participated in the design of the experiments and discussion of the data here presented.

Summary

Abstract

It has been already demonstrated that the oligosaccharide chain (OligoGM1) of the ganglioside GM1, β-Gal-(1-3)-β-GalNAc-(1-4)-[α-Neu5Ac-(2-3)]-β-Gal-(1-4)-β-Glc-(1-1)-Ceramide, promotes neurodifferentiation in the Neuro2a murine neuroblastoma cells, used as a model, by directly interacting with the NGF specific receptor TrkA, leading to the activation of ERK1/2 downstream pathway. In this context, my PhD work aimed to investigate which other biochemical pathways, in addition to TrkA-MAPK cascade activation, are prompted by OligoGM1, with an emphasis on Ca^{2+} modulating factors.

A proteomic analysis (nLC-ESi-MS-MS) performed on Neuro2a cells treated with 50 μM OligoGM1 for 24 hours led to the identification and quantification of 324 proteins exclusively expressed by OligoGM1-treated cells. Interestingly, some of these proteins are involved in the regulation of Ca^{2+} homeostasis and in Ca^{2+}-dependent differentiative pathways. In order to evaluate if OligoGM1 administration was able to modulate Ca^{2+} flow, we performed calcium-imaging experiments on Neuro2a cells using the Ca^{2+}-sensitive Fluo-4 probe. Starting from 5 minutes upon OligoGM1 administration to undifferentiated Neuro2a, a significant increase in Ca^{2+} influx occurs. At the same time an increased activation of TrkA membrane receptor was observed and, importantly, the addition of a specific TrkA inhibitor abolished the OligoGM1 mediated increase of the cytosolic Ca^{2+}, suggesting that the opening of the cell Ca^{2+} channels following OligoGM1 administration depends on the activation of TrkA receptor. To unveil which cellular pathway activated by OligoGM1 could lead to the increase of intracellular Ca^{2+}, time-course immunoblotting analyses were performed. The data revealed that following TrkA activation, OligoGM1 induced the activation of phospholipase PLCγ1 which converts phosphatidylinositol 4,5-bisphosphate (PIP_2) to diacyglycerol (DAG) and inositol 1,4,5-trisphosphate (IP_3), the second messengers that propagate cellular signalling via Ca^{2+} mobilization. Moreover, we observed a hyperphosphorylation of the DAG substrate, protein kinase C (PKC), which is a priming event that enables its catalytic activation in response to lipid second messengers, and we found its enrichment in lipid rafts, events that consolidate its activation. When calcium-imaging experiments where performed in the presence of xestospongin C, a potent inhibitor of IP_3 receptors on endoplasmic reticulum, a reduction of about 50% of Ca^{2+} influx was observed, suggesting that the Ca^{2+} flows moved by the OligoGM1 come not only from intracellular storages, but probably also from the extracellular environment. Accordingly, in the presence of both extracellular (EGTA) and intracellular (BAPTA-AM) Ca^{2+} chelators the neuritogenic effect induced by OligoGM1 was abolished.

The work described in this thesis confirms that the effects of GM1 ganglioside on neuronal differentiation are mediated by its oligosaccharide portion.

In particular, here I highlight that the oligosaccharide, initiating a signalling cascade on the cell surface, is responsible alone for the balancing of the intracellular Ca^{2+} levels that underlie neurite sprouting, which have historically been attributed to the whole GM1 ganglioside and its role as lipid inserted into the plasma membrane. In this way, these data give additional information on the molecular characterization of the mechanisms by which GM1 exerts its neuronal functions.

Abbreviations:

BSA: bovine serum albumin

Ca^{2+}: calcium ion

CGN: cerebellar granule neurons

CTRL: control

Ctx-B: B subunit of cholera toxin

DAG: diacyglycerol

DMEM HG: Dulbecco's modified Eagles' medium high glucose

DRM: detergent resistant membrane

ERK1/2: extracellular signal-regulated protein kinases 1 and 2

FAK: focal adhesion kinase

FBS: fetal bovine serum

GDNF: glial cell-derived neurotrophic factor

HBSS+: Hank's Balanced Salt Solution with Mg^{2+} and Ca^{2+} ions

IP3: inositol 1,4,5-trisphosphat

MAPK: mitogen activated protein kinase

MPTP: 1-Methyl-4-phenyl-1,2,3,6-tetrahydropyridine hydrochloride

N2a: Neuro2a cells

NCX: Na/Ca exchanger

NGF: nerve growth factor

OligoGM1: GM1-oligosaccharide

PBS: phosphate saline buffer

PD: Parkinson's Disease

PKC: Protein Kinase C

PLC: Phospholipase C

PMCA: plasma membrane calcium ATPase

PNS: post nuclear supernatant

PVDF: polyvinylidene difluoride

SDS: sodium-dodecyl-sulphate

TBS: Tris-buffered saline

Trk: tropomyosin receptor kinase

TRPC5: Transient receptor potential channel 5

Introduction

1. GM1 structure and physico-chemical properties

Ganglioside GM1 has been defined as a "*factotum* of nature" because of its relevant implication and key role in many signalling systems and cell regulatory pathways (Fang et al. 2000; Ledeen and Wu 2015; Aureli et al. 2016). Abounding in all mammalian brains, GM1 interacts with a wide range of membrane receptors as well as with extracellular ligands, modulating mechanisms such as ion transport, neuronal differentiation, neuronal recovery, and neuroprotective signalling (Schengrund and Mummert 1998; Schengrund and Ringler 1989; Ledeen and Wu 2015; Aureli et al. 2016; Chiricozzi et al. 2020).

Thanks to its properties, GM1 is one of the best studied gangliosides, a particular class of glycosphingolipids containing sialic acids in the glycan chain. Gangliosides are composed by the ceramide, which represents the hydrophobic core, resulting from a long chain fatty acid incorporation on the second position of a sphingosine basis, and by a hydrophilic head, the oligosaccharide chain, always characterized by the presence of one or more residues of sialic acid. There are different types of ceramides consisting of a basic long hydrophobic chain, called sphingosine (Sph), attached to a fatty acid by an amide bond (figure I1). Within the brain, sphingosine has 18 or 20 carbon atoms (C18- or C20-sphingosine). The two structures show different ratios in relationship with the brain age (Karlsson 1970), the C20-sphingosine being barely detectable in the foetus but becoming the most represented sphingosine in adult human brain (Sonnino and Chigorno 2000). Regarding the fatty acid of ceramide, stearic acid (C18) accounts for 90% of those present in the nervous system.

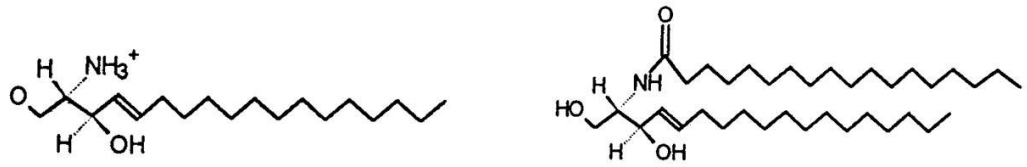

Sphingosine Ceramide

Figure I1: chemical structure of sphingosine and ceramide. Ceramide represents the hydrophobic core of all gangliosides and consists of a carbon amino alcohol chain base, the sphingosine, attached to a fatty acid by an amidic bond.

Although small amounts of gangliosides have been found also in the membrane of the mitochondria, nucleus and in the endoplasmic reticulum as well as in soluble form in the cytoplasm, they are mostly concentrated in the plasma membrane. In particular, they are inserted in the outer half of the bilayer,

integrated in the lipid core through the hydrophobic moiety, while the hydrophilic oligosaccharide chain protrudes towards the extracellular space, interacting with soluble extracellular molecules, with neighbouring membrane components (cis-interactions), and with membrane components of neighbouring cells (trans-interactions) (Ledeen and Wu 2018b; Bertoli et al. 1981; Kolter 2012; Schengrund 2015).

Gangliosides are particularly enriched in the nervous system, and five of them, namely GM1, GD1a, GD1b, GT1b and GQ1b, cover altogether over 95%–97% of the total content in adult mammals. They abound especially in the membranes of neurons but have also been identified in glial cells and GM1 has also been found in astrocytes, oligodendrocytes and microglia (Svennerholm 1964; Hansson, Holmgren, and Svennerholm 1977; Senn et al. 1989; Kolter 2012).

The structure of GM1, established in 1963, contains a single residue of sialic acid and belongs to the ganglio-tetrahexosyl series, with formula β-Gal-(1-3)-β-GalNAc-(1-4)-[α-Neu5Ac-(2-3)-]-β-Gal-(1-4)-Glc-(1-1)-Ceramide (figure I2 A). The specific names for the gangliosides provide information about their structure, according to International Union of Pure and Applied Chemistry (IUPAC)-International Union of Biochemistry (IUB) nomenclature (Chester 1998). The capital letter G refers to ganglioside and the subscript M indicates that the molecule contains one unit of sialic acid. The numbered subscript refers to the carbohydrate sequence that is attached to the ceramide. In particular, 1 stands for Gg_4 neutral series, i.e. β-Gal-(1-3)-β-GalNAc-(1-4)-β-Gal-(1-4)-β-Glc oligosaccharide structure (Aureli et al. 2016).

The other three major ganglio-series gangliosides GD1a, GD1b, and GT1b, contain the GM1 structure with additional sialic acids attached (figure I2 B). These additional units are susceptible to hydrolytic removal by endogenous sialidase enzymes (Miyagi and Yamaguchi 2012; Sonnino et al. 2011), while this does not happen for the sialic acid of GM1, which is resistant to most forms of mammalian sialidase. Thus, sialidase induces elevation of GM1 at the expense of oligosialo-homologs during GM1-requiring processes.

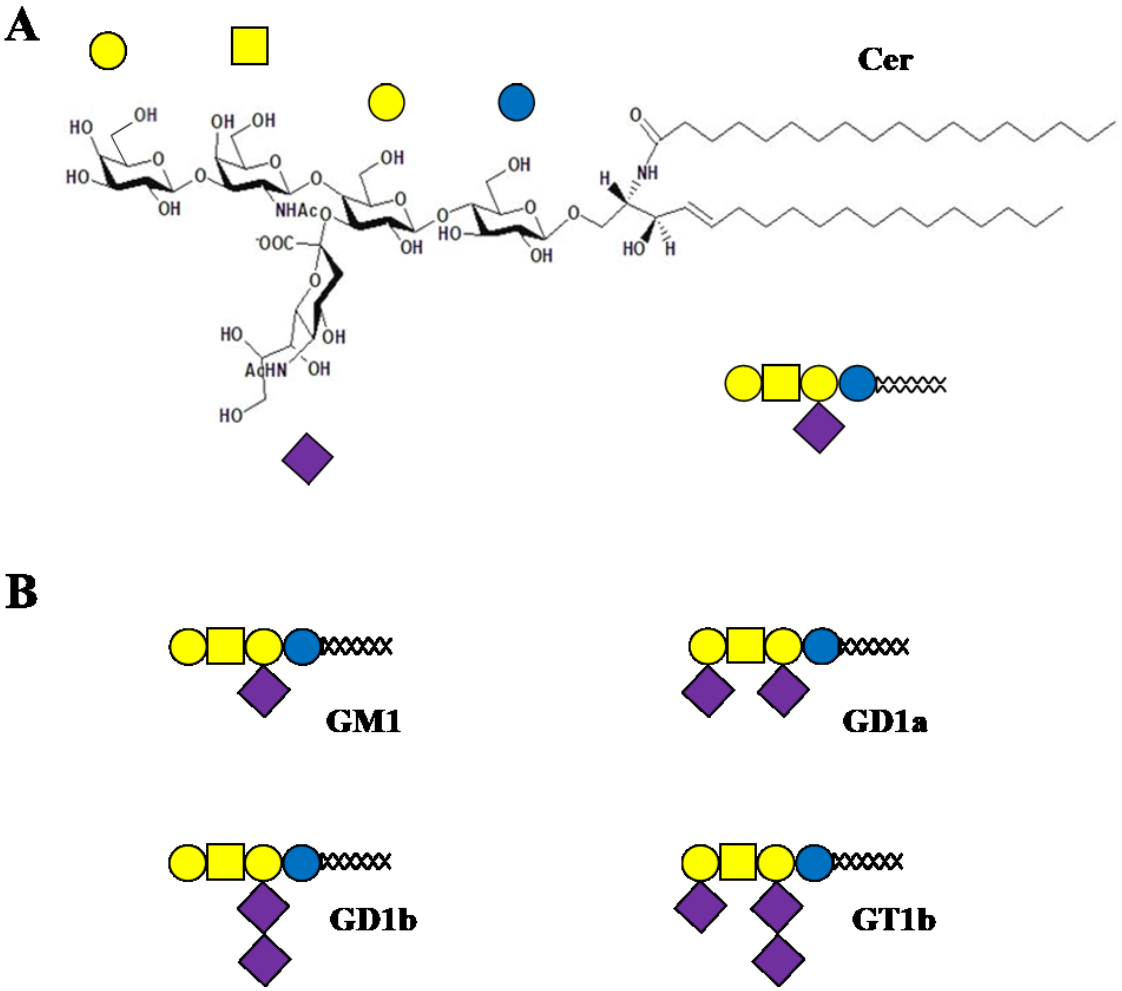

Figure I2: schematic representation of gangliosides. A: GM1 ganglioside consists of neutral core structure Galβ3-GalNAcβ4-Galβ4-Glcβ1-Cer and one N-acetylneuraminic acid (Neu5Ac) attached to the inner galactose. **B:** Schematic representation of major gangliosides in vertebrate brain: GM1, GD1a, GD1b and GT1b. Blu circle = glucose; yellow circle = galactose; yellow square = N-acetylgalactosamine (GalNAc), purple rhombus = Neu5Ac. Symbols for ganglioside saccharide unites are in accordance with the glycan symbol nomenclature updated in the Second Edition of Essentials of Glycobiology (Varki et al. 2009).

In biological environments, GM1 has a net negative charge due to the presence of sialic acid. A high degree of hydrophilicity is conferred by the presence of the pentasaccharide portion, due both to the presence of the sialic acid and to the intrinsic hydrophilicity of sugars. The combination of the hydrophobic lipid chain and the hydrophilic oligosaccharide portion gives to the GM1 molecule an amphiphilic character that determines its chemical-physical behaviors and the biological ones.

GM1 is soluble in aqueous solution, where it tends to form small ellipsoidal micelles due to the geometry of the monomer presenting a large hydrophilic head (Cantu et al. 1986). GM1 micelles are formed at very low concentration. In fact, the critical micellar concentration (c.m.c.) of GM1 is in the range of 10^{-8}-10^{-9} M, indicating that, regardless of its concentration, in aqueous solution GM1 free

monomers in equilibrium with the aggregates cannot exceed the c.m.c. (Sonnino et al. 1994; Corti et al. 1980; Ulrich-Bott and Wiegandt 1984).

The intrinsic aggregation properties of the gangliosides, which contribute to determine the distribution of gangliosides in the membrane, are important parameters that can influence gangliosides capability to modulate membrane protein activities, probably originating from a specific ganglioside-protein interaction process occurring at the membrane level. Aggregative properties are of significant relevance when gangliosides are administered to cells. In fact, experimental evidences derived from GM1 exogenous administration to cultured neurons report that only the GM1 monomers become part of the cell plasma membrane through lipid-lipid interactions, while the micelles bind to the plasma membrane through interactions with proteins and are internalized by endocytosis, reaching the lysosomes (figure I3) (Valsecchi et al. 1992; Saqr, Pearl, and Yates 1993). A prolonged treatment was proven to advance the insertion of GM1 monomers into the plasma membrane. On the other hand, the gradually augmenting in GM1 concentration over the c.m.c. increase the aggregative process (Tomasi et al. 1980; Venerando et al. 1982; Facci et al. 1984).

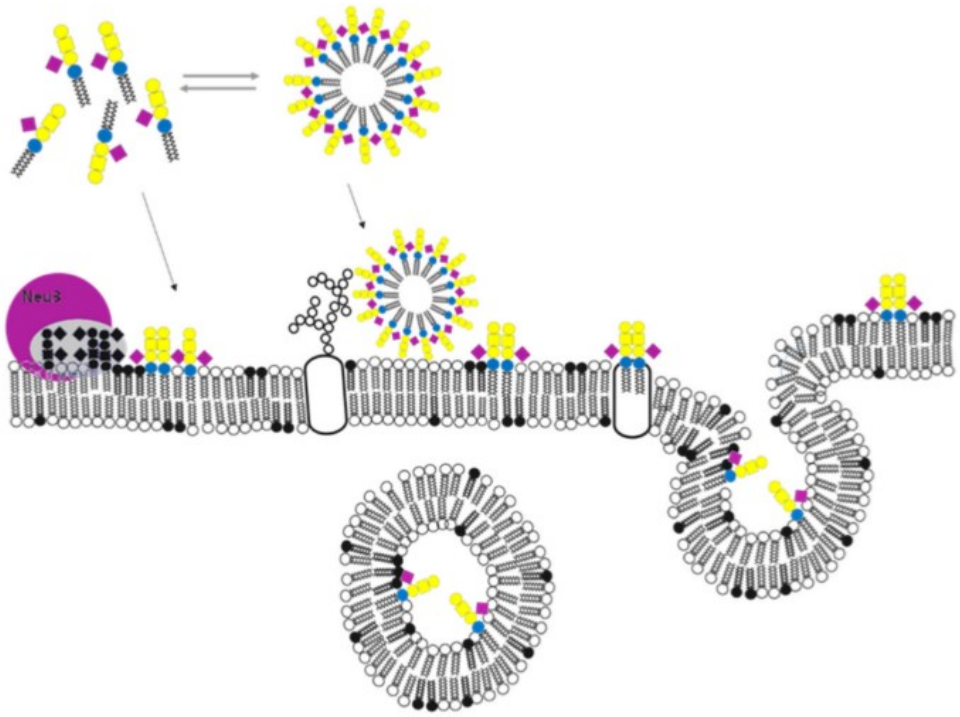

Figure I3: association of exogenous administered GM1 to cell culture. GM1 in water forms small ellipsoidal micelles above a certain concentration (10^{-9} M), called the critical micelle concentration, whereas below this concentration it is found as monomers. The two forms are found in equilibrium to each other. When GM1 is administered to cells, the GM1 monomers become part of the cell plasma membrane, while the micelles bind to the plasma membrane and are internalized by endocytosis, reaching the lysosomes (modified from (Chiricozzi et al. 2020).

In the plasma membrane, GM1 and gangliosides occur predominantly within lipid rafts, membrane microdomains enriched in dipalmitoylphosphatidylcholine, cholesterol, sphingomyelin, phosphatidylinositols, and lipid-modified proteins. Lipid rafts represent important cellular signaling platforms through which cells receive signals from outside and transfer them inside the cell (figure I4). Operationally, the lipid rafts are detergent-resistant assemblages that are isolated as low-density fractions by density-gradient ultracentrifugation (Simons and Sampaio 2011). Despite the cholesterol and sphingolipid enrichment, glycerophospholipids were shown to constitute over 50% of lipids in lipid rafts from cerebellar granule cells, while gangliosides as a whole represented only 6–7% of the total lipids (Sonnino et al. 2007). Moreover, GM1 was found to be the less abundant member; GD1a and GT1b, for example, occurred at nearly three and four times the GM1 level, respectively. However, a major role for GD1a is that of reserve pool for GM1, consistent with its easy conversion by endogenous sialidase (Miyagi and Yamaguchi 2012; Sonnino et al. 2011). Despite their relative paucity, gangliosides are known to have an active role in the formation, stabilization, and dynamics of lipid microdomains (Furukawa et al. 2011). This is supported by the finding of distorted microdomains from genetically altered mice deficient in gangliosides (Ohmi et al. 2012).

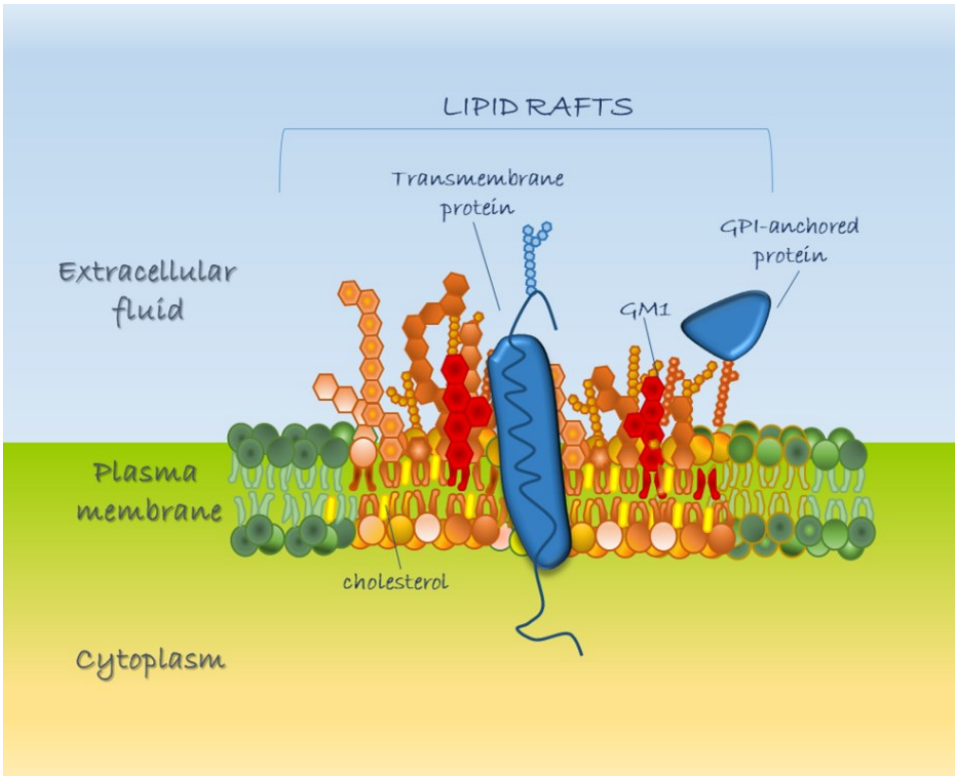

Figure I4: schematic representation of membrane lipid rafts. Lipid rafts are membrane microdomains enriched in gangliosides, cholesterol, glycolipids, transmembrane proteins (glycosylated and not) and glycosylphosphatidylinositol (GPI)-anchored proteins.

2. GM1 in neuronal development

Gangliosides are particularly represented in the grey matter of the central and peripheral nervous system, especially localized in presynaptic and postsynaptic membranes of neurons. Mammalian differentiated neurons present a ganglioside content up to ten folds higher than the one of non-neuronal cells. The content of gangliosides in brain drastically increases during development and the expression pattern changes during differentiation and aging (Ngamukote et al. 2007; Yu, Nakatani, and Yanagisawa 2009). In particular, during the early phases of neuron migration and mitosis simple gangliosides, such as GM3 and GD3, are mainly expressed, whereas a rapid upregulation of GM1 and other complex gangliosides such as GD1a, GD1b and GT1b occurs during the process of outgrowth and synaptogenesis (Aureli et al. 2011). During aging, the amount of brain gangliosides shows a progressive decrease (figure I5) (Svennerholm et al. 1994).

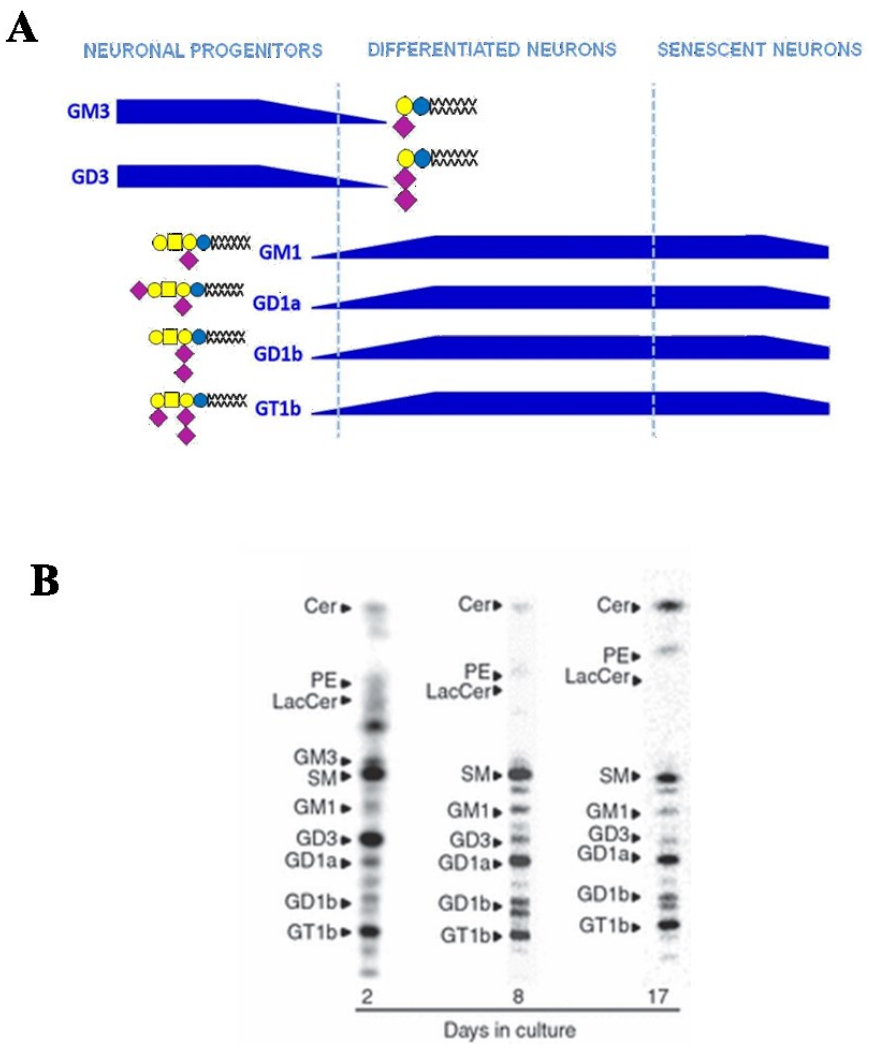

Figure I5: ganglioside changing in neurodifferentiation. A: modification in neuron ganglioside pattern during neurodifferentiation suggests an important role of oligosaccharide chains in the process (modified from Yu et al. 2008). **B:** changes in lipid patterns in rat cerebellar granule cells during development and aging

in vitro. Patterns of radioactive lipids in homogenates obtained from rat cerebellar granule cells at the 2nd, 8th and 17th day in culture. Total content of ganglioside increases during development. GD3 represents the most component in immature neurons, whereas during maturation complex gangliosides augment. At the 17th day in culture GM1 content is considerably reduced (modified from Aureli et al. 2011).

3. GM1 modulation of neuronal functions

The biological importance of GM1 derives from its ability to modulate neuronal functions mainly related to differentiation, protection and neuronal integrity maintenance. In the literature, GM1 is described as a key molecule for the development and homeostasis of central and peripheral nervous system, since it takes part to many cell processes such as neurites sprouting, axon guidance and in the restoration of lesioned neurons, both *in vitro* and *in vivo* (Ledeen and Wu 2015; Schengrund 2015; Aureli et al. 2016; Chiricozzi et al. 2020).

The neurotrophic and neuroprotective effects exerted by GM1 increase in membrane lipid micro-domains (Hakomori et al. 1998) can be due to a membrane reorganization, which alters its properties ensuring the requirement of the physical parameters for proper protein function, or to a GM1 oligosaccharide–protein direct interaction, which modify the protein conformation and function (Coskun and Simons 2011).

GM1 properties have been studied by two different approaches: via application of exogenous GM1 or through manipulation of endogenous GM1. The latter approach may involve different techniques: the use of exogenous sialidase, which locally modifies the ganglioside composition of plasma membrane microdomains by reducing the polysialogangliosides in favor of GM1 increase (Valaperta et al. 2007), and the administration of the B subunit of cholera toxin (Ctx-B) or GM1-specific polyvalent antibodies (of the IgM series), alone or combined (O'Hanlon, Hirst, and Willison 2003). Ctx-B and GM1-antibodies act as cross-linking agents, leading to the clustering of endogenous GM1 molecules and concomitantly of proteins containing ganglioside-binding domains, thus modulating the activation of downstream pathways.

3.1 GM1 and calcium signalling

Calcium ion (Ca^{2+}) represents an important second messenger, especially in neurons, where its intracellular levels are finely modulated to orchestrate the processes of neuronal differentiation and survival (Ledeen and Wu 2018).

It has been extensively studied how modulation of GM1 levels is responsible for the induction of neurite outgrowth and neuroprotective phenomena. Underlying many of these trophic effects is GM1 ability to modulate cellular calcium levels, accomplished through modulation of Ca^{2+} influx channels, Ca^{2+} exchangers, and various Ca^{2+}-utilizing enzymes that are regulated by association with the ganglioside (Ledeen and Wu 2015).

Elevation of plasma membrane GM1 in mouse neuroblastoma cells Neuro-2a (N2a) and other neuroblastoma cells by exogenous sialidase induced Ca^{2+} influx via low-threshold voltage-dependent T type channels (Wu and Ledeen 1991). The increase of intracellular Ca^{2+} in these cells is accompanied by extension of neurites, which were shown to have axonal character (Wu et al. 1998). Exogenous applied GM1 also caused both Ca^{2+} influx and neurite outgrowth, where instead such extensions have dendritic features (Wu et al. 1998). Although Ca^{2+} influx occurred in both cases, differences in the mode of entry were apparently critical in determining which signalling pathway was activated.

Interestingly, the regeneration of injured peripheral nerve promoted by GM1 elevation in the membrane due to local Neu3-sialidase action is associated to the increase in Ca^{2+} influx (Kappagantula et al. 2014).

An alternative GM1-mediated mechanism for Ca^{2+} influx resides in use of the Ctx-B or anti-GM1 antibodies as GM1-crosslinking agents, that were shown to induce Ca^{2+} influx and axonogenesis in N18 neuroblastoma cells and in both central (Wu et al. 1996) and peripheral neurons (Milani et al. 1992). The mechanism of this mode of Ca^{2+} influx was shown to involve the transient receptor potential channel 5 (TRPC5) channel, whose activation was triggered by GM1 crosslinking (Wu et al. 2007). The binding of CtxB to GM1 induces the crosslinking of α5β1 integrin heterodimer, which is associated to GM1. This association in turn induces the autophosphorylation of associated focal adhesion kinase (FAK) and consequently activates PLCγ and PI3K, leading to the opening of TRPC5. Additionally, cultured neurons from the *β4galnt1* knock out (KO) mouse deficient in ganglio-series gangliosides showed impaired Ca^{2+} regulatory capability, which translates in significantly retarded outgrowth (Wu et al. 2004; Wu et al. 2001) and in increased vulnerability to KCl and glutamate excitotoxicity, which is rescued after GM1 application (Wu et al. 2004).

In N2a cells the exogenous administration of GM1 restores Ca^{2+} homeostasis following intracellular calcium elevation induced by calcium ionophore application, protecting cells from death (Nakamura, Wu, and Ledeen 1992). Similar effects have been observed in cultures of primary neurons exposed to massive glutamate concentration, which induces an excessive Ca^{2+} influx, leading to cell death (Avrova et al. 1998). Glutamate cytotoxicity was reduced by GM1 in murine cerebellar granule cells (Bachis et al. 2002; Sokolova, Rychkova, and Avrova 2014), and in cortical neurons (Park et al. 2016).

The finding that GM1 protected neurons from the toxic effects induced by glutamate and the calcium ionophore suggests that GM1 is involved in the maintaining of intracellular Ca^{2+} homeostasis, regulating also its extrusion.

Ca^{2+} efflux from cytoplasm was found to be modulated through GM1 regulation of Na^{+}/Ca^{2+} exchanger (NCX). NCX in the nuclear envelope was found to be associated with and modulated by GM1 (Xie et al. 2002), suggesting a mechanism of regulation of nucleoplasmic Ca^{2+} levels. The NCX/GM1 complex mediates the transfer of Ca^{2+} from the nucleoplasm to the luminal space of the nuclear envelope, which is continuous with the lumen of the endoplasmic reticulum; since nucleoplasmic Ca^{2+} is substantially in equilibrium with cytosolic free Ca^{2+} via nuclear pores, the NCX/GM1 complex at the inner membrane constitutes a gating mechanism for Ca^{2+} transfer from cytosol to endoplasmic reticulum (Wu et al. 2009).

Finally, GM1 can regulate cytoplasmatic Ca^{2+} level by modulating the plasma membrane calcium ATPase (PMCA). In neurons membrane PMCA isoform 2 is the most expressed (Burette et al. 2003) and was found to be slightly inhibited by GM1 (Zhao et al. 2004).

A schematic summary of the regulation of calcium flows by GM1 at various cellular levels is shown in the figure I6.

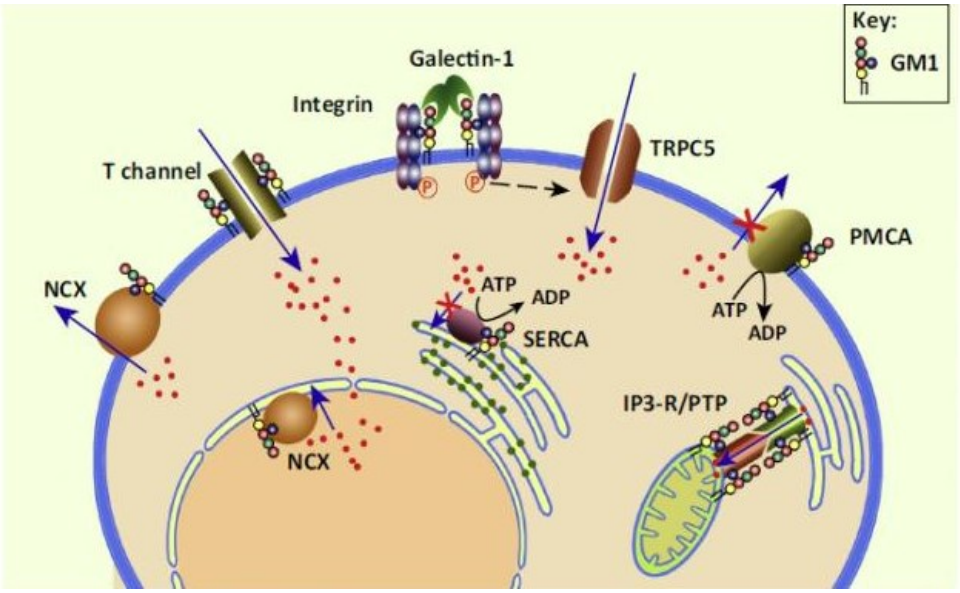

Figure I6: schematic representation of GM1 regulation of calcium flux. GM1 can interact directly or indirectly with different proteins responsible to mediate influx or efflux of Ca^{2+} across cell membranes. NCX, Na^{+}/Ca^{2+} exchanger; TRPC5, transient receptor potential channel 5; PMCA, plasma membrane Ca^{2+}-ATPase pump; SERCA, sarco/endoplasmic Ca^{2+}-ATPase pump; PTP, IP_3-R, inositol-3-phosphate receptor; PTP, permeability transition pore (modified from (Ledeen and Wu 2015).

3.2 GM1 influence on neurotrophic receptors

Neurotrophins and their receptors have been shown to be in contact with ganglioside GM1, contributing to explain the neurotrophic and protective effects of GM1, thanks to a specific protein-oligosaccharide interaction in the extracellular space (Ferrari et al. 1995; Mutoh et al. 1995; Farooqui et al. 1997; Bachis et al. 2002).

The main neurotrophic factors include nerve growth factor (NGF), brain-derived neurotrophic factor (BDNF), and glial cell-derived neurotrophic factor (GDNF), that respectively binds to TrkA, TrkB, and Ret tyrosine kinase receptors. Neurotrophin binding to their receptors induces receptor dimerization and autophosphorylation, therefore initiating complex cascade of signal transduction events necessary for neuronal differentiation, survival and maturation (figure I7).

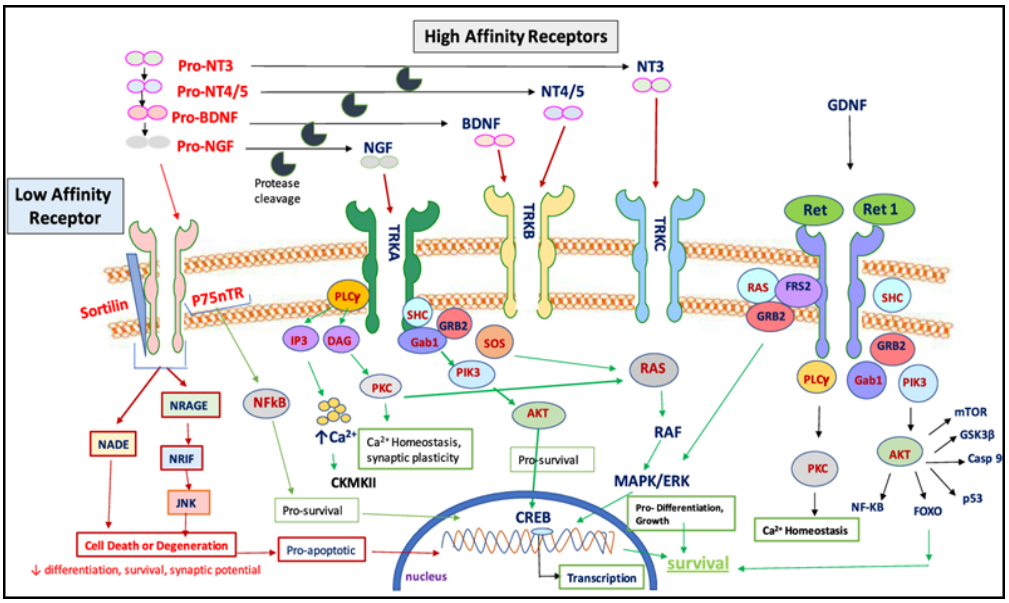

Figure I7: schematic illustration of neurotrophins' signaling sustaining neuron differentiation, growth and survival. NT = neurotrophins, BDNF = brain-derived neurotrophic factor, TRK = tyrosine receptor kinase, GDNF = glial-derived neurotrophic factor, PLC = phospholipase C, RAS = Ras proteins, GRB = growth factor receptor-bound protein 2, PIK3 = phosphatidylinositol-4,5-bisphosphate 3-kinase, AKT =AKT serine/threonine–protein kinases, FOXO = The forkhead box O transcription factor, PKC = protein kinase C, CREB= the cAMP-responsive element-binding protein (modified from (Kashyap et al. 2018).

GM1 ganglioside was shown to be able to activate TrkA receptor in different cell lines (Mutoh et al. 1995; Rabin and Mocchetti 1995) and primary neurons (Da Silva et al. 2005). In cells lacking endogenous GM1, it has been demonstrated that NGF did not induce the autophosphorylation of TrkA, but the rescue of GM1 content recovered the reaction of Trk to its ligand (Mutoh et al. 2002), suggesting that GM1 is necessary for the normal functioning of TrkA in inducing neuronal differentiation and neuritogenesis. Also the protective role of GM1 has been found to depend on TrkA activation (Sokolova, Rychkova, and Avrova 2014) coupled to ERK1/2 and Akt downstream pathways (Zakharova et al. 2014).

GM1 associates also with TrkB (Pitto et al. 1998; Bachis et al. 2002) and with the GDNF receptor complex comprised of Ret, the tyrosine kinase component, and GFRα, a GPI-anchored co-receptor. The important role of GM1 in interaction with neurotrophic receptors it is highlighted once again since the Ret association with GFRα was severely impaired in neurons totally or even partially devoid of GM1 (Hadaczek et al. 2015).

4. GM1 mechanism of action: the oligosaccharide chain as the functional portion

Despite the several studies relating the GM1 neuronal functions, the precise GM1 mechanism of action remained elusive.

In 1988, Schengrund and Prouty observed that the GM1 oligosaccharide (OligoGM1) promoted neuritogenesis in neuroblastoma cells S20Y (Schengrund and Prouty 1988). In 2012, Ledeen found that the hydrophilic GM1 derivative LIGA20, modified on the ceramide moiety but keeping the entire oligosaccharide intact, still maintained the GM1 properties, including the rescue of parkinsonian symptoms of *B4galnt1*$^{+/-}$ mice (Wu et al. 2012; Costa et al. 1993; Polo et al. 1994). This suggested that the ceramide structure is not critically related to GM1 modulatory effects.

Furthermore, the already mentioned evidence of neurodifferentiating and protective effects deriving from endogenous GM1 increase after Neu3 sialidase treatment both *in vitro* and *in vivo* (Schneider, Seyfried, et al. 2015), suggest an important role for GM1 oligosaccharide chain in the regulation of the processes that occur at the plasma membrane level.

4.1 GM1-oligosaccharide neurodifferentiative properties

Recent studies have investigated the OligoGM1 differentiative properties, confirming its neuritogenic potential in N2a murine neuroblastoma cells (Chiricozzi et al. 2017). In this study, OligoGM1 administered to N2a reduced cell proliferation without altering cell viability and induced the emission of neurite prolongations and the elevation of the neurofilament proteins analogously to what observed following the application of the entire GM1. Moreover, it was demonstrated that the effect exerted by OligoGM1 was strictly dependent from its structure. In fact, residues of the total structure, such as sialic acid, galactose, sialyllactose, Neu5Ac-Gg3 and Gg4, did not show neuritogenic properties. On the other hand, fucosylated OligoGM1, containing a α-fucose linked to position 2 of the external galactose, showed the same neuritogenic effect. This suggests that the β-Gal-(1-3)-β-GalNAc-(1-4)-[α-Neu5Ac-(2-3)]-β-Gal-(1-4)-Glc represented the minimal structure required by the oligosaccharide to exert its neuronal functions and the terminal α-Fuc-(1-2)-β-Gal linkage does not change the saccharide conformation necessary for the activation of the sprouting process.

Importantly, OligoGM1 exerts its neuritogenic effect without entering into the cells but interacting with cell surface. Accordingly, OligoGM1 was found to elicit the activation of TrkA-ERK1/2 pathway (figure I8), confirming what was previously demonstrated for GM1. In fact, in conditions of TrkA silencing or inhibition, the addition of OligoGM1 to N2a cells did not promote neurite sprouting nor reduced the cell proliferation.

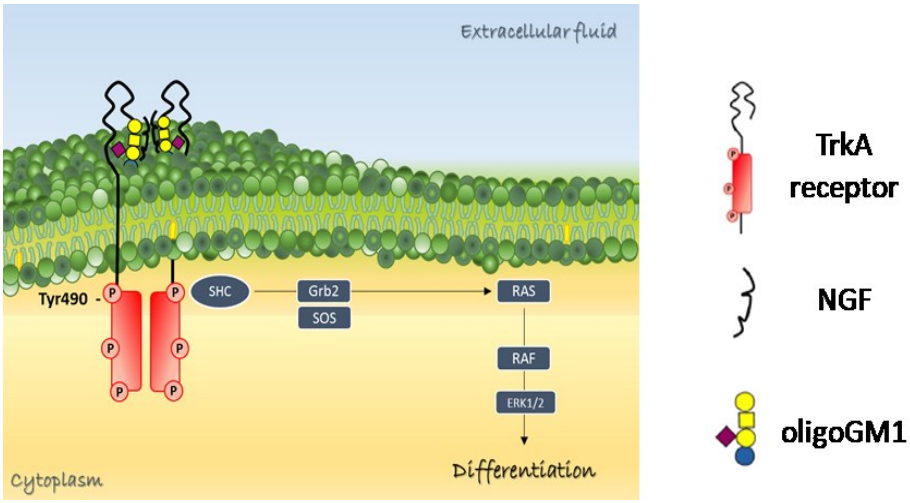

Figure I8: scheme of the proposed mechanism underling GM1 neuritogenic effect in N2a. OligoGM1 directly interacts with an extracellular domain of TrkA stabilizing TrkA–NGF complex, enhancing TrkA phosphorylation on tyr490. TrkA activation induces MAPK differentiative pathway. ERK, extracellular signal-regulated protein kinases 1 and 2; Grb2, growth factor receptor-bound protein 2; Gab1, Grb2-associated binder-1; RAS, GTP-binding protein; RAF, serine/ threonine kinase; SHC, transforming protein 1; SOS, son of sevenless (modified from (Chiricozzi et al. 2017).

OligoGM1 neurotrophic properties were further confirmed using primary cerebellar granule neurons (CGN) obtained from mice (Di Biase et al. 2020). Accordingly, OligoGM1 administered to mice CGN induces TrkA-MAP kinase pathway activation enhancing neuron clustering, neurite sprouting and networking (figure I9).

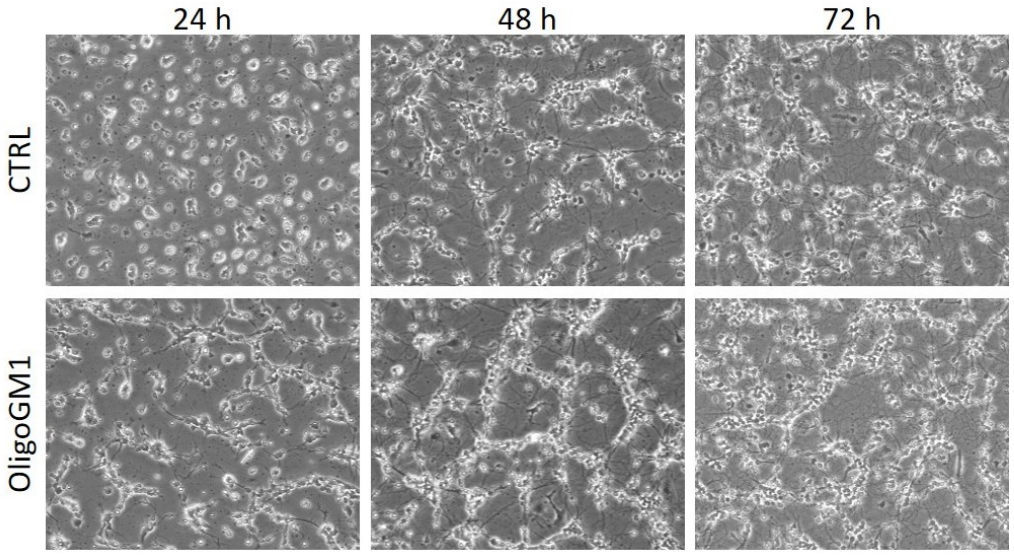

Figure I9: Morphological effect of exogenous administration of OligoGM1 to cerebellar granule neurons during development. CGN plated in the presence of 50 µM OligoGM1 show an acceleration of the clustering and the neuritogenesis with respect to the untreated control cells (modified from (Di Biase et al. 2020).

Moreover, a higher phosphorylation rate of FAK and Src proteins, the intracellular key regulators of neuronal motility, was observed. In parallel, OligoGM1 receiving cells express increased level of neuronal maturation markers and anticipate the expression of complex gangliosides reducing the level of simplest ones, suggesting an advanced stage of maturation compared to controls (figure I10).

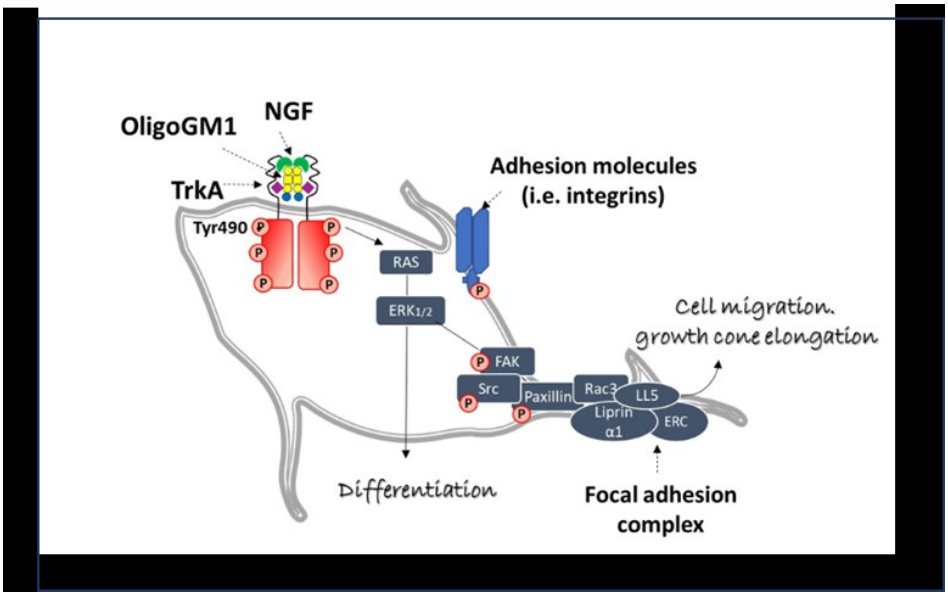

Figure I10: schematic representation of the hypothesized molecular mechanism underling OligoGM1 enhanced neuronal maturation. OligoGM1 enhances the activation of TrkA-MAPK pathway which could be associated to an increase of FAK and Src activation, regulators of neuronal motility and axon growth. ERC, ELKS/Rab6-interacting/CAST family; ERK, extracellular signal-regulated protein kinases; FAK, Focal adhesion kinase; LL5, Pleckstrin homology-like domain family B; Rac3, Ras-related C3 botulinum toxin substrate 3; RAS, GTP-binding protein; Src, proto-oncogene tyrosine-protein kinase Src (modified from (Di Biase et al. 2020).

4.2 GM1-oligosaccharide and TrkA interaction

The specific interaction between TrkA and GM1 has been reported by several authors (Bachis et al. 2002; Farooqui et al. 1997; Mutoh et al. 1995; Da Silva et al. 2005; Ferrari et al. 1995; Rodriguez et al. 2001). By photolabeling experiments (figure I11c), a direct interaction between the GM1 oligosaccharide and the extracellular domain of TrkA receptor was shown (Chiricozzi et al. 2017; Chiricozzi, Biase, et al. 2019). In these studies, a derivative of OligoGM1 pentasaccharide, containing both a tritium and a photoactivable phenylazide group was added to N2a cells; the subsequent UV-light exposition transformed the photoactivable group into a nitrene, which rapidly binds neighbouring compounds in a covalent manner (Mauri et al. 2004). After SDS–PAGE separation and radio-imaging of the blotted material, the authors recognized a band of molecular mass equal to that of the TrkA. Using a specific anti-TrkA antibody on the same PVDF, a specific signal overlapping the radiolabelled band was found, suggesting a direct interaction between OligoGM1 and TrkA.

This evidence was further confirmed (figure I11 A&B) by using two modified forms of radiolabeled GM1: one carrying the photoactivatable group associated with the oligosaccharide chain, and the other one carrying the same group within the lipid portion (Chiricozzi, Biase, et al. 2019). The overlapping between the radioactive and the chemiluminescent signals was obtained only by using the radiolabeled-GM1 derivative containing the photoactivable group inserted in the oligosaccharide head. This finding clearly indicated that the interaction between TrkA and ganglioside GM1 occurs outside the cell through the oligosaccharide chain.

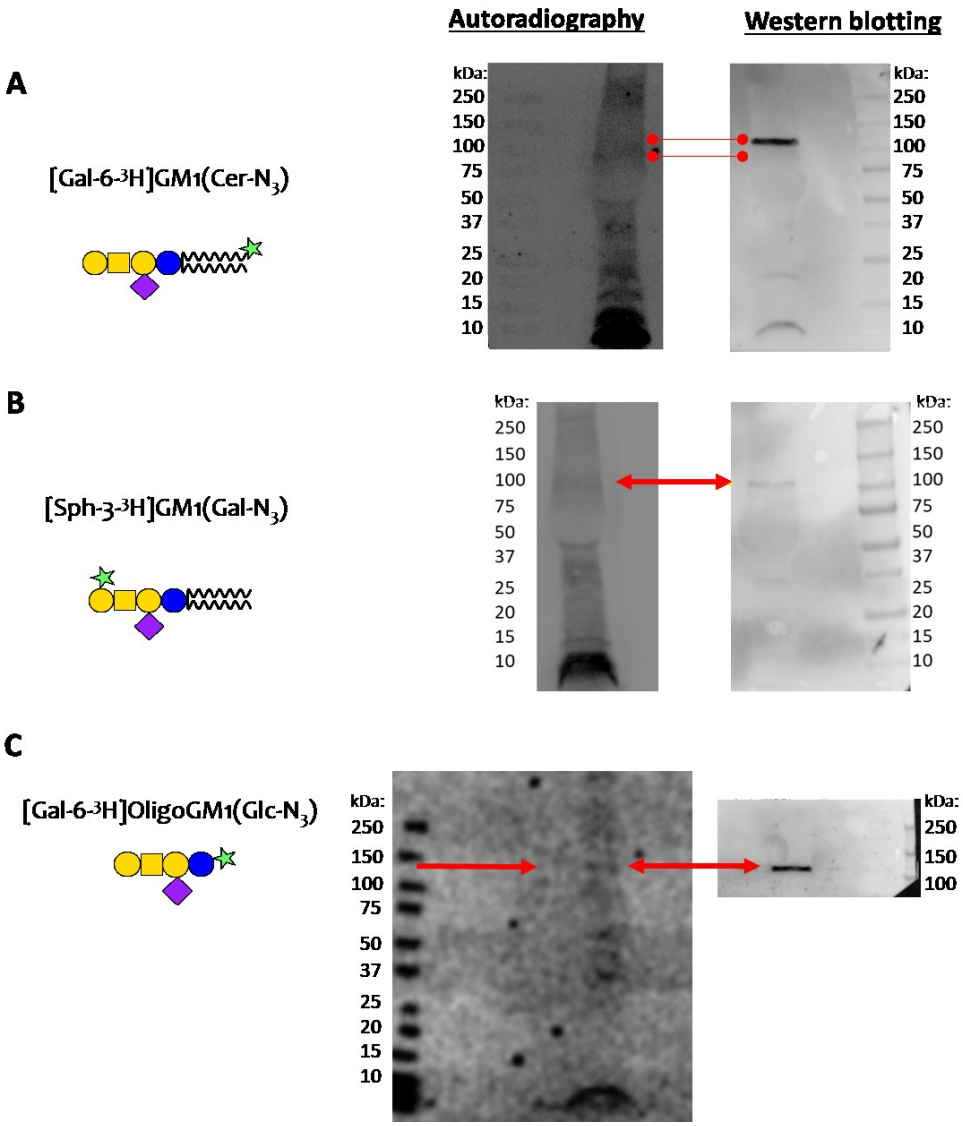

Figure I11: Interaction between TrkA and GM1 occurs through GM1-oligosaccharide in N2a cells. Radiolabel derivatives of GM1 carrying the photoactivable group, represented by the green star in the symbolic representation, were administered to cells. UV light was used to induce crosslinking between GM1-derivates and surrounding molecules. After radiography of cell protein pattern and TrkA immunoblotting, overlapping between radio-signal and chemiluminescent signal was only found with OligoGM1 and GM1 carrying photoactive group on the oligosaccharide (modified from (Chiricozzi, Biase, et al. 2019; Chiricozzi et al. 2017).

In 2015, Fantini reported on the presence of a GM1-binding domain in the extracellular domain of Trk receptor, suggesting that GM1 oligosaccharide could act as an endogenous activator of TrkA receptor (Fantini and Yahi 2015). Accordingly, a molecular modelling tool was used to predict whether OligoGM1 could increase the TrkA-NGF complex stability, favouring receptor-ligand intermolecular interactions (figure I12). The crystallized structure of TrkA-NGF complex was resolved as a dimer that presented a pocket in the interface of receptor-ligand interaction. By *in silico* molecular docking studies it was found that the OligoGM1 perfectly fits in the pocket, reducing the free energy associated to the TrkA-NGF complex from approx. −7 kcal/mol to approx. −12 kcal/mol (Chiricozzi et al. 2017), indicating that GM1 oligosaccharide stabilizes TrkA-NGF association.

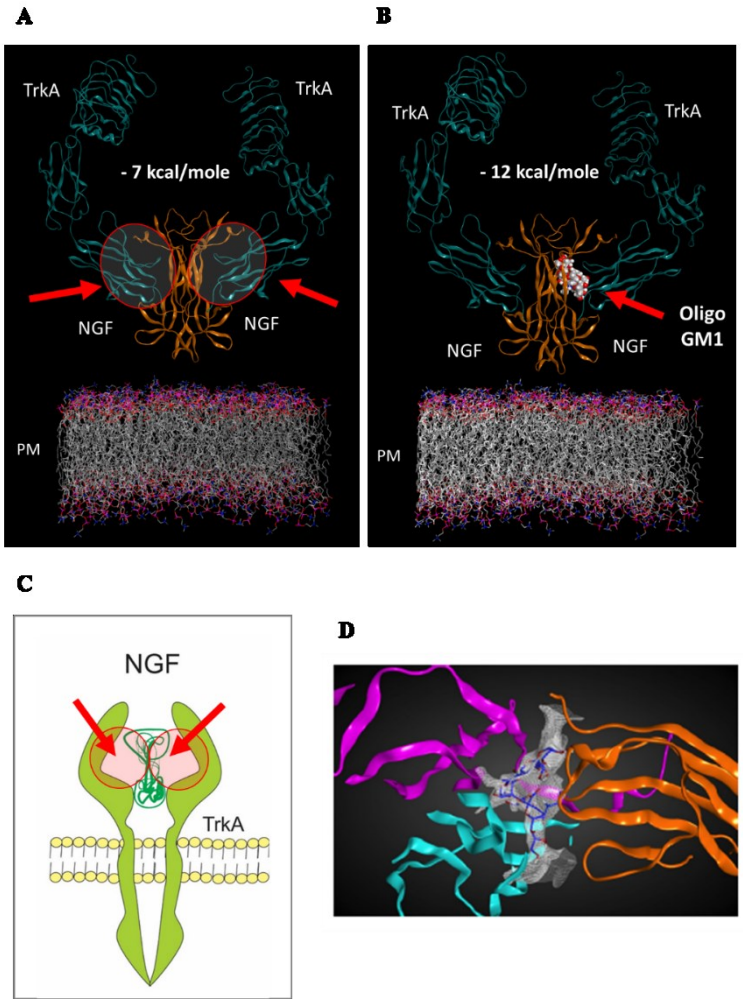

Figure I12: Modeling of the interaction between NGF-TrkA complex and OligoGM1. A: crystallized structure of TrkA receptor, which is resolved as a dimer in the presence of its natural ligand, the NGF, also present as a dimer. **B:** TrkA-NGF complex owns a pocket in the interface of receptor-ligand that can accommodate OligoGM1. When OligoGM1 is present the free energy of the TrkA-NGF structure is reduced from -7 kcal/moles to -12kCal/mol. **C:** schematic representation of TrkA-NGF complex. **D:** TrkA in orange ribbons; two NGF molecules: one in cyan ribbons and one in magenta ribbons. OligoGM1 is represented in sticks, with blue color for carbon atoms and red color for oxygen atoms. Van der Waals interaction surface between oligoGM1and proteins is represented as a white mesh map (modified from (Chiricozzi et al. 2017).

4.3 GM1-oligosaccharide neuroprotective properties

A later study demonstrated that also GM1 neuroprotective effects, at least in N2a cells, are related to its oligosaccharide chain (Chiricozzi, Maggioni, et al. 2019).

In particular, it was demonstrated that a 24 hours pre-treatment with OligoGM1 conferred cell protection against 1-methyl-4-phenyl-1,2,3,6-tetrahydropyridine (MPTP), a pro-neurotoxin that, upon cell oxidative conversion into 1-methyl-4-phenylpyridinium (MPP^+), inhibits the complex I of mitochondria electron transport chain inducing ATP depletion, ROS production and finally cell death. In particular, it has been demonstrated that OligoGM1 reduced mitochondrial ROS production preventing oxidative stress and reducing N2a cell death.

The inhibition of TrkA receptor abolished the OligoGM1 protective effect against MPTP treatment, confirming that OligoGM1 protective effect is dependent on TrkA pathway activation.

4.4. GM1-oligosaccharide as mitochondria regulator

Mitochondria are fundamental organelles of eukaryotic cells responsible for supplying cellular energy and for regulating cell survival. They take part in many cellular processes, including calcium signaling, cell growth and differentiation (Osellame, Blacker, and Duchen 2012). Mitochondrial impairment can be found in a large number of human diseases and has been taking huge consideration as promotor of neurodegenerative disorders including Parkinson's Disease (PD), since dopaminergic neurons are remarkably vulnerable to mitochondrial alterations (Winklhofer and Haass 2010). Multiple aspects of mitochondrial biology are affected in PD, so that impairments of mitochondrial integrity and function have been linked to the pathogenesis of PD (Winklhofer and Haass 2010). Considering its devastating effects on mitochondria, the MPTP molecule has been widely employed to induce the neurological lesions typically occurring in PD. In this context, the protective effects against MPTP-toxicity (Chiricozzi, Maggioni, et al. 2019) led to hypothesize a possible regulatory effect of GM1 oligosaccharide on mitochondria. Accordingly, it was demonstrated that in N2a cells the administration of OligoGM1 promotes a mitochondriogenic effect, shown as an increased expression of mtDNA and of mitochondrial proteins (Fazzari et al. 2020). In addition, OligoGM1 treatment induced an upregulation of Tom20 and HTRA2, two proteins that interestingly have been found to correlate with PD onset when their cellular expression is altered. In particular, the deletion of HTRA2 protease determined an increase of ROS levels and misfolded proteins in murine brain mitochondria (Moisoi et al. 2009), while HTRA2 loss of function mutations were found in PD patients (Strauss et al. 2005).

Transmission electron microscopy analyses of OligoGM1 treated N2a cells showed more electron-dense mitochondria suggesting an enhanced mitochondrial activity. This was confirmed by increased expression of some subunits of electron transport chain (ETC complexes, by enhanced respiration and by incremented ATP levels following OligoGM1 administration.

Finally, OligoGM1 was found to rescue impaired mitochondria function in a N2a model with a chemically induced mitochondrial dysfunction (Audano et al. 2019) (Fazzari et al. 2020), enhancing the activity of complex I and II of the ETC which function was reported to be impaired in PD.

A schematic representation of the proposed mechanism for OligoGM1 modulation of mitochondrial function is shown in figure I13.

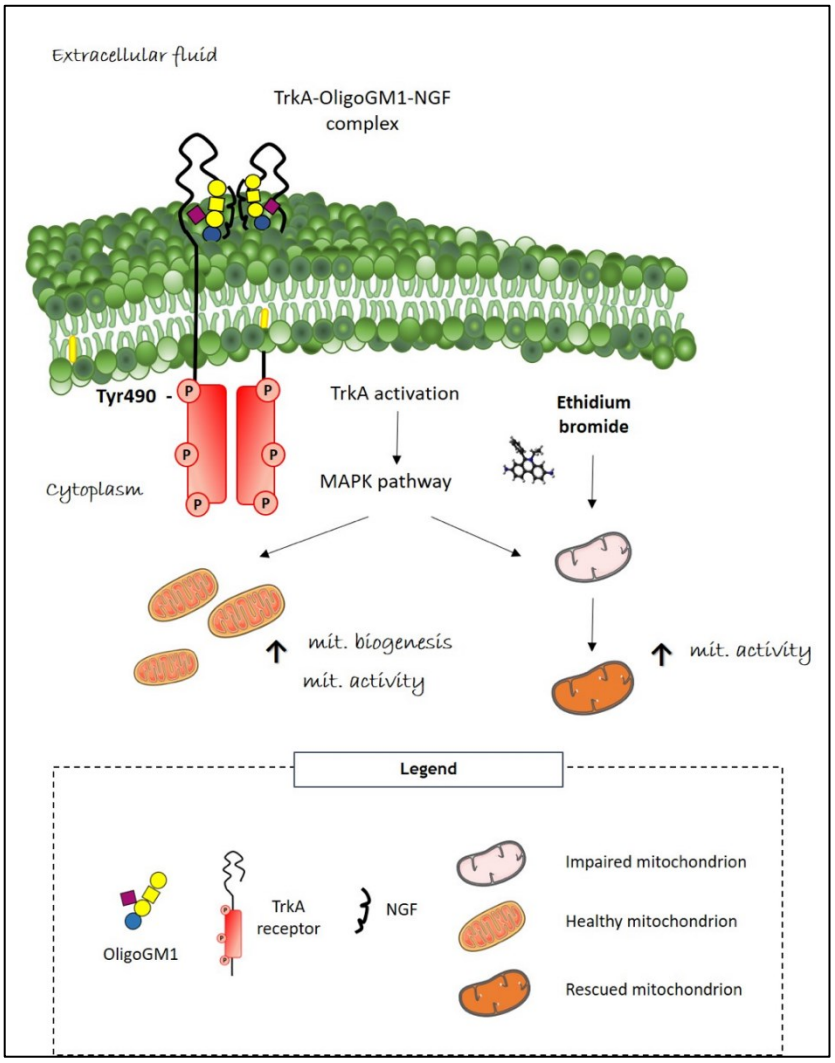

Figure I13: Diagram of the proposed mechanism for OligoGM1 modulation of mitochondrial function at the plasma membrane level. OligoGM1 interacts with TrkA receptor and, by stabilizing the NGF-TrkA complex, induces its autophosphorylation and the activation of MAPK signaling pathway. Both in healthy and in ethidium bromide mitochondria defective cells, this leads to an increase of mitochondrial bioenergetics (modified from (Fazzari et al. 2020).

5. GM1 and Parkinson's disease

The several studies demonstrating neurotrophic and neuroprotective effects of ganglioside GM1 led inevitably to think about it as a possible therapeutic agent. Since the 80s GM1 ganglioside, alone or in combination with other gangliosides has been used as therapeutic drugs for the treatment of peripheral neuropathies, neurodegenerative diseases and cerebral/spinal cord injuries (Chiricozzi et al. 2020; Magistretti et al. 2019).

Among other disorders, Parkinson's disease elicited particular interest regarding GM1-based therapy. PD is a neurodegenerative disorder characterized by the progressive death of dopamine producing neurons in the *substantia nigra* of the brain. Pathognomonic histopathological sign of the disease is the accumulation in the affected brain areas of the Lewy bodies composed mainly of fibrillary aggregates of the alpha-synuclein protein. The processes underlying the generation of these accumulations over time and the mechanisms associated with their pathogenicity are still largely unknown, so far. Moreover, most of PD cases are idiopathic and are treated only with symptomatic interventions since drugs blocking neuronal loss are not available yet. In the past, the exogenous administration of GM1 ganglioside showed significant efficacy in partially recover behavioural and biochemical alterations in chemically induced PD mouse (Schneider et al. 1995) and primates models (Schneider et al. 1992). Alterations of the plasma membrane ganglioside content have been reported in neurodegenerative diseases and dementias (Piccinini et al. 2010; Breiden and Sandhoff 2018; Magistretti et al. 2019). This is particularly true for PD, where reduced levels of GM1 were detected in nigrostriatal neurons of the *substantia nigra pars compacta*, in occipital cortex, and in various peripheral tissues of PD patients compared to healthy subjects of the same age (Schneider 2018; Hadaczek et al. 2015; Ledeen and Wu 2018a). These observations gave rise to the development of a new theory regarding a possible role for decreased expression levels of ganglioside GM1 and its precursor GD1a in the *aetiopathogenesis* of sporadic form of PD (Ledeen and Wu 2018b; Ledeen and Wu 2018a). This theory was further supported by recent studies showing that gangliosides-deficient *B4galnt1*$^{+/-}$ mice with half of the normal level of GM1 manifested impaired movement and all the neuropathological symptoms of PD (Wu et al. 2011; Wu et al. 2012).

From a mechanistic point of view subnormal plasma membrane levels of GM1 could induce neuronal degeneration by a failure of trophic signalling, since neurotrophic factors' receptors require GM1 association to facilitate neuron survival, together with a reduction of clearance promoting the alpha-synuclein accumulation.

In fact, GM1 was found to bind to the soluble alpha-synuclein, promoting the maintenance of the non-aggregating helical conformation of the protein (Martinez et al. 2007). This association is

enhanced by N-terminal acetylation of alpha-synuclein, which significantly increases GM1-binding specificity and resistance of alpha-synuclein to aggregation (Bartels et al. 2014). Since alpha-synuclein oligomerization and fibrillation cause neuronal toxicity and the spreading of the disease, the prevention of such fibrillation could protect neurons from degeneration. Significantly, application of GM1 to a rat model of PD overexpressing the human alpha-synuclein reduced the aggregation of the protein (Schneider et al. 2019). Overall, these data suggest that subnormal level of brain GM1 could favour misfolding of alpha-synuclein protein, thus representing the leading cause responsible for the onset of idiopathic PD.

Accordingly, GM1 replacement therapy demonstrated a modest but significant efficacy in a monocentric controlled, delayed start trial on patient with sporadic PD, where patients recorded improvements in motor and cognitive outcomes compared to the placebo-receiving counterpart (Schneider et al. 2010; Schneider et al. 2013; Schneider, Cambi, et al. 2015). However, an important and fundamental limitation in GM1 clinical application is that, due to its chemo-physical properties (i.e. amphiphilic characteristic), GM1 hardly crosses the blood-brain barrier (BBB) and thus a too small quantity of GM1 may reach the damaged neurons. In fact, a significant amount of GM1 had to be injected to obtain a relevant result in PD patients (Schneider et al. 2010).

5.1 GM1 oligosaccharide role in PD

Considering all the evidence about OligoGM1 ability to replace GM1 properties *in vitro*, its neuroprotective potential was also addressed *in vivo* (Chiricozzi, Mauri, et al. 2019). Firstly, OligoGM1 capability to reach more efficiently the central nervous system than the entire GM1 was assessed. Following the intraperitoneal injection of tritium labeled OligoGM1, [^{3}H]OligoGM1, in adult mice, the radioactivity was found to be associated with all brain areas, including the *substantia nigra*. Importantly, OligoGM1 maintained its metabolic stability when was extracted from brain tissues as verified by chromatography assay.

To verify OligoGM1 therapeutic potential, the *B4galnt1*$^{+/-}$ mice were used as model of sporadic PD. As already mentioned above, these mice present reduced brain content of GM1 and GD1a and develop progressively many of the PD features: alteration of neurotrophic signaling, alpha-synuclein elevation and aggregation in the *substantia nigra*, loss of dopaminergic neurons, striatal degeneration, and increasing motor dysfunction (Wu et al. 2012; Wu et al. 2011). Impressively, OligoGM1 treatment of these mice (20 mg/kg, intraperitoneally, daily for 28 days) completely rescued physical symptoms, reduced nigral alpha-synuclein aggregates, and restored the expression of nigral tyrosine

hydroxylase (marker of dopaminergic neurons) together with striatal neurotransmitter levels, matching the wild type healthy condition.

These impressive *in vivo* data together with previous *in vitro* findings suggest that GM1 trophic and protective functions in PD affected brain areas relay on the interaction and modulation of plasma membrane proteins and receptors by its oligosaccharide chain, which could likely be used as a more efficient tool to sustain neuronal survival over GM1.

Aim

GM1 ganglioside has been abundantly studied because of its essential role in neuronal differentiation, protection and restoration (Schengrund 2015; Ledeen and Wu 2015; Aureli et al. 2016). GM1 trophic effects are determined by the interaction with specific proteins expressed on the plasma membrane, such as TrkA receptor, and by changes in cellular calcium level, accomplished through modulation of Ca^{2+} influx channels, Ca^{2+} exchange proteins, and various Ca^{2+}-dependent enzymes that are modulated through association with GM1 (Ledeen and Wu 2015; Wu et al. 1998; Wu et al. 2009).

In fact, the Ca^{2+} ion is a highly versatile and ubiquitous signalling messenger that plays an essential role in the development of the nervous system, modulating neuronal proliferation, migration, and differentiation (Toth, Shum, and Prakriya 2016). The difference in Ca^{2+} concentration between the extracellular space and the cytosol creates a gradient that allows the Ca^{2+} to rapidly flow into the cell, where it exerts regulatory effects on multitude of downstream enzymes and proteins (Toth, Shum, and Prakriya 2016).

Even if the neurotrophic properties of GM1 have been extensively studied both *in vitro* and *in vivo*, the molecular basis of its mechanism of action is currently not entirely clear.

However, investigating the molecular mechanisms at the base of GM1 action is not such a simple experimental procedure. Using the GM1 as a whole molecule (exogenous administration or increasing by modulation of sialiadase), if on one hand may be advantageous, on the other it induces not negligible macroscopic changes. In fact, GM1 increase at the cell surface can alter the characteristics of the membrane impacting on signal transduction mechanisms, and it also can be internalized reaching the lysosomes where its catabolic fragments are then recycled for the biosynthesis of all sphingolipids. This can certainly be important to evaluate the effects of GM1 as a soluble cytoplasmic molecule (Wu, Lu, and Ledeen 1995) but for what concerns the membrane signalling it risks being counterproductive.

However, the GM1 signalling at the plasma membrane level may be due to the oligosaccharide chain, which protruding into the cellular environment can interact with the exposed extracellular domains of membrane receptors.

With the aim of shedding light on GM1 mode of action starting at the plasma membrane level, the oligosaccharide chain was chemically separated from the GM1 ceramide and purified to be used experimentally (Chiricozzi et al. 2017; Chiricozzi, Biase, et al. 2019; Chiricozzi, Maggioni, et al. 2019).

Importantly, it was discovered that within the entire molecule, the oligosaccharide chain β-Gal-(1-3)-β-GalNAc-(1-4)-[α-Neu5Ac-(2-3)]-β-Gal-(1-4)-β-Glc of GM1 is actually the bioactive moiety responsible for the ganglioside neurodifferentiative and neuroprotective properties (Chiricozzi et al. 2017; Chiricozzi, Biase, et al. 2019; Chiricozzi, Maggioni, et al. 2019). Precisely, OligoGM1 was

found to induce the emission of neurite prolongations in mouse neuroblastoma cells (Chiricozzi et al. 2017; Chiricozzi, Biase, et al. 2019) and to enhance neuron clustering, neurite sprouting and networking in a neuronal primary culture (Di Biase et al. 2020). Moreover, OligoGM1 has been found to be protective against MPTP neurotoxicity in mouse neuroblastoma cells by specifically increasing mitochondria biogenesis and energetics (Chiricozzi, Maggioni, et al. 2019; Fazzari et al. 2020).

Thus, GM1 exerts its activities through its hydrophilic head, which protrudes into the extracellular environment and therefore acts at the cell surface by interacting with plasma membrane proteins. In particular, OligoGM1 was found to directly interact with NGF specific receptor TrkA at the plasma membrane level, leading to the activation of ERK1/2 downstream pathway (Chiricozzi et al. 2017; Chiricozzi, Biase, et al. 2019; Chiricozzi, Maggioni, et al. 2019; Di Biase et al. 2020).

Given the importance of the Ca^{2+} signaling in the GM1 mediated neuronal functions, the aim of the present doctoral project was to investigate the mechanism of action underlying the neurotrophic functions of GM1 focusing on the role of its oligosaccharide in the modulation of Ca^{2+} flow and its possible involvement in OligoGM1-mediated neuronal differentiation.

To answer these questions, mouse neuroblastoma cells N2a has been employed in the present study since represent a cellular model widely used to demonstrate the neurotrophic properties of GM1, including its modulation on calcium homeostasis (Wu and Ledeen 1991; Spoerri, Dozier, and Roisen 1990; Fang et al. 2000) and already used to shown the OligoGM1 neuronal functions (Chiricozzi et al. 2017; Chiricozzi, Biase, et al. 2019; Chiricozzi, Maggioni, et al. 2019; Fazzari et al. 2020).

In the present study, the oligosaccharide chain of GM1 was employed as a tool to provide knowledge regarding the mechanism by which the specific sugar code of GM1 influences calcium homeostasis through the modulation of plasma membrane signaling.

Materials and methods

Materials

Commercial chemicals were of the highest purity available, common solvents were distilled before use and water was doubly distilled in a glass apparatus.

Phosphate buffered saline (PBS), sodium orthovanadate (Na_3VO_4), phenylmethanesulfonyl fluoride (PMSF), aprotinin, protease inhibitor cocktail (IP), ethylenediamine tetraacetic acid (EDTA), bovine serum albumin (BSA), Xestspongin C, calcium ionophore A23187, ethylene glycol tetraacetic acid (EGTA), 1,2-bis(o-aminophenoxy)ethane-N,N,N′,N′-tetraacetic acid (acetoxymethyl ester) (BAPTA-AM) and mouse anti-alpha-tubulin (RRID: AB_477579) antibody were from Sigma-Aldrich (St. Louis, MO, USA).

TrkA-inhibitor (CAS 388626-12-8) was from Merk Millipore (Billerica, MA, USA).

Fluo-4 AM, Hank's Balanced Salt Solution containing calcium and magnesium ($HBSS^+$) and Sodium pyruvate were from Thermo Fisher Scientific (Waltham, MA, USA).

Rabbit anti-TrkA (RRID: AB_10695253), rabbit anti-phospho-TrkA (Tyr 490) (RRID: AB_10235585), rabbit anti-Flotillin-1 (RRID: AB_2773040), and goat anti-rabbit IgG (RRID: AB_2099233) antibodies were from Cell Signaling Technology (Danvers, MA, USA).

Mouse anti-PLCγ1 (RRID: AB_628119), p-PLC γ1 (Tyr 783) (RRID: AB_2163561), PKC (RRID: AB_628139), pPKCα (Ser 657) (RRID not found) antibodies were from Santa Cruz Biotechnology (Dallas, TX, USA).

Mouse anti-Calnexin (RRID: AB_397884) antibody was from BD Biosciences.

Chemiluminescent kit for western blot was from Cyanagen (Bologna, Italy).

4 –20% Mini-PROTEAN® TGX™ Precast Protein Gels, Turbo Polyvinylidene difluoride (PVDF) Mini-Midi membrane and DC™ protein assay kit were from BioRad (Hercules, CA, USA).

Triton X-100 were from Merk Millipore (Frankfurten, Germany).

Corning® cell culture flasks, dishes, and Corning® Costar® cell culture plates were purchased from Corning (Corning, NY, USA).

Dulbecco's modified Eagle's high glucose medium (DMEM HG), fetal bovine serum (FBS), L-glutamine (L-Glut), Penicillin/streptomycin (10.000 Units/mL), and acrylamide, were purchased from EuroClone (Paignton, UK).

Methods

1. Chemical synthesis and preparation of ganglioside GM1 and its oligosaccharide

1.1 GM1 purification

GM1 ganglioside (II^3Neu5Ac-Gg_4-Cer) was purified from the total ganglioside mixture extracted from fresh pig brains collected at the slaughterhouse of the Galbani Company (Melzo, Italy), according to the procedure developed previously (Tettamanti et al. 1973). High amount of GM1 was obtained by the sialidase treatment of the total pig brain ganglioside mixture. This simplified the purification process as the major part of polysialogangliosides were transformed into GM1 (Acquotti et al. 1990). The ganglioside mixture, 5 g as sialic acid, was dissolved in pre-warmed (36°C) 500 mL of 0.05 M sodium acetate, 1 mM $CaCl_2$ buffer pH 5.5. *Vibrio cholerae* sialidase (1 unit) was added to the solution every 12 h. Incubation at 36°C and magnetic stirring was maintained for two days, and the solution dialyzed at 23°C for 4 days against 10 L of water changed 5 times a day. The sialidase treated ganglioside mixture was subjected to 150 cm x 2 cm silica gel 100 column chromatography equilibrated and eluted with chloroform/methanol/water, 60:35:5 by vol. The fractions containing GM1, identified by thin layer chromatography (TLC), were pooled, dried and submitted to a further column chromatographic purification using the above experimental conditions. Fractions containing pure GM1 were collected and dried. The residue was dissolved in chloroform/methanol (2:1 v/v) and precipitated by adding 4 volumes of cold acetone. After centrifugation (15.000 *x* g) the GM1 pellet was separated from the acetone, dried, dissolved in 50 mL of deionized water and lyophilized giving 1350 mg of white powder which was stored at -20°C.

1.2 GM1 oligosaccharide preparation

The oligosaccharide II^3Neu5Ac-Gg_4 (OligoGM1) was prepared by ozonolysis followed by alkaline degradation (Wiegandt and Bucking 1970) from GM1 (figure M1). Briefly, GM1 was dissolved in methanol and slowly saturated with ozone at 23°C. Triethylamine/water (5:1) was added to the mixture bringing the pH to 10.5–11.0 and the reaction continued for three days. Then, solvent was evaporated and GM1 oligosaccharide was purified by flash chromatography using chloroform/methanol/2-propanol/water 60:35:5:5 v/v/v/v as eluent. The oligosaccharide was dissolved in methanol and stored at 4°C.

Altogether, NMR, MS, HPTLC and autoradiographic analyses showed a homogeneity over 99% for the prepared ganglioside and oligosaccharide (figure M2).

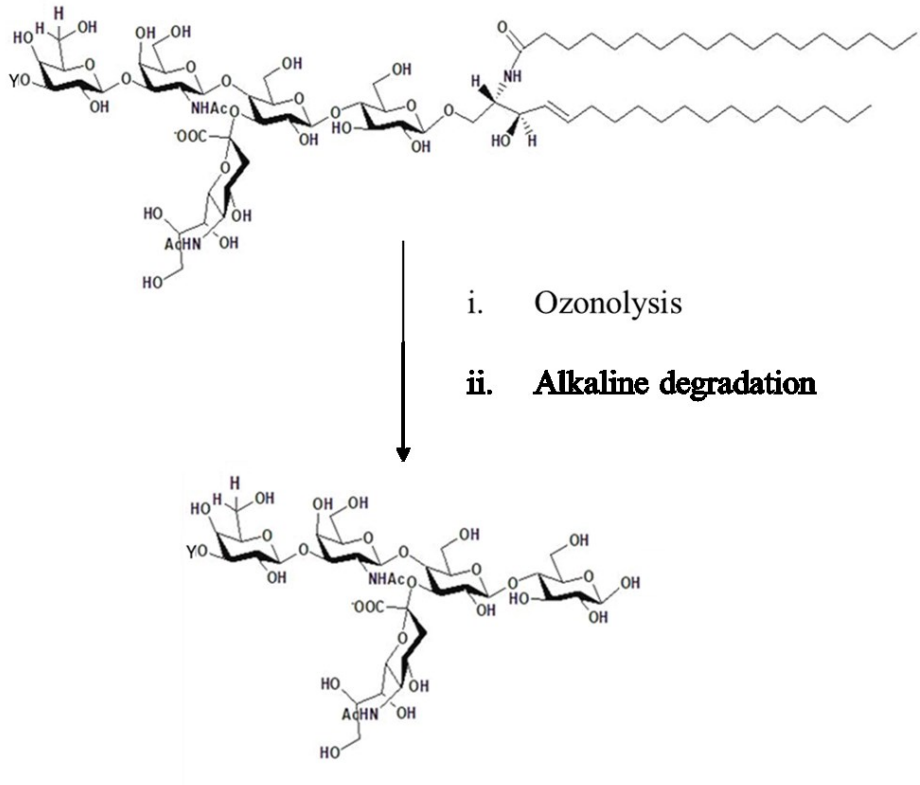

Figure M1: Chemical synthesis of GM1 oligosaccharide. Ozone-alkali fragmentation procedure was used to obtain desphingosino-gangliosides. Ozonolysis organic reaction cleaved unsaturated bond between sphingosine 4 and 5 carbons. Subsequently, the alkaline degradation with triethylamine released the oligosaccharide chain form the residue.

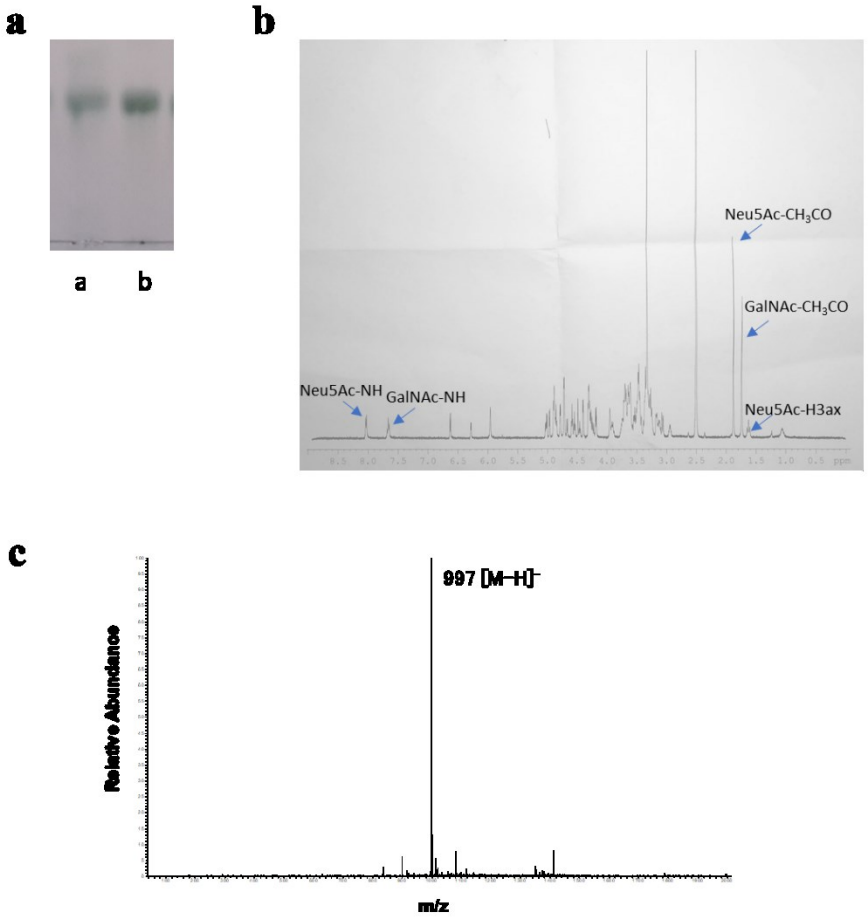

Figure M2: a) HPTLC representative images. TLC were developed with the solvent system chloroform/methanol/KCl 50mM, 30:50:13 by vol. Two amounts of OligoGM1, Erlich colorimetric revealing; b) 500 MHz 1H-NMR spectrum in DMSO-d6 at 303K of OligoGM1; c) MS profile ESI-MS (negative-ion mode): m/z= 997 $[M - H]^-$.

2. N2a cell culture

N2a cells were cultured and propagated on 75 cm^2 flasks in DMEM HG supplemented with 10% FBS, 1% L-glutamine and 1% penicillin/streptomycin, 1% sodium pyruvate (v/v), at 37°C in a humidify atmosphere of 95% air / 5% CO_2. Cells were sub-cultured to a fresh culture twice a week at the reaching of 90% confluence (i.e. every 3-4 days). In sub-cultures passages cells were washed twice with PBS and detached by 0.02% EDTA - 0.6% glucose in PBS (w/v).

N2a cells were bought from Sigma-Aldrich to which they were supplied by European Collection of Authenticated Cell Cultures (ECACC) (Catalogue No. 89121404; Lot No. 13K010, RRID: CVCL_0470).

N2a cells were employed in experiments between the 5th and the 20th passages.

For all cell culture procedures sterilized condition were maintained by using sterile solutions and by working under the laminar flow cabinet.

2.1 OligoGM1 treatment

N2a cells were plated at 5 x 10^3 / cm^2 on 6-well plates in complete DMEM HG medium. Cells were counted by Bürker chamber system (Denham et al. 1971). 24 hours after plating, growth medium was removed and N2a cells were pre-incubated in pre-warmed (37°C) DMEM HG medium containing 2% FBS, 1% L-glutamine, and 1% penicillin/streptomycin, for 30 minutes at 37°C.
Subsequently, to perform cell treatment, GM1 oligosaccharide was solubilized in water at 2 mM concentration by vortex agitation and sonication in water bath 3 times for 30 seconds. Solubilized OligoGM1 was administered to cells at the final concentration of 50 μM (Chiricozzi et al. 2017). Control cells were incubated under the same experimental conditions but omitting any addition of OligoGM1.

2.2 Inhibition of TrkA Receptor

To block TrkA activity in N2a cells, TrkA inhibitor (120 nM) was added to the incubation medium 1 hour before the addition of OligoGM1 (Wood et al. 2004; Chiricozzi et al. 2017).

2.3 EGTA and BAPTA-AM treatment

To chelate Ca^{2+} ions in N2a cells, the extracellular Ca^{2+} chelating agent EGTA (100 μM) or the intracellular Ca^{2+} chelating agent BAPTA-AM (1 μM) were added to the incubation medium together with OligoGM1 (Chiricozzi et al. 2010).

3. Morphological analysis and neurite outgrowth evaluation

Cultured cells untreated (control) or treated with 50 μM OligoGM1 in presence or absence of EGTA/BAPTA-AM for 24 hours were observed by phase contrast microscopy (Olympus BX50 microscope; Olympus, Tokyo, Japan).
The neurite-like processes length was measured after treatment with OligoGM1 on bidimensional images acquired with 200X magnification with phase contrast microscopy and expressed as the ratio between neurite length and cell body diameter (Schengrund and Prouty 1988; Sato, Matsuda, and

Kitajima 2002; Chiricozzi et al. 2017). Five random fields were examined from each well, giving a total cell count of at least 200 cells per well.

4. Proteomic Analysis

N2a cells were incubated in the absence (control) or in the presence of 50 μM OligoGM1 for 24 hours. Then, medium was removed and cells were rinsed twice with 1 mM Na_3VO_4, 1 mM PMSF, 2% (v/v) aprotinin, and 1% (v/v) IP in cold PBS. Cells were scraped in the same buffer and centrifuged 800 × g for 5 minutes at 4°C. Pellets were immediately frozen by liquid nitrogen and conserved at -80°C before proteomic analysis by a shotgun label-free proteomic approach for the identification and quantification of expressed proteins. Proteins were subjected to reduction with 13 mM DTE (30 minutes at 55 °C) and alkylation with 26 mM iodoacetamide (30 minutes at 23 °C). Peptide digestion was conducted using sequence-grade trypsin (Roche) for 16 hours at 37 °C using a protein/trypsin ratio of 20:1 (Ragg et al. 2006). The proteolytic digested was desalted using Zip-Tip C18 (Millipore) before MS analysis. LC-ESI-MS/MS analysis was performed on a DionexUltiMate 3000 HPLC System with a PicoFritProteoPrep C18 column (200 mm, internal diameter of 75 μm) (New Objective, USA). Gradient: 2% ACN in 0.1% formic acid for 10 minutes, 2–4% ACN in 0.1% formic acid for 6 minutes, 4–30% ACN in 0.1% formic acid for 147 minutes, and 30–50% ACN in 0.1% formic for 3 minutes at a flow rate of 0.3 μL/minute. The eluate was electrosprayed into an LTQ OrbitrapVelos (Thermo Fisher Scientific, Bremen, Germany) through a Proxeon nanoelectrospray ion source (Thermo Fisher Scientific) as described from Dell'Orco (Dell'Orco et al. 2016). The LTQ-Orbitrap was operated in positive mode in data-dependent acquisition mode to automatically alternate between a full scan (m/z 350–2000) in the Orbitrap (at resolution 60,000, AGC target 1,000,000) and subsequent CID MS/MS in the linear ion trap of the 20 most intense peaks from full scan (normalized collision energy of 35%, 10-ms activation). Isolation window, 3 Da; unassigned charge states, rejected; charge state 1, rejected; charge states 2+, 3+, 4+, not rejected; dynamic exclusion enabled (60 seconds; exclusion list size, 200). Data acquisition was controlled by Xcalibur 2.0 and Tune 2.4 software (Thermo Fisher Scientific).

4.1 Data Analysis

MS spectra were searched against the mouse Uniprot sequence database (release 31.07.2017) by MaxQuant (version 1.3.0.5) (Coccetti et al. 2008). The following parameters were used: initial

maximum allowed mass deviation of 15 ppm for monoisotopic precursor ions and 0.5 Da for MS/MS peaks, trypsin enzyme specificity, a maximum of two missed cleavages, carbamidomethyl cysteine as fixed modification, N-terminal acetylation, methionine oxidation, asparagine/glutamine deamidation, and serine/threonine/tyrosine phosphorylation as variable modifications. False protein identification rate (5%) was estimated by searching MS/MS spectra against the corresponding reversed-sequence (decoy) database. The minimum required peptide length was set to 6 amino acids and the minimum number of unique peptide supporting protein identification was set to 1. Quantification in MaxQuant was performed using the built-in label-free quantification (LFQ) algorithms based on extracted ion intensity of precursor ions. Three biological replicates, each one replicated twice, were carried out for treated and control cells. Only proteins present and quantified in at least 2 out of 3 biological repeats were considered as positively identified in a sample and used for statistical analyses performed by the Perseus software module (version 1.5.5.3, www.biochem.mpg.de/mann/tools/). A t test (p value ≤ 0.01) was carried out to identify proteins differentially expressed among the two different conditions. Proteins were considered to be differentially expressed if they were present only in treated or control samples or showed significant t test difference. Bioinformatic analyses were carried out by Panther (version 10.0) and DAVID software (release 6.7) to cluster enriched annotation groups of molecular function, biological processes, pathways, and networks within the set of identified proteins. Functional grouping was based on p value ≤ 0.05 and at least two counts. The MS proteomics data have been deposited to the ProteomeXchange Consortium via the PRIDE partner repository with the data set identifier PXD011682.

5. Isolation of detergent-resistant membrane (DRM) fractions

To verify the presence of PKCα in the plasma membrane microdomain, N2a cells were incubated in the absence (control) or in the presence of 50 μM GM1 or OligoGM1 for 3 hours at 37°C. Detergent-resistant membrane (DRM) were prepared by ultracentrifugation on discontinuous sucrose gradient of cells subjected to homogenization with 1% Triton X-100, as previously described (Chiricozzi et al. 2015; Schiumarini et al. 2017). Briefly, cells were mechanically harvested in PBS 1X and centrifuged at 270 x g for 10 minutes at 4°C. Cell pellet was lysed in 1.2 mL of 1% Triton X-100 in TNEV buffer (10 mM TrisHCl pH 10, 150 mM NaCl, 5 mM EDTA pH 7.5) in the presence of 1 mM Na_3VO_4, 1mM PMSF, and 75 mU/mL aprotinin and homogenized for 11-folds with tight Dounce. Cell lysate (2 mg of cell protein/mL) was centrifuged for 5 minutes at 1300 x g at 4°C to remove

nuclei and cellular debris and obtain a post nuclear supernatant (PNS). A volume of 1 mL of PNS was mixed with an equal volume of 85% sucrose (w/v) in TNEV buffer containing 1 mM Na_3VO_4, placed at the bottom of a discontinuous sucrose gradient (30–5%), and centrifuged for 17 hours at 200,000 *x* g at 4°C. After ultracentrifugation, 12 fractions were collected starting from the top of the tube. The light scattering band, corresponding to the DRM fraction, was located at the interface between 5 and 30% sucrose corresponding to fractions 4-6. The entire procedure was performed at 0–4° C on ice immersion. Equal amounts from each fraction were diluted with Laemmli sample buffer (0.15 M DTT, 94 mM Tris-HCl, 3% SDS w/v, 0.015% blue bromophenol, v/v) without glycerol and used for protein analysis as reported in paragraph 7.

6. Protein determination

Protein concentration of samples was assessed using a DC™ protein assay kit according to manufacturer's instructions, using BSA as standard.

7. Protein analysis

N2a cells were washed with cold PBS containing 1 mM Na_3VO_4 and lysed by hot Laemmli sample buffer (0.15 M DTT, 94 mM Tris-HCl, 15% glycerol v/v, 3% SDS w/v, 0.015% blue bromophenol v/v). After the probe sonication (50 W, 30 kHz) and the boiling of the lysed samples for 5 minutes at 99°C, equal amounts of denatured proteins derived from treated and untreated cells were separated on 4-20% precast polyacrylamide gels, and transferred to PVDF membranes using the Trans -Blot® Turbo™ Transfer System (Bio -Rad).

PVDF membranes were blocked with 5% milk (w/v) in TBS-0.1% tween (v/v) at 23°C for 1 hour under gently shaking.

The presence of TrkA and p-TrkA was determined by using specific rabbit primary antibodies, diluted 1:1,000 in 5% BSA (w/v) in TBS-0.1% tween. PLCγ1, P-PLCγ1, PKCα, P-PKCα were detected by the specific mouse primary antibodies diluted 1:500 in 5% milk (w/v) in TBS-0.1% tween (v/v). Flotillin was detected by the specific rabbit primary antibody diluted 1:1,000 in 5% milk (w/v) in TBS-0.1% tween (v/v). α-tubulin and calnexin, used as loading controls, were detected by the specific mouse primary antibodies diluted 1:40,000 in 5% milk (w/v) in TBS-0.1% tween (v/v) and 1:1,000 in 5% BSA (w/v) in TBS-0.1% tween, respectively. The incubation was performed overnight at 4 °C under gently shaking.

Following, PVDF membranes were washed three times with TBS-0.1% tween. The reaction with secondary horseradish peroxidase (HRP)-conjugated antibodies was following performed at 23°C 1 hour in agitation. The data acquisition and analysis were performed using Alliance Uvitec (Eppendorf, Germany).

8. Calcium-imaging

N2a cells were plated at 7.5 x 10^3 / cm^2 on a 24 mm coverglass in complete DMEM HG medium. 48 hours after plating medium was removed and cells were rinsed three times with $HBSS^+$. After washing, cells were incubated with 2.5 μM Fluo-4 AM (494/506 nm) in $HBSS^+$ for 30 minutes at 23°C in the dark. Subsequently cells were washed three times with $HBSS^+$ to remove any dye that is not specifically associated with the cell surface and then incubated in $HBSS^+$. Fluorescent emission was examined by live cell analysis using Axio Observer (Zeiss Axio Observer.Z1 with Hamamatsu EMCCD 9100 - 02) with 400X magnification. The frames were acquired every 5 seconds for 20 minutes. After 3 minutes of acquisition, OligoGM1 50 μM solubilized in $HBSS^+$ was administered to the cells and after 15 minutes the Ca^{2+} ionophore A23187 (2 μM) in $HBSS^+$ was added to the cells. Control cells were subjected to the same experimental conditions but $HBSS^+$ was administer instead of OligoGM1. Only ionophore responsive cells were analysed. At least 6 cells for field were quantified. The fluorescence for each acquisition (F) was related to the basal fluorescence (Fmin) according to the following formula:

$$\frac{F - Fmin}{Fmin}$$

To evaluate the involvement of TrkA receptor in the induction of Ca^{2+} influx by the OligoGM1, the TrkA inhibitor (120 nM) was added to the growth medium 30 minutes before the incubation with Fluo-4. After 30 minutes, cells were washed three times with $HBSS^+$ and then incubated with Fluo-4 AM in $HBSS^+$ containing 120 nM TrkA inhibitor for 30 minutes at 23°C in the dark. Subsequently, cells were washed three times with $HBSS^+$ and incubated in $HBSS^+$ with 120 nM TrkA inhibitor.
To inhibit the IP_3-receptors, xestospongin C (2.5 μM) was administered together with Fluo-4 for 30 minutes. After washing with $HBSS^+$, xestospongin C was added again to working solution and left for the entire duration of the experiment.

9. Statistical analysis

Data are expressed as mean ± SEM. The analysis was performed with Prism software (GraphPad Software, Inc. La Jolla, CA, USA). The normality distribution was verified using Kolmogorov–Smirnov, D' Agostino & Pearson and Shapiro-Wilk tests; in case of a non-Gaussian distribution of data, non-parametric tests were used as indicated in the legend of the figures. A p-value < 0.05 was considered significant.

10. Other analytical methods

NMR spectra were recorded with a Bruker AVANCE-500 spectrometer at a sample temperature of 298 K. NMR spectra were recorded in CDCl3 or CD3OD and calibrate using the TMS signal as internal reference. Mass spectrometric analysis were performed in positive or negative ESI-MS. MS spectra were recorded on a Thermo Quest Finningan LCQTM DECA ion trap mass spectrometer, equipped with a Finnigan ESI interface; data were processed by Finnigan Xcalibur software system. All reactions were monitored by TLC on silica gel 60 plates (Merck).

Results

1. Proteomic Profile of OligoGM1-Treated Cells

It has been reported that the oligosaccharide chain of ganglioside GM1 (OligoGM1) is responsible for the neurotrophic and neuroprotective functions of GM1 through the interaction with the extracellular domain of TrkA receptor (Chiricozzi et al. 2017; Chiricozzi, Biase, et al. 2019). In order to investigate which other biochemical pathways, in addition to TrkA-MAPK cascade activation, are prompted by OligoGM1 in modulating neuritogenic, neurotrophic and neuroprotective phenomena, we performed a proteomic analysis of N2a cells treated with 50 μM OligoGM1 for 24 hours (Chiricozzi, Maggioni, et al. 2019)

Proteins were identified by a shotgun proteomic approach, using label free quantification for determine the relative quantity of their expression levels. The proteomic analysis led to the identification of 3166 proteins expressed in treated cells and 3132 in control cells with Pearson's correlation of 0.94, suggesting that the two data sets are very similar in terms of protein composition (Fig. R1a). As shown in the Venn diagram (Fig. R1b), 2842 proteins are commonly expressed in control and in OligoGM1-treated cells and among these, 23 proteins are upregulated (Table 1, Appendix I) and 47 downregulated (Table 2, Appendix I) in OligoGM1-treated cells in comparison to controls. Finally 350 (Table 3, Appendix I) and 324 (Table 4, Appendix I) proteins are expressed exclusively in control cells and in OligoGM1-treated cells respectively (Chiricozzi, Maggioni, et al. 2019).

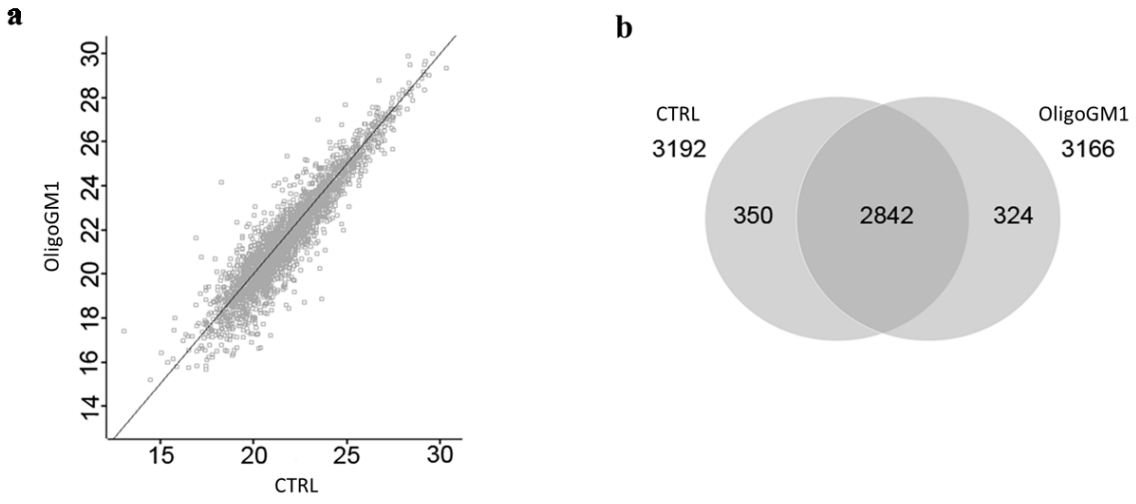

Figure R1: proteomic characterization of OligoGM1-treated cells and control cells. **a.** Scatter plot of the proteome of N2a cells treated (OligoGM1) and untreated (CTRL) with OligoGM1. Pearson's correlation coefficient R = 0.94. **b.** Venn diagram showing the proteins identified in at least 2/3 replicates. Proteins common to both data sets were considered for differential expression.

In order to further elaborate the effect of OligoGM1, we focused our attention on the proteins exclusively expressed in OligoGM1-treated cells. By using the software DAVID, OligoGM1-only proteins were grouped on the base of biological properties and molecular functions (Chiricozzi, Maggioni, et al. 2019). This analysis (p value ≤ 0.05, at least 2 counts) showed that there is a significant enrichment of gene ontology terms related to endocytic trafficking, ribosome biogenesis, regulation of transcription, regulation of cell cycle, mitochondrion, fatty acid metabolism, and cell adhesion (Table 5, Appendix I).

Importantly, the DAVID analysis highlighted that a large portion of proteins exclusively expressed in OligoGM1-treated cells are involved in neuronal differentiation and neurite extension, confirming the biochemical data (Chiricozzi et al. 2017).

Additionally, this bioinformatic analysis brought out the specific expression of a gene set involved in the modulation of Ca^{2+} homeostasis in OligoGM1-treated cells (Table R1) (Lunghi et al. 2020). Since Ca^{2+} regulates the neuronal differentiation process among others, it was possible to think that the neuritogenic effect promoted by the administration of OligoGM1 could be linked to the modulation of cellular Ca^{2+} flows. In fact, Ca^{2+} ions are necessary for the function of some of proteins involved in the processes of differentiation, emphasizing the importance of calcium signalling. Among these proteins, we found the cadherins (PCDHB6, PCDH11X, FAT1, CDHR1, PCDH15, RET), Ca^{2+}-dependent cell-adhesion proteins that play an essential role for cell polarization, cell migration and cell-cell contact (Suzuki and Takeichi 2008; Seong, Yuan, and Arikkath 2015).

Ca^{2+} ions are also involved in organelles transport, endocytic trafficking and in the polymerization/depolymerization and enzymatic degradation of many different cytoskeletal components, all necessary for the differentiation process. Among the proteins identified upon OligoGM1 treatment, Intersectin1 (ITSN-1) is a Ca^{2+}-dependent adapter protein that provides a link between the endocytic membrane traffic and the actin assembly machinery and is involved in brain development, in the positive regulation of dendritic spine development and in membrane organization (Jakob et al. 2017; Herrero-Garcia and O'Bryan 2017). Nidogen-1 (NID1) is a glycoprotein widely distributed in the extracellular matrix and tightly associated with laminin and collagen IV. It probably has a role in cell-extracellular matrix interactions, in nerve development, and in promoting nerve fibre growth during regeneration after injury (Lee et al. 2009). Protein-arginine deiminase 6 (PADI6) is a Ca^{2+}-dependent enzyme involved in cytoskeleton organization (Kan et al. 2011). Neuronal calcium sensor 1 (NCS1) is a neuronal Ca^{2+} sensor, involved in long-term synaptic plasticity and in neuronal differentiation through inhibition of the activity of N-type voltage-gated Ca^{2+} channel (Hui et al. 2007).

Ca^{2+} signalling also plays an important role in gene expression. Among proteins expressed only in treated cells, Ca^{2+}-dependent transcriptional regulators are also included: striatin-3 (STRN3) binds calmodulin in a Ca^{2+}-dependent manner and can positively or negatively regulate gene transcription (Chen et al. 2014; Petta et al. 2017). Serine/threonine-protein phosphatase 2B catalytic subunit alpha and gamma isoforms (PPP3CA/PPP3CC) are Ca^{2+}-dependent, calmodulin-stimulated proteins phosphatases, which play an essential role in the transduction of intracellular Ca^{2+}-mediated signals (Kilka et al. 2009). In response to increased Ca^{2+} levels, they regulate NFAT-mediated transcription by dephosphorylating NFAT and promoting its nuclear translocation. Calcineurin-NFAT signalling pathway is important in axonal growth and guidance during development (Nguyen and Di Giovanni 2008). They also dephosphorylate and inactivate transcription factor ELK1 that plays important roles in long-term memory formation, drug addiction, Alzheimer's disease, and depression (Besnard et al. 2011). Finally, helicase SRCAP (SRCAP) acts as a coactivator for CREB-mediated transcription, which is induced by increased intracellular Ca^{2+} level (Monroy et al. 2001).

Table R1 Calcium dependent proteins exclusively expressed by OligoGM1-trated cells (Lunghi et al. 2020).

Majority protein IDs	Protein names	Gene names
P35546	Proto-oncogene tyrosine-protein kinase receptor Ret	Ret
A0A0A6YX01	Protocadherin beta-6	Pcdhb6
E9Q622	Protocadherin 11 X-linked	Pcdh11x
A0A1L1SQU7	FAT atypical cadherin 1	Fat1
Q8VHP6	Cadherin-related family member 1	Cdhr1
Q99PJ1	Protocadherin-15	Pcdh15
F8WJ23	Hornerin	Hrnr
Q91ZZ3	Beta-synuclein	Sncb
Q8BNY6	Neuronal calcium sensor 1	Ncs1
P10493	Nidogen-1	Nid1
E9Q0N0	Intersectin-1	Itsn1
B2RPV6	Multimerin-1	Mmrn1
Q8C845	EF-hand domain-containing protein D2	Efhd2
Q8K3V4	Protein-arginine deiminase type-6	Padi6
Q704Y3	Transient receptor potential cation channel subfamily V member 1	Trpv1
Q9WTR1	Transient receptor potential cation channel subfamily V member 2	Trpv2
B2RQS1	Striatin-3	Strn3
V9GXI9	Striatin-4	Strn4
P48455	Serine/threonine-protein phosphatase 2B catalytic subunit gamma isoform	Ppp3cc
P63328	Serine/threonine-protein phosphatase 2B catalytic subunit alpha isoform	Ppp3ca
A0A087WQ44	Snf2-related CREBBP activator protein	Srcap
Q9QVP9	Protein-tyrosine kinase 2-beta	Ptk2b

2. OligoGM1 modulation of intracellular calcium level

Since GM1 has been shown to be a valid modulator of Ca^{2+} flux (Ledeen and Wu 2015) and since the proteomic analysis suggests that OligoGM1 could be the GM1 portion involved also in the modulation of this process, we decided to verify possible changes of intracellular calcium level upon OligoGM1 administration.

To do that, we performed calcium-imaging experiments on N2a cells using Fluo-4 probe, an indicator that allows measuring Ca^{2+} concentration inside living cells. The binding of Fluo-4 to Ca^{2+} results in increased fluorescence excitation at 488 nm and consequently higher fluorescence signal levels (Lunghi et al. 2020).

As detailed described in Methods section, cells plated on a cover glass were incubated at 23°C with 2.5 μM Fluo-4 AM in $HBSS^{+}$ for 30 minutes and, after washing, cells were examined at the Widefields Zeiss Axio Observer.Z1. The frames were acquired every 5 seconds for 20 minutes. After the first 3 minutes of basal acquisition, $HBSS^{+}$ without (CTRL) or with the addition of 50 μM OligoGM1 was administered to the cells. As positive control, to confirm the cellular responsiveness to the stimuli, Ca^{2+} ionophore A23187 (2 μM) was added to the cells after 15 minutes. Only ionophore responsive cells were analysed. The fluorescence for each acquisition was related to the fluorescence of the basal condition.

Video cutouts representing some of the acquired fields are shown in figure R2a.

Importantly we find out that the administration of OligoGM1 to undifferentiated N2a cells induces a significant Ca^{2+} influx, starting from 5 minutes from OligoGM1 administration as shown in the graph reported in figure R2b. On the contrary, no increase in fluorescence is observed in control cells.

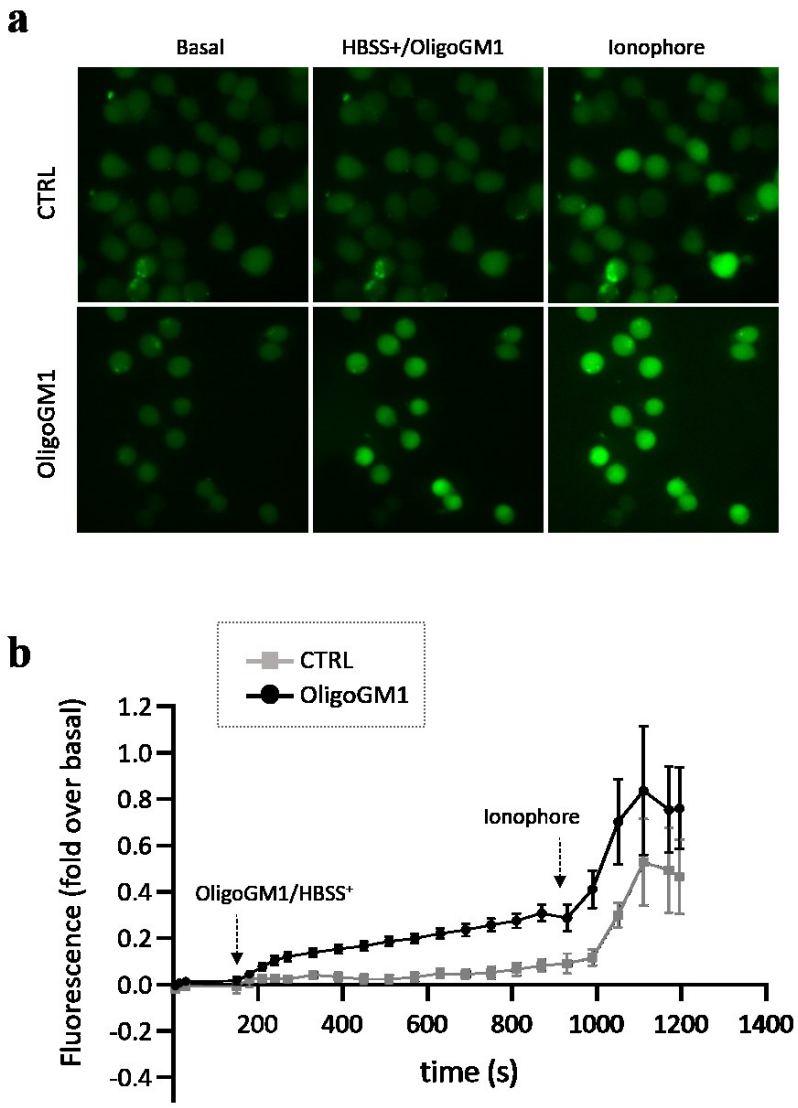

Figure R2: OligoGM1 modulation of intracellular calcium level. Intracellular Ca^{2+} level of N2a cells untreated (CTRL) or treated with OligoGM1 was analysed by single-cell based measuring of the variation of the emission fluorescence intensity of the internalized Fluo-4 probe. The frames were acquired every 5 seconds for 20 minutes with Widefields Zeiss Axio Observer.Z1 with a 400X magnification. After 3 minutes of basal acquisition, $HBSS^+$ alone (CTRL) or added with OligoGM1 for a final concentration of 50 µM was administered to the cells and, after 15 minutes, 2 µM Ca^{2+} ionophore A23187 was added. Only ionophore responsive cells were analysed. **a.** Representative frames of basal condition, cell response to OligoGM1/$HBSS^+$ and after ionopohore administration; **b.** Green fluorescence quantification. For each cell, the fluorescence of each frame (F) was related to the basal fluorescence (Fmin) (F-Fmin/Fmin). At least 6 cells were analyzed for each experiment. Results are expressed as the mean ± SEM of fluorescence intensity changes of at least three independent experiments experiments (OligoGM1 *p = 0.0258 vs. basal, one-way ANOVA, n = 11; OligoGM1 ** vs. CTRL, two-way ANOVA; CTRL no significant (NS) vs. basal, one-way ANOVA, n = 5).

3. TrkA as the mediator of OligoGM1 induction of calcium influx

In primary neurons, as well as in N2a neuroblastoma line, the OligoGM1 is not internalized by the cells, so its effects could be probably due to an action at the plasma membrane level (Chiricozzi et al. 2017). Furthermore, taking into account the reported effect prompted by GM1 on TrkA mediated neuronal differentiation (Farooqui et al. 1997; Singleton et al. 2000; Duchemin et al. 2002; Da Silva et al. 2005; Mocchetti 2005; Zakharova et al. 2014) and considering the recent results in N2a cells and primary neurons, where OligoGM1 was found to increase TrkA phosphorylation (Chiricozzi et al. 2017; Chiricozzi, Biase, et al. 2019; Di Biase et al. 2020), we investigated if also Ca^{2+} flow modulation could be a molecular event downstream of TrkA activation induced by OligoGM1.

To evaluate the involvement of TrkA receptor, we repeated the calcium-imaging experiment in the presence of a cell-permeable, reversible, potent, and highly selective TrkA inhibitor, able to significantly reduce the TrkA autophosphorylation at tyrosine 490 (Wood et al. 2004; Chiricozzi et al. 2017).

As shown in figure R3, the specific TrkA activation induced by 50 μM OligoGM1 after 5 and 30 minutes was prevented by the addition of TrkA inhibitor (figure R3) (Lunghi et al. 2020)

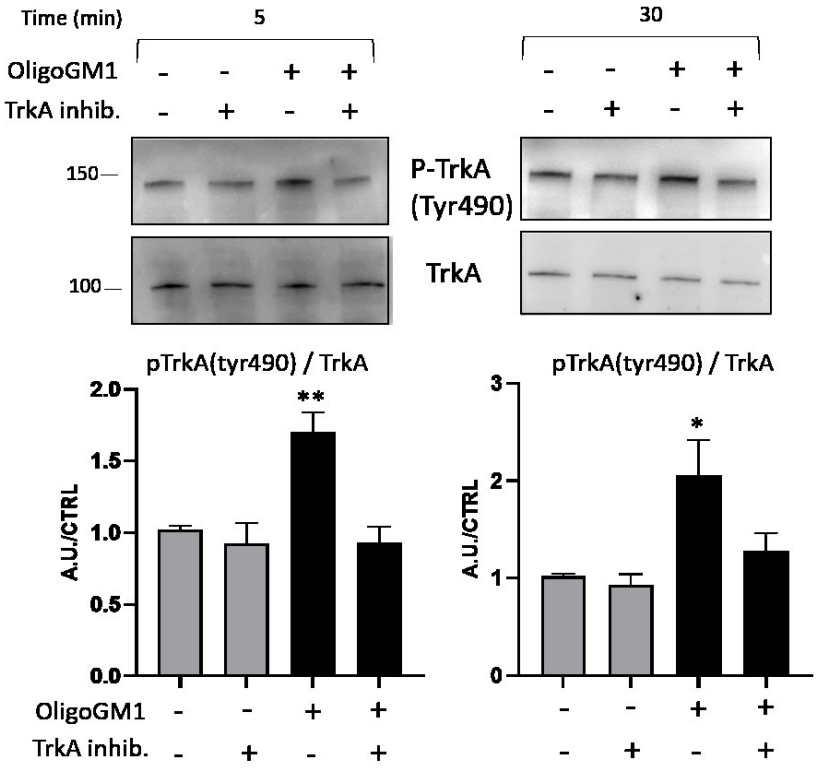

Figure R3: Effect of TrkA receptor inhibitor on TrkA autophosforilation. The TrkA receptor inhibitor (120 nM) was added to the N2a cells one hour before the administration of 50 μM OligoGM1. Expression of TrkA and phosphorylated TrkA (tyrosine 490, Tyr490) was evaluated 5 and 30 minutes after OligoGM1 treatment by western blot using specific antibodies and revealed by enhanced chemiluminescence. Top: immunoblotting images are shown. Bottom: Semiquantitative analysis of phosphorylated TrkA related to total level of TrkA. Data are expressed as fold increase over control of the mean SEM from three different experiments (*$p < 0.05$, **$p < 0.005$, two-way ANOVA, $n = 3$).

For calcium-imaging experiment, the TrkA-inhibitor (120 nM) was added to the culture medium for 30 minutes before Fluo-4 administration and left for the duration of the experiment as reported in the Methods section. The calcium-imaging representative frames and the graph reported in figure R4 clearly show that in presence of the TrkA inhibitor there is no significant increase of the fluorescence signal, as for the control condition, suggesting that the opening of the cell Ca^{2+} channels and the Ca^{2+} influx following OligoGM1 administration is mediated by the activation of TrkA receptor (Lunghi et al. 2020).

.

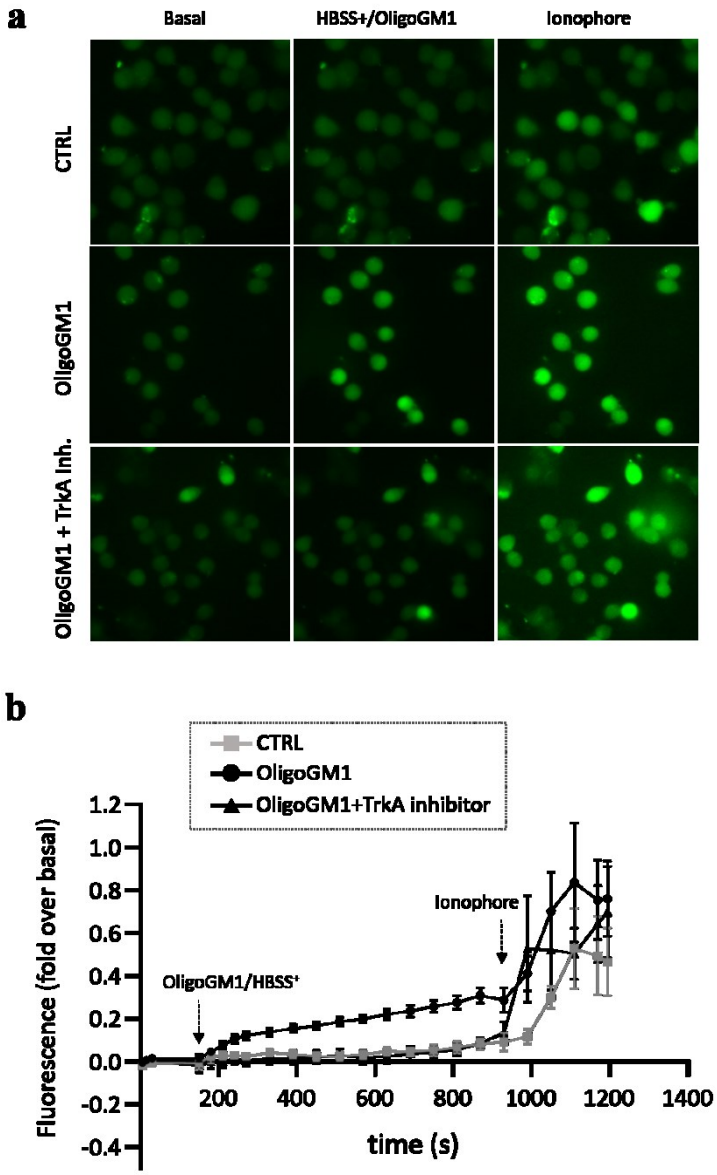

Figure R4: OligoGM1 calcium modulation depends on TrkA activation. Intracellular Ca^{2+} level of N2a cells untreated or treated with OligoGM1 (50 µM) was analysed by the single-cell measuring of the green fluorescence emission intensity of internalized Fluo-4 (2.5 µM). The frames were acquired every 5 seconds for 20 minutes with Widefields Zeiss Axio Observer.Z1 (400X magnification). The TrkA inhibitor (120 nM) was added to the culture medium 30 minutes before Fluo-4 administration and left for the duration of the experiment. After 3 minutes of basal acquisition, $HBSS^+$ alone (CTRL) or supplemented with OligoGM1 (50 µM) was administered to the cells and after 15 minutes the calcium ionophore A23187 (2 µM) was added. Only ionophore responsive cells were analysed. **a.** Representative frames of basal condition, cell response to OligoGM1/$HBSS^+$ and after ionophore administration. **b.** Green fluorescence quantification. For each cell, the fluorescence of each frame (F) was related to the basal fluorescence (Fmin) (F-Fmin/Fmin). At least 6 cells were analyzed for each experiment. Results are expressed as the mean ± SEM of fluorescence intensity changes of at least three independent experiments (OligoGM1 *p = 0.0258 vs. basal, one-way ANOVA, *n* = 11; OligoGM1 ** vs. CTRL, two-way ANOVA; OligoGM1 + TrkA inhibitor NS vs. basal, one-way ANOVA, *n* = 5; OligoGM1 + TrkA inhibitor NS vs. CTRL, two-way ANOVA).

4. Identification of the cellular pathways involved in OligoGM1-mediated calcium influx

To biochemically characterize the effect of OligoGM1 on Ca^{2+} flux in N2a cells following TrkA activation, we investigated the involvement of PLCγ and PKC. It is reported that the activation of TrkA receptor can trigger the phosphorylation of PLCγ that converts phosphatidylinositol 4,5-bisphosphate (PIP_2) to inositol 1,4,5-trisphosphate (IP_3) and diacyglycerol (DAG), which in turn activates PKC, finally leading to an increase in the intracellular Ca^{2+} (Huang and Reichardt 2003).
To unveil if OligoGM1 administration could lead to the increase of intracellular Ca^{2+} through this cellular pathway, we performed an immunoblotting analysis evaluating the phosphorylation status of the TrkA receptor, PLCγ1 and PKCα on N2a cells after 5 minutes, 30 minutes, and 1 hour following OligoGM1 administration (50 μM). As shown in figure R5 we found that 5 minutes after OligoGM1 administration there is an activation of TrkA receptor, confirming what we previously found (Chiricozzi et al. 2017). The TrkA activation is followed by an enhanced activation of PLCγ1 starting from 5 minutes after OligoGM1 administration and by a hyperphosphorylation of PKCα, which is a priming event that enables its catalytic activation, after 1 hour (Fig. R5) (Lunghi et al. 2020).

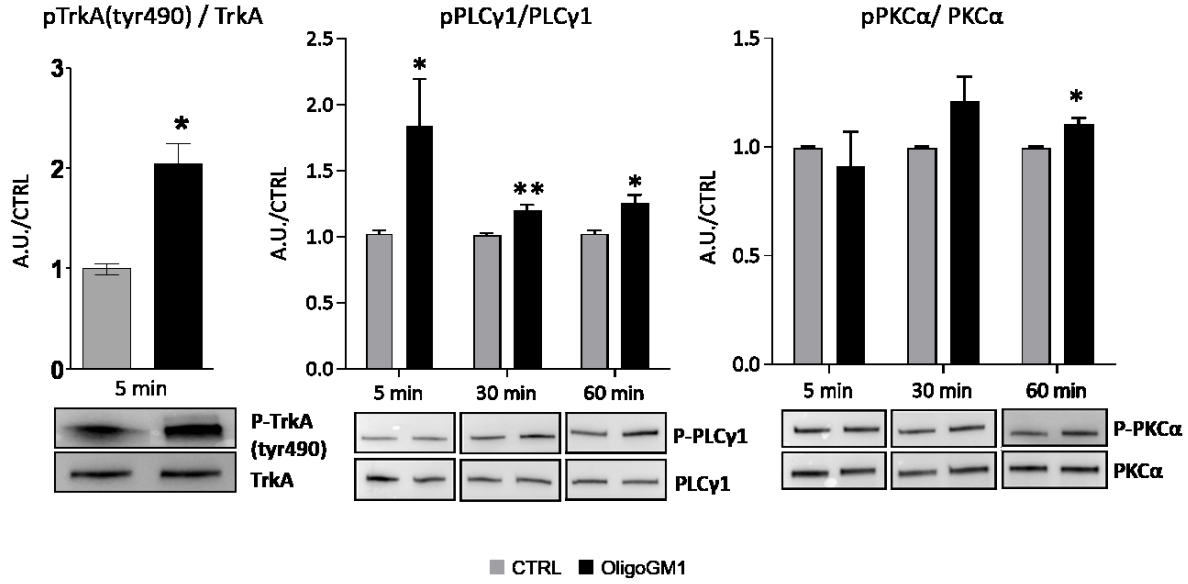

Figure R5: OligoGM1 effect on TrkA-PLC-PKC pathway. N2a were cultured in the absence (CTRL) or in the presence of 50 μM OligoGM1. Expression of TrkA, pTrkA (Tyr490), PLCγ1, pPLCγ1, PKCα and pPKCα was evaluated 5 minutes, 30 minutes and 1 hour after OligoGM1 treatment by western blot using specific antibodies and revealed by enhanced chemiluminescence. Top: semi-quantitative analysis of signals of phosphorylated TrkA, PLCγ1 and PKCα related to signals of total TrkA, PLCγ1 and PKCα, respectively. Bottom: representative immunoblotting images. Data are expressed as mean ± SEM of the fold increase over control from at least three experiments (*$p < 0.05$, **$p < 0.005$, Student's t-test, $n = 3$-5).

Although the phosphorylation is a key event for the catalytic activity of PKC, it is known that its activation depends on its translocation to the plasma membrane (Freeley, Kelleher, and Long 2011; Igumenova 2015).

Therefore, we verified whether the administration of OligoGM1 was followed by an enrichment of PKC in lipid rafts.

Given their particular composition, lipid rafts are insoluble in 1% Triton-X 100 detergent and can be isolated by flotation in a sucrose density gradient where they distribute in fractions 4 to 6 of the gradient (Simons and Sampaio 2011; Chiricozzi et al. 2015). For this reason, these fractions are defined as detergent resistant membrane (DRM). The last fractions, 10 to 12, defined as high density fractions (HD), contain all the other membranes solubilized by the detergent and the soluble proteins.

After 3 hours from OligoGM1 administration, N2a cells were lysed and centrifuged to obtain the post nuclear supernatant (PNS). The PNS was loaded on a discontinuous sucrose gradient and ultra-centrifuged at 200,000 *x* g for 17 hours and 12 fractions were collected from the top of the tube. As control we used N2a cells not treated with OligoGM1.

To examine the distribution of PKCα on the membrane fractions, we performed immunoblotting analysis as shown in figure R6. We pointed out an enrichment of PKCα in DRM fractions in the condition of treatment with OligoGM1 (Lunghi et al. 2020).

These events could be responsible for the opening of Ca^{2+} channels on both plasma membrane and intracellular storages (i.e. endoplasmic reticulum), resulting in an increase of intracellular Ca^{2+}.

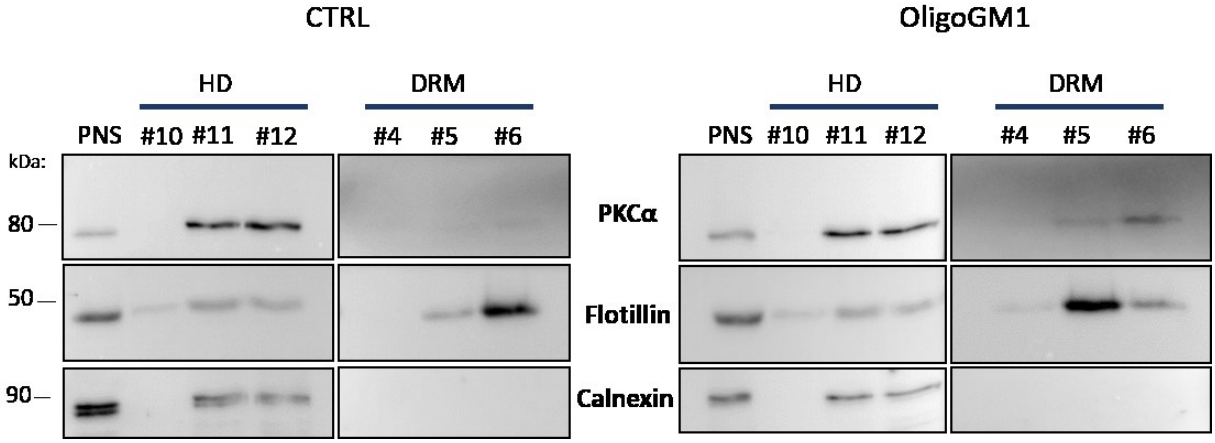

Figure R6: PKCα translocation in lipid rafts microdomains upon OligoGM1 treatment. N2a cells were incubated in the absence (CTRL), or in the presence of 50 μM OligoGM1 for 3 hours at 37°C. Cells were subsequently subjected to sucrose gradient ultracentrifugation to prepare plasma membrane microdomains. Twelve fractions were collected from the top of the tube, with fractions 4-6 corresponding to the detergent resistant membrane (DRM) fractions and fractions 10-12 corresponding to high density (HD) fractions. Expression of PKCα, Flotillin (DRM marker) and Calnexin (HD marker) was evaluated by western blot using specific antibodies and revealed by enhanced chemiluminescence. Images are representative of three independent cell culture preparations (*n* = 3).

To disclose if the intracellular Ca^{2+} increased after OligoGM1 administration derives from the extracellular environment through the plasma membrane Ca^{2+} channels or from the intracellular storages, the calcium-imaging experiment was performed in the presence of Xestospongin C, a selective, reversible and potent inhibitor of IP_3 receptors on endoplasmic reticulum (Gafni et al. 1997). The Xestospongin C (2.5 μM) was added to the cells together with Fluo-4 for 30 minutes before starting the acquisitions and left for the entire duration of the experiment. The calcium-imaging representative frames and the relative graph shown in figure R7 (panel a and b) demonstrate that in the presence of the IP_3 receptors inhibitor the cytoplasmic Ca^{2+} influx following OligoGM1 administration is reduced but is not completely abolished, suggesting that both plasma membrane and intracellular channels may be modulated by OligoGM1 administration (Lunghi et al. 2020).

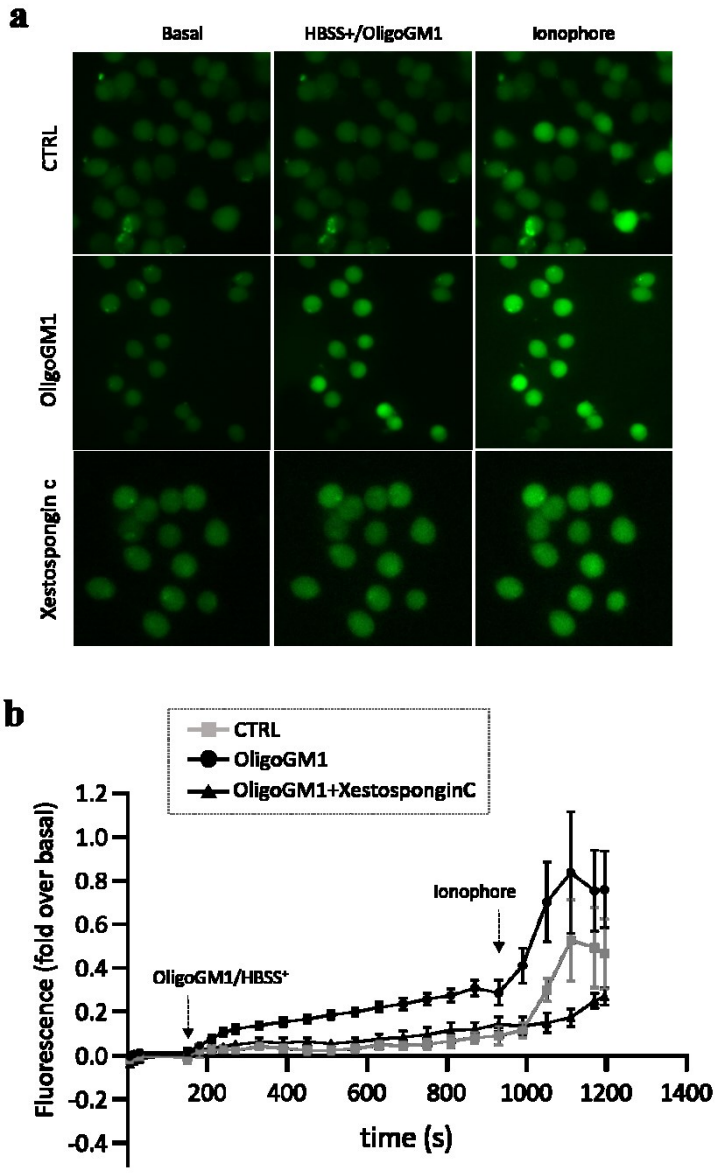

Figure R7: OligoGM1-modulated Ca^{2+} derives from both the extracellular environment and the intracellular storages. Intracellular Ca^{2+} level of N2a cells untreated (CTRL) or treated with 50 µM OligoGM1 was analysed by single-cell based measuring of the green fluorescence emission intensity variation of internalized Fluo-4 (2.5 µM). The frames were acquired every 5 seconds for 20 minutes with Widefields Zeiss Axio Observer.Z1 (400X magnification). The IP3 receptor inhibitor, Xestospongin C (2.5 µM) was added to the cells together with Fluo-4 for 30 minutes before starting the acquisitions and left for the entire duration of the experiment. After 3 minutes of basal acquisition, $HBSS^+$ alone (CTRL) or added with OligoGM1 50µM was administered to the cells and after 15 minutes the Ca^{2+} ionophore A23187 (2 µM) was added. Only ionophore responsive cells were analysed. **a.** Representative frames of basal condition, cell response to OligoGM1/$HBSS^+$ and after ionophore administration. **b.** Green fluorescence quantification. For each cell, the fluorescence of each frame (F) was related to the basal fluorescence (Fmin) (F-Fmin/Fmin). At least 6 cells were analyzed for each experiment. Results are expressed as the mean ± SEM of fluorescence intensity of at least three independent experiments (OligoGM1 * $p = 0.0258$ vs. basal, one-way ANOVA, $n = 11$; OligoGM1 ** vs. CTRL, two-way ANOVA; OligoGM1 + Xestospongin C $p = 0.0389$ vs. basal, one-way ANOVA, $n = 5$; OligoGM1 + Xestospongin C NS vs. CTRL, two-way ANOVA).

5. Calcium influence on OligoGM1-dependent neuritogenesis

It has been known for long time that exogenously administered GM1 and its endogenous increase induces the differentiation of murine neuroblastoma cells as well as the maturation state of primary neurons (Ledeen and Wu 2015; Schengrund 2015). Importantly, the GM1 mediated neurite outgrowth is known to be strictly dependent on calcium influx (Masco, Van de Walle, and Spiegel 1991; Fang et al. 2000; Wu and Ledeen 1994).

It has recently been observed that the administration of the oligosaccharide component alone induces the same neuritogenic effect, demonstrating that GM1 sugar is responsible for this outcome (Chiricozzi et al. 2017; Di Biase et al. 2020). Thus, we decided to investigate if also the neuronal differentiation mediated by OligoGM1 may depend on Ca^{2+} signaling.

To investigate this, 50 μM OligoGM1 was administered to N2a cells in the presence or absence of subtoxic concentrations of extracellular (EGTA, 100 μM) or intracellular (BAPTA-AM, 1 μM) Ca^{2+} chelators for 24 hours (Wie et al. 2001; Spoerri, Dozier, and Roisen 1990).

As highlighted in the images reported in figure R8a, the presence of both extracellular and intracellular Ca^{2+} chelators abolishes the neurite sprouting induced by OligoGM1 after 24 hours. The neurite extensions, observed after 24 hours of treatment with OligoGM1, were also quantified by measuring the ratio between the length of neurites and the diameter of the cell body (Schengrund and Prouty 1988; Sato, Matsuda, and Kitajima 2002; Chiricozzi et al. 2017). As it emerges from the graph in figure R8b, the length of the neuritis in cells incubated with OligoGM1 resulted at least two fold higher compared to the control cells but equalized the control condition when Ca^{2+} chelators was administered in combination with OligoGM1 (Lunghi et al. 2020).

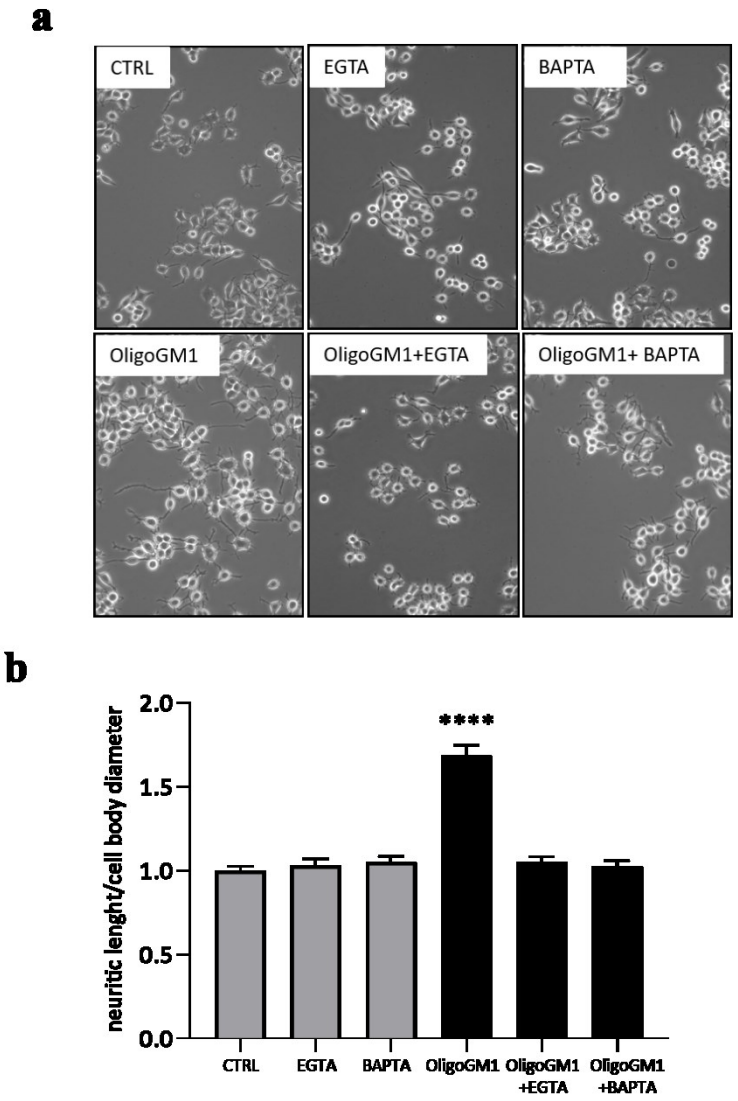

Figure R8: Morphological outcomes of N2a cells treated with 50 µM OligoGM1 in presence or absence of EGTA (100 µM) or BAPTA-AM (1 µM) for 24 hours. a. Cells were observed by phase contrast microscopy with 200X magnification. Images are representative of 3 independent experiments (n = 3). **b.** Evaluation of neurite sprouting and elongation in N2a cells. Neurite extensions were evaluated as the ratio between process length and cell body diameter. The bars show the mean values ± SEM from 3 different experiments (n = 3, OligoGM1 **** $p < 0.0001$ vs CTRL, OligoGM1 + EGTA, OligoGM1 + BAPTA, non-parametric one-way ANOVA).

This result suggests that, as already reported for GM1 (Ledeen and Wu 2015), the increase of intracellular Ca^{2+} is responsible of OligoGM1-mediated neuronal differentiation.

Discussion

GM1 ganglioside has been considered as a master regulator of the nervous system in light of its essential role in neuronal differentiation, protection and restoration (Schengrund 2015; Ledeen and Wu 2015; Aureli et al. 2016; Chiricozzi et al. 2020). GM1 trophic effects are determined by the cooperation with several modulators expressed on the plasma membrane, and particularly the specific interaction with neurotrophin receptors belonging to the Trk family, which seems to be fundamental for neuronal survival, differentiation and protection (Mutoh et al. 1995; Rabin and Mocchetti 1995; Ledeen and Wu 2015).

Despite the long-standing research on the GM1 functions in relation to differentiating and protective actions, the fine molecular mechanism still has some shadows. In fact, any endogenous increase of GM1 at the cell surface modifies the entire ganglioside metabolic processes, i.e. ganglioside membrane half-life, ganglioside intracellular trafficking and ganglioside lysosomal catabolism. On the other hand, the administered exogenous ganglioside in part modifies the ganglioside membrane content, and in part reaches the cytosol and the lysosomes where its catabolic fragments are then recycled for the biosynthesis of all sphingolipids.

An important information, which has not been fully investigated until 2017, bring us back to 1988 when Shengrund and Prouty observed that the GM1 oligosaccharide promoted the neuritogenesis process of neuroblastoma cells (Schengrund and Prouty 1988). This suggested that GM1 exerts its bioactive features through the hydrophilic head, which, protruding in the extracellular environment, could act at cell surface level through the interaction with plasma membrane proteins. This pioneering hypothesis was confirmed in 2017, when it was observed that within the entire molecule, the oligosaccharide chain β-Gal-(1-3)-β-GalNAc-(1-4)-[α-Neu5Ac-(2-3)]-β-Gal-(1-4)-β-Glc (OligoGM1) represents, alone, the bioactive component of GM1 ganglioside (Chiricozzi et al. 2017). Following its isolation from parental compound, the GM1 oligosaccharide was added to the culture medium of N2a neuroblastoma cells and was observed to induce the process of neuritogenesis as equimolar concentration of GM1 did (Chiricozzi et al. 2017), confirming the Shengrund's findings. These results were subsequently translated in a more physiological context by using primary cultures of murine granule cerebellar neurons (GCN) (Di Biase et al. 2020). According to this study, OligoGM1 administered to GCN enhanced neuron clustering, neurite sprouting and networking, thus confirming the specific role of the oligosaccharide chain in the processes of neuronal differentiation and maturation, known to be regulated by the entire GM1.

Additionally, the OligoGM1 was found to induce protection from MPTP neurotoxicity in N2a neuroblastoma cells (Chiricozzi, Maggioni, et al. 2019).

Both in neuroblastoma cells and in primary cerebellar neurons, the exogenous administered GM1 oligosaccharide was found to be mostly associated with the plasma membrane, indicating that it

remains in the extracellular environment without being internalized by the cells (Chiricozzi et al. 2017; Di Biase et al. 2020). This finding suggested that the OligoGM1 acts at plasma membrane level, probably interacting with some membrane receptors.

In accordance, it has been demonstrated that OligoGM1, similarly to the entire GM1, exerts its effect by enhancing the phosphorylation of the TrkA receptor on the tyrosine 490, followed by the increase in ERK1/2 phosphorylation (Chiricozzi et al. 2017; Di Biase et al. 2020; Chiricozzi, Biase, et al. 2019). More detailed *in silico* studies and experiments employing photoactivable analogues highlighted that OligoGM1 directly binds to extracellular domain of the nerve growth factor (NGF) specific receptor TrkA, stabilizing the NGF-TrkA complex. In fact, when OligoGM1 binds the complex, the binding free energy is reduced from -7 kcal/mol to approximately -11.5 kcal/mol, thus acting as a bridge able to increase and stabilize the TrkA-NGF molecular interactions (Chiricozzi et al. 2017).

It has been reported that the interaction of GM1 with TrkA is followed by changes in cellular Ca^{2+} level, accomplished through the modulation of Ca^{2+} influx channels and Ca^{2+} exchange proteins. GM1-induced Ca^{2+} influx was found to involve the voltage-dependent T type channels (Wu and Ledeen 1991) and TRPC5, which activation was triggered by GM1 crosslinking (Wu et al. 2007), while Ca^{2+} efflux from cytoplasm was found to be modulated through GM1 regulation of NCX (Xie et al. 2002).

Therefore, here, we examine the hypothesis that the GM1 oligosaccharide could be responsible for the modulation of cellular Ca^{2+} flow attributed to the ganglioside using mouse neuroblastoma cells, N2a, as experimental model.

To do that, we first investigated the landscape of events that follows the interaction between the OligoGM1 and TrkA receptor at the cell surface, by a proteomic analysis on N2a cells treated with 50 μM OligoGM1 for 24 hours.

Comparing the protein patterns of OligoGM1 treated cells and control cells (untreated), we found a differential expression of a specific gene set (Table 1 and 2 in Appendix I section) and, importantly, 324 proteins exclusively expressed in cells treated with the OligoGM1 (Table 4 in Appendix I section), possibly as a consequence of the downstream molecular cascade promoted by TrkA activation (Chiricozzi, Maggioni, et al. 2019). The analysis of OligoGM1-only proteins based on biological properties and molecular functions using the software DAVID, showed that a large portion of proteins exclusively expressed in OligoGM1-treated cells is involved in neuronal differentiation and neurite extension (Chiricozzi, Maggioni, et al. 2019).

The activity of many of these proteins (Table R1) depends on the presence of Ca^{2+} ions (Lunghi et al. 2020), suggesting that the modulation of Ca^{2+} homeostasis could be a fundamental mechanism for OligoGM1-mediated neuritogenic effect, as reported for GM1 (Wu et al. 1998).

Indeed, the administration of 50 μM OligoGM1 to undifferentiated N2a is capable of inducing a significant Ca^{2+} intake starting from 5 minutes after GM1 oligosaccharide application as shown by calcium-imaging experiments (figure R2) (Lunghi et al. 2020). This latency time suggests that the entry of Ca^{2+} is not due to the direct interaction of OligoGM1 with Ca^{2+} channels on the plasma membrane neither with intracellular channels, since it was demonstrated in primary neurons (Di Biase et al. 2020) and in N2a cells (Chiricozzi et al. 2017) that the OligoGM1 is not internalized by the cells but rather it could be a result of the activation of plasma membrane receptors and downstream signaling pathways.

As already mentioned, OligoGM1 carries out its neurotrophic and neuroprotective activities interacting with the TrkA receptor on plasma membrane, allowing the stabilization of TrkA-NGF complex and consequently the receptor activation. Thus to verify a direct participation of TrkA in the OligoGM1 mediated Ca^{2+} modulation, the calcium-imaging experiment was performed in the presence of the TrkA inhibitor. Importantly, in this case no Ca^{2+} influx was observed following OligoGM1 administration, indicating that TrkA receptor activation is an upstream event modulating Ca^{2+} flux upon OligoGM1 addition (figure R4) (Lunghi et al. 2020). Accordingly, OligoGM1 was found to elicit TrkA activation 5 minutes following its cellular administration (figure R5).

Subsequently, we studied in more detail the involvement of the transducing factors downstream of the signalling cascade initiated by the OligoGM1-TrkA interaction, responsible for mobilizing intracellular Ca^{2+} flows. TrkA is recognized to phosphorylate and activate the phospholipase PLCγ, which is involved in the Ca^{2+} regulation (Lunghi et al. 2020).

PLCγ is a membrane-associated enzyme that cleaves PIP_2 into DAG and IP_3 (Fukami et al. 2010). The two products of the PLC catalysed reaction, DAG and IP_3, are important second messengers that control diverse cellular processes (Carpenter and Ji 1999). These products propagate and regulate cellular signalling via Ca^{2+} mobilization and activation of protein kinases, such as PKC, and ion channels (Fukami et al. 2010). When PIP_2 is cleaved, DAG remains bound to the membrane, whereas IP_3 is released as a soluble molecule into the cytosol. IP_3 diffuses through the cytosol to bind IP_3 receptors, IP_3-sensitive intracellular Ca^{2+} channels predominately located in the membrane of the endoplasmic reticulum, regulating the Ca^{2+} flux from intracellular stores to the cytosol (Alzayady et al. 2016). This finally leads to an increase of the cytosolic Ca^{2+} concentration, causing the activation of intracellular signalling cascade. The other product, DAG, also triggers extracellular Ca^{2+} influx independently from IP_3 activity by directing plasma membrane TRP channels (Hofmann et al. 1999)

and activating PKC (Huang 1989). The function of the PKC is regulated by two mechanisms. First, the enzyme is rendered catalytically competent by phosphorylation that correctly aligns residues for the catalysis. Second, the increase in the intracellular Ca^{2+} concentration triggers the membrane translocation of PKC and its association with DAG at the plasma membrane microdomains stimulating the enzyme activity (Freeley, Kelleher, and Long 2011; Huang 1989; Igumenova 2015). Additionally, PKC phosphorylates other molecules, modulating several cellular events: activation of PKC in the nervous system has been involved in the regulation of ion channels activity, neurotransmitter release, growth, differentiation, and neural plasticity (Huang 1989).

For this reason, we evaluated the possible activation of PLCγ and PKC following the administration of OligoGM1. In agreement, by immunoblotting analysis we found a hyperphosphorylation of PLCγ occurring 30 minutes upon OligoGM1 administration (figure R5), followed by a hyperphosphorylation of PKC after 1 hour from OligoGM1 administration and by its enrichment in lipid rafts, confirming its activation (figures R5 and R6) (Lunghi et al. 2020).

To examine the involvement of IP_3 in mobilizing Ca^{2+} from the intracellular stores, we performed calcium-imaging experiments by administering OligoGM1 together with the selective IP_3 inhibitor, Xestospongin C. Interestingly, in this case a 50% lower increase in intracellular Ca^{2+} level was recorded (figure R7) (Lunghi et al. 2020). However the Ca^{2+} influx was not completely abolished, suggesting the involvement of Ca^{2+} channels of both the intracellular and plasma membranes in the modulation of the cytoplasmic Ca^{2+} levels, which are activated by IP_3 and DAG respectively.

The increase of cytosolic Ca^{2+} is essential for the morphological difference accompanying the neurodifferentiative properties prompted by GM1 (Wu et al. 1998; Kappagantula et al. 2014; Wu et al. 1996; Milani et al. 1992; Bachis et al. 2002; Sokolova, Rychkova, and Avrova 2014; Park et al. 2016). Thus, we finally proved that GM1 neuritogenic effect is mediated by an increase in intracellular Ca^{2+} following the OligoGM1-TrkA interaction at the plasma membrane level, leading to the recruitment and activation of multiple intracellular players eventually promoting neurite sprouting. In fact, we observed that OligoGM1 is not able to induce neurite emission in N2a cells if Ca^{2+} ions, both intracellular and extracellular, are chelated (figure R8) (Lunghi et al. 2020). Since Ca^{2+} is fundamental for many essential cell functions, for this experiment sub-toxic low concentrations of Ca^{2+} chelators have been used.

This result suggests that the modulation of cytosolic Ca^{2+} levels by OligoGM1 is fundamental for the execution of its neurodifferentiative properties, and that the amount of intracellular Ca^{2+} must exceed a certain threshold to trigger the neurite extension in N2a cells induced by OligoGM1.

The present work demonstrates that the GM1 oligosaccharide is responsible on its own also for the GM1 modulation of Ca^{2+} homeostasis in relation to its neuroproperties. As summarized in the diagram of figure D1, OligoGM1 exogenously administered to N2a cells acts at the cell surface activating the TrkA receptor that in turn triggers the activation of PLCγ1. This leads to the formation of second messengers IP_3 and DAG and to the activation of PKC that are responsible together for the increase of cytosolic Ca^{2+} ions deriving from the extracellular environment and from intracellular stores. The regulation of Ca^{2+} signaling is a fundamental molecular mechanism at the base of OligoGM1 neurogenic action, partially revealing the mechanism of action of the oligosaccharide chain of ganglioside GM1.

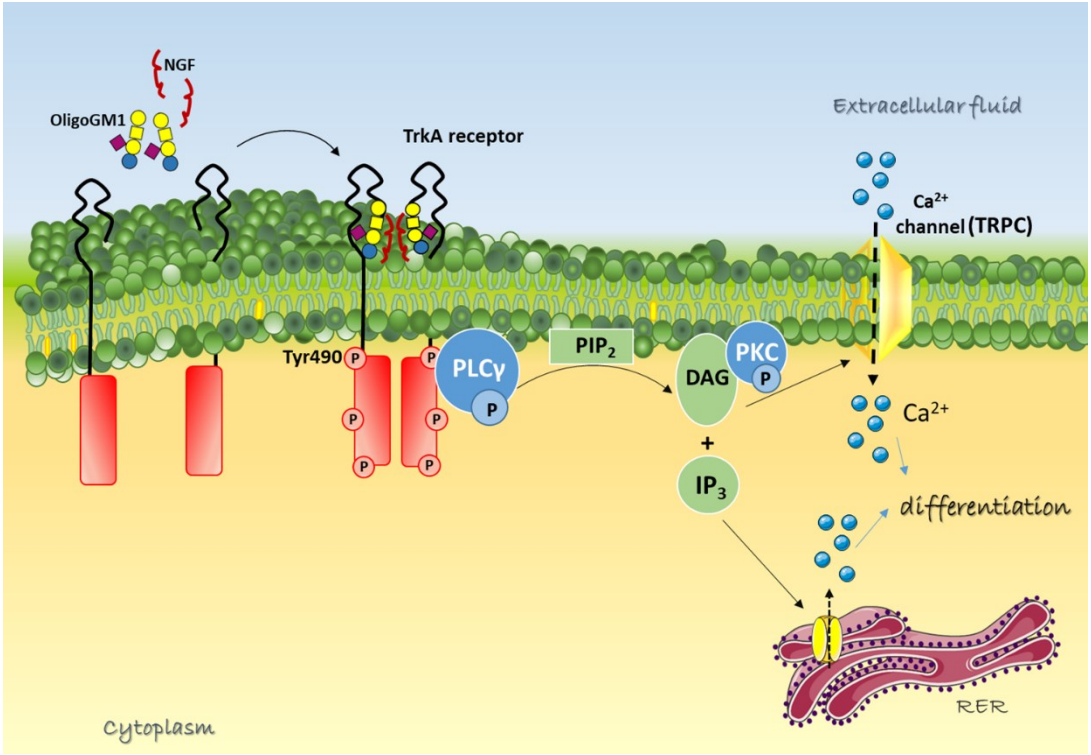

Figure D1. Schematic representation of molecular mechanism underling GM1-oligosaccharide neurotrophic function. OligoGM1 enhances the activation of TrkA-MAPK pathway, which could be associated to an increased activation of PLCγ1, leading to the formation of second messengers DAG and IP_3. These events bring to the opening of Ca^{2+} channels on the plasma membrane and on endoplasmic reticulum, leading to an increase of cytosolic Ca^{2+} responsible for N2a differentiation. PLCγ, phospholipase C gamma; PIP2, phosphatidylinositol 4,5-bisphosphate; DAG, diacyl-glycerol; IP_3, inositol 1,4,5-trisphosphate; PKC, protein kinase C; TRPC, transient receptor potential channel; RER, rough endoplasmic reticulum.

Appendix I

Table 1 List of the proteins upregulated in OligoGM1 vs CONTROL N2a cells

Student's T-test OLIGO vs CTRL	Majority protein IDs	Protein names	Gene names
0,273	Q99LC8	Translation initiation factor eIF-2B subunit alpha	Eif2b1
0,310	Q8VE73	Cullin-7	Cul7
0,451	Q9EQI8	39S ribosomal protein L46, mitochondrial	Mrpl46
0,485	G5E8R4	Serine/threonine-protein phosphatase 6 regulatory subunit 3	Ppp6r3
0,550	Q60790	Ras GTPase-activating protein 3	Rasa3
0,657	E9Q0S6	Tensin 1	Tns1
0,700	Q3U9G9	Lamin-B receptor	Lbr
0,716	A0A087WPU8	Transcription factor Dp-2	Tfdp2
0,724	P53994	Ras-related protein Rab-2A	Rab2a
0,868	Q6PDI6	Protein FAM63B	Fam63b
0,886	Q64378	Peptidyl-prolyl cis-trans isomerase FKBP5	Fkbp5
0,972	P36552	Coproporphyrinogen-III oxidase, mitochondrial	Cpox
1,024	P62827	GTP-binding nuclear protein Ran	Ran
1,114	P61514	60S ribosomal protein L37a	Rpl37a
1,212	A0A0U1RNX8	B-cell CLL/lymphoma 7 protein family member C	Bcl7c
1,253	Q6GQT9	Nodal modulator 1	Nomo1
1,334	P29595	NEDD8	Nedd8
1,353	P62281	40S ribosomal protein S11	Rps11
1,534	P35550	rRNA 2-O-methyltransferase fibrillarin	Fbl
1,609	P62889	60S ribosomal protein L30	Rpl30
1,777	Q6PIU9	Uncharacterized protein FLJ45252 homolog	N/A
1,844	Q8CBB6	Histone H2B	Gm13646
2,892	P02301	Histone H3.3C	H3f3c

Table 2 List of the proteins downregulated in OligoGM1 vs CONTROL N2a cells

Student's T-test OLIGO vs CTRL	Majority protein IDs	Protein names	Gene names
-3,980	E9QMV2	Costars family protein ABRACL	Abracl
-3,193	Q9CQR2	40S ribosomal protein S21	Rps21
-3,074	Q9CQZ1	Heat shock factor-binding protein 1	Hsbp1
-3,009	Q3TIX9	U4/U6.U5 tri-snRNP-associated protein 2	Usp39
-2,893	P60710	Actin, cytoplasmic 1	Actb
-2,473	Q9CWZ3	RNA-binding protein 8A	Rbm8a
-2,461	P55105	Bone morphogenetic protein 8B	Bmp8b
-2,128	Q6ZWV3	60S ribosomal protein L10	Rpl10
-2,003	A6H6S0	Hect domain and RLD 3	Herc3
-1,924	Q8BJA2	Solute carrier family 41 member 1	Slc41a1
-1,913	Q9ESW4	Acylglycerol kinase, mitochondrial	Agk
-1,757	Q8VIB5	BarH-like 2 homeobox protein	Barhl2
-1,682	P11157	Ribonucleoside-diphosphate reductase subunit M2	Rrm2
-1,620	A0A0R4J0I2	Transmembrane protein 132D	Tmem132d
-1,528	E9Q2G7	Solute carrier family 2, facilitated glucose transporter member 3	Slc2a3
-1,520	P54103	DnaJ homolog subfamily C member 2	Dnajc2
-1,495	P58389	Serine/threonine-protein phosphatase 2A activator	Ppp2r4
-1,405	E9PW66	Nucleosome assembly protein 1-like 1	Nap1l1
-1,380	Q9Z1R2	Large proline-rich protein BAG6	Bag6
-1,374	Q8VEH6	COBW domain-containing protein 1	Cbwd1
-1,374	Q9CWF2	Tubulin beta-2B chain	Tubb2b
-1,314	Q924T2	28S ribosomal protein S2, mitochondrial	Mrps2
-1,312	Q9QZD8	Mitochondrial dicarboxylate carrier	Slc25a10
-1,235	G3X8Y3	N-alpha-acetyltransferase 15, NatA auxiliary subunit	Naa15
-1,211	A0A0R4J008	Histone deacetylase 2	Hdac2
-1,148	E9Q6G4	ATP-binding cassette sub-family A member 7	Abca7
-1,137	Q9Z2Q6	Septin-5	Sept5
-1,125	Q4FE56	Ubiquitin carboxyl-terminal hydrolase	Usp9x
-1,093	Q0VBD2	Protein MCM10 homolog	Mcm10
-1,063	Q6P1J1	Crmp1 protein	Crmp1
-0,962	A2AFI6	Transmembrane 9 superfamily member	Gm364
-0,908	D3Z780	Translation initiation factor eIF-2B subunit delta	Eif2b4
-0,878	E9QM77	Ataxin-2	Atxn2
-0,840	Q9R0P4	Small acidic protein	Smap
-0,831	Q9Z0V8	Mitochondrial import inner membrane translocase subunit Tim17-A	Timm17a
-0,815	I1E4X0	Disks large-associated protein 4	Dlgap4
-0,801	E9Q1P8	Interferon regulatory factor 2-binding protein 2	Irf2bp2
-0,751	Q62465	Synaptic vesicle membrane protein VAT-1 homolog	Vat1
-0,708	E9Q616	AHNAK nucleoprotein (desmoyokin)	Ahnak
-0,703	Q9CQ22	Ragulator complex protein LAMTOR1	Lamtor1
-0,644	P56480	ATP synthase subunit beta, mitochondrial	Atp5b
-0,641	Q9DAP7	Histone chaperone ASF1B	Asf1b
-0,509	Q9Z1N5	Spliceosome RNA helicase Ddx39b	Ddx39b

-0,448	Q8BTW3	Exosome complex component MTR3	Exosc6
-0,387	Q6PAM1	Alpha-taxilin	Txlna
-0,368	Q9WTM5	RuvB-like 2	Ruvbl2
-0,316	Q3UHJ0	AP2-associated protein kinase 1	Aak1

Table 3 List of the proteins only expressed in CONTROL cells in the comparison OligoGM1 vs CONTROL N2a cells

Majority protein IDs	Protein names	Gene names
A0A075B5Z7	T cell receptor alpha variable 5-1	Trav5-1
A0A087WPL5	ATP-dependent RNA helicase A	Dhx9
Q9CWU4	UPF0690 protein C1orf52 homolog	2410004B18Rik
Q8BXK8	Arf-GAP with GTPase, ANK repeat and PH domain-containing protein 1	Agap1
A0A087WRX8	Serine/arginine repetitive matrix protein 2	Srrm2
Q60862	Origin recognition complex subunit 2	Orc2
A0A087WSQ9	Zinc finger CCHC domain-containing protein 2	Zcchc2
G3UZM1	Probable JmjC domain-containing histone demethylation protein 2C	Jmjd1c
B7ZCJ1	Rho GTPase-activating protein 21	Arhgap21
A0A0A6YVS2	Transmembrane and coiled-coil domain-containing protein 1	Tmco1
Q64735	Complement component receptor 1-like protein	Cr1l
A0A0A6YVW3	Immunoglobulin heavy variable V1-23	Ighv1-23
A0A0A6YXG9	Uridine-cytidine kinase 2	Uck2
A0A0B4J1J5	Immunoglobulin heavy variable V9-3	Ighv9-3
E9PZ43	Microtubule-associated protein	Mtap4
A0A0G2JEG1	Serine/arginine-rich-splicing factor 11	Srsf11
O54946	DnaJ homolog subfamily B member 6	Dnajb6
A0A0G2JFP4	Ferric-chelate reductase 1	FRRS1
Q8BXV2	BRI3-binding protein	Bri3bp
A0A0G2LB90	Tubulin polyglutamylase TTLL7	Ttll7
A0A0J9YTZ5	Protein FAM193A	Fam193a
O35427	DNA-directed RNA polymerase III subunit RPC9	Crcp
F7BJB9	MORC family CW-type zinc finger protein 3	Morc3
Q3UEZ8	Sodium/bile acid cotransporter 4	Slc10a4
Q4VC33	Macrophage erythroblast attacher	Maea
P17183	Gamma-enolase	Eno2
Q80V62	Fanconi anemia group D2 protein homolog	Fancd2
Q9CQR6	Serine/threonine-protein phosphatase 6 catalytic subunit	Ppp6c
A0A0N4SVR5	RasGEF domain family, member 1A	Rasgef1a
A0A0R4J023	Methylglutaconyl-CoA hydratase, mitochondrial	Auh
A0A0R4J0D1	Store-operated calcium entry-associated regulatory factor	Tmem66
A0A0R4J0H8	Fibronectin type III domain-containing protein 3B	Fndc3b
A0A0R4J0J4	Atypical chemokine receptor 1	Ackr1
A0A0R4J0P1	Isobutyryl-CoA dehydrogenase, mitochondrial	Acad8
A0A0R4J0T5	CUGBP Elav-like family member 1	Celf1
A0A0R4J1C6	Butyrophilin-like protein 10	Btnl10
A0A0R4J1K1	CCR4-NOT transcription complex subunit 4	Cnot4
Q9QZR5	Homeodomain-interacting protein kinase 2	Hipk2
A0A0R4J220	Atypical chemokine receptor 1	Kifc3
A0A0R4J259	Heterogeneous nuclear ribonucleoprotein Q	Syncrip

Q8BX09	Retinoblastoma-binding protein 5	Rbbp5
A0A0U1RNX4	Unconventional prefoldin RPB5 interactor	Uri1
A0A140LJ04	Zinc finger ZZ-type and EF-hand domain-containing protein 1	Zzef1
A0A140LJ70	Protein arginine N-methyltransferase 1	Prmt1
O55222	Integrin-linked protein kinase	Ilk
Q6PD31	Trafficking kinesin-binding protein 1	Trak1
Q3TIR3	Synembryn-A	Ric8a
G5E8I8	Calcium homeostasis endoplasmic reticulum protein	Cherp
E9PZW8	Unconventional myosin-IXb	Myo9b
O54833	Casein kinase II subunit alpha	Csnk2a2
Q7TR45	Olfactory receptor	Olfr1131
Q9WU63	Heme-binding protein 2	Hebp2
Q8R4S0	Protein phosphatase 1 regulatory subunit 14C	Ppp1r14c
A0A1L1SUG9	Cadherin EGF LAG seven-pass G-type receptor 3	Celsr3
Q4VBF2	R3H domain-containing protein 4	R3hdm4
K3W4Q9	Golgi-associated PDZ and coiled-coil motif-containing protein	Gopc
Q8VHR5	Transcriptional repressor p66-beta	Gatad2b
A2A432	Cullin-4B	Cul4b
P02535	Keratin, type I cytoskeletal 10	Krt10
A2A654	Bromodomain PHD finger transcription factor	Bptf
A2AE27	AMP deaminase 2	Ampd2
Q9D711	Pirin	Pir
A2AIR7	Voltage-dependent N-type calcium channel subunit alpha-1B	Cacna1b
A2AMD0	Predicted gene 12666	Gm12666
A2AML7	Zinc finger protein 352	Zfp352
Q8JZX4	Splicing factor 45	Rbm17
A2APR8	Mitotic checkpoint serine/threonine-protein kinase BUB1	Bub1
Q80TY0	Formin-binding protein 1	Fnbp1
A2ASI5	Sodium channel protein type 3 subunit alpha	Scn3a
A2AUD5	Tumor protein D54	Tpd52l2
A2AVR2	HEAT repeat-containing protein 8	Heatr8
A2AWI7	Endophilin-B2	Sh3glb2
Q9D868	Peptidyl-prolyl cis-trans isomerase H	Ppih
A3KFM7	Chromodomain-helicase-DNA-binding protein 6	Chd6
A4FUP9	Glycosyltransferase 1 domain-containing protein 1	Glt1d1
A6H630	UPF0364 protein C6orf211 homolog	Armt1
Q9D3L3	Synaptosomal-associated protein	Snap23
Q9WTT4	V-type proton ATPase subunit G 2	Atp6v1g2
B1AQW2	Microtubule-associated protein	Mapt
Q9QWI6	SRC kinase signaling inhibitor 1	Srcin1
B1AUN2	Eukaryotic translation initiation factor 2B, subunit 3	Eif2b3
B1AVB2	Scm polycomb group protein-like 2	Scml2
B1AZM2	Predicted gene 15091	Gm15091
O35317	Pre-B-cell leukemia transcription factor 3	Pbx3
B2M1R6	Heterogeneous nuclear ribonucleoprotein K	Hnrnpk
B2RXS4	Plexin-B2	Plxnb2

B7ZC40	Glutaredoxin-2, mitochondrial	Glrx2
P47934	Carnitine O-acetyltransferase	Crat
B8JJZ4	Zinc finger protein 808	Zfp808
G3UZF7	Centrosomal protein C10orf90 homolog	D7Ertd443e
P62843	40S ribosomal protein S15	Rps15
E9Q425	Tubulin polyglutamylase TTLL5	Ttll5
P17515	C-X-C motif chemokine 10	Cxcl10
Q9Z1M4	Ribosomal protein S6 kinase beta-2	Rps6kb2
D3YXS5	Kinesin-like protein KLP6	Klp6
D3YXW1	Protein LLP homolog	Llph
Q99MN9	Propionyl-CoA carboxylase beta chain, mitochondrial	Pccb
Q9D6K7	Tetratricopeptide repeat protein 33	Ttc33
D3Z2J4	AKT-interacting protein	Aktip
Q9WTZ1	RING-box protein 2	Rnf7
Q9CQB5	CDGSH iron-sulfur domain-containing protein 2	Cisd2
D3Z4U8	DDB1- and CUL4-associated factor 11	Dcaf11
D3Z6B7	DNA damage-regulated autophagy modulator protein 2	Dram2
D3Z7P4	Glutaminase kidney isoform, mitochondrial	Gls
P97785	GDNF family receptor alpha-1	Gfra1
Q8CIG9	F-box/LRR-repeat protein 8	Fbxl8
D6RJI8	TBC1 domain family member 13	Tbc1d13
Q5SUQ9	CST complex subunit CTC1	Ctc1
E0CXT7	Cleavage and polyadenylation specificity factor subunit 4	Cpsf4
E9PU87	Serine/threonine-protein kinase SIK3	Sik3
P70170	ATP-binding cassette sub-family C member 9	Abcc9
E9PUR1	Opticin	Optc
P48774	Glutathione S-transferase Mu 5	Gstm5
E9PVN6	Synaptojanin-2-binding protein	Gm20498
E9PVZ8	Golgi autoantigen, golgin subfamily b, macrogolgin 1	Golgb1
E9PWQ7	Zonadhesin	Zan
Q8CCB4	Vacuolar protein sorting-associated protein 53 homolog	Vps53
E9PXU1	Integrator complex subunit 6-like	Ddx26b
E9PYD5	Transcription elongation factor A protein 1	Tcea1
Q6NZN0	RNA-binding protein 26	Rbm26
E9Q430		Gm2832
O08532	Voltage-dependent calcium channel subunit alpha-2/delta-1	Cacna2d1
Q8R0F3	Sulfatase-modifying factor 1	Sumf1
E9Q2E4	HECT domain E3 ubiquitin protein ligase 4	Gm15800
E9Q2N4	Vomeronasal type-1 receptor	Vmn1r184
E9Q394	A-kinase anchor protein 13	Akap13
E9Q4K7	Kinesin family member 13B	Kif13b
E9Q4R1	Protein FAM102B	Fam102b
E9Q545	Olfactory receptor	Olfr552
E9Q5L3	Short/branched chain specific acyl-CoA dehydrogenase, mitochondrial	Acadsb
G5E8P0	Gamma-tubulin complex component 6	Tubgcp6
E9Q7E2	AT-rich interactive domain-containing protein 2	Arid2

Q3UQ84	Threonine--tRNA ligase, mitochondrial	Tars2
E9Q7P5	Olfactory receptor	Olfr640
E9Q9J4	Inositol hexakisphosphate and diphosphoinositol-pentakisphosphate kinase 2	Ppip5k2
Q6ZPL9	ATP-dependent RNA helicase DDX55	Ddx55
H3BJQ9	Homeobox protein cut-like 1	Cux1
F6QYZ5	Peptidase inhibitor 16	Pi16
F6S169	Tankyrase-2	Tnks2
O88384	Vesicle transport through interaction with t-SNAREs homolog 1B	Vti1b
Q810U5	Coiled-coil domain-containing protein 50	Ccdc50
Q6DFZ2	Nesprin-2	Syne2
F6XVH0	Predicted gene 12830	Gm12830
Q9CR21	Acyl carrier protein, mitochondrial	Ndufab1
F6ZGR6	RIKEN cDNA D430041D05 gene	D430041D05Rik
J3QPW1	Phosphatidylinositol transfer protein alpha isoform	Pitpna
Q69ZR2	E3 ubiquitin-protein ligase HECTD1	Hectd1
Q99N84	28S ribosomal protein S18b, mitochondrial	Mrps18b
P19426	Negative elongation factor E	Rdbp
Q80VJ2	Steroid receptor RNA activator 1	Sra1
G3X9H5	Huntingtin	Htt
G3X9Z8	Innate immunity activator protein	5730559C18Rik
G5E852	Tyrosine-protein kinase	Jak2
H3BLL4	Heterogeneous nuclear ribonucleoprotein K	Hnrnpk
Q60766	Immunity-related GTPase family M protein 1	Irgm1
K4DI67	Condensin-2 complex subunit D3	Ncapd3
K7N678	Olfactory receptor	Olfr893
M9MMK5	Olfactory receptor	Olfr329-ps
O08675	Proteinase-activated receptor 3	F2rl2
O35350	Calpain-1 catalytic subunit	Capn1
O54732	Matrix metalloproteinase-15	Mmp15
O54774	AP-3 complex subunit delta-1	Ap3d1
O70456	14-3-3 protein sigma	Sfn
P01649	Ig kappa chain V-V regions	
P01897	H-2 class I histocompatibility antigen, L-D alpha chain	H2-L
P01942	Hemoglobin subunit alpha	Hba
P02772	Alpha-fetoprotein	Afp
P08122	Collagen alpha-2(IV) chain	Col4a2
P10922	Histone H1.0	H1f0
P13542	Myosin-8	Myh8
P15533	Tripartite motif-containing protein 30A	Trim30a
P20060	Beta-hexosaminidase subunit beta	Hexb
P22437	Prostaglandin G/H synthase 1	Ptgs1
P31938	Dual specificity mitogen-activated protein kinase kinase 1	Map2k1
P35585	AP-1 complex subunit mu-1	Ap1m1
P42227	Signal transducer and activator of transcription 3	Stat3
P43247	DNA mismatch repair protein Msh2	Msh2
P48432	Transcription factor SOX-2	Sox2

P49586	Choline-phosphate cytidylyltransferase A	Pcyt1a
Q922U2	Keratin, type II cytoskeletal 5	Krt5
P51125	Calpastatin	Cast
P51807	Dynein light chain Tctex-type 1	Dynlt1
P51943	Cyclin-A2	Ccna2
P55200	Histone-lysine N-methyltransferase MLL	Mll
P57716	Nicastrin	Ncstn
P58058	NAD kinase	Nadk
P58871	182 kDa tankyrase-1-binding protein	Tnks1bp1
P59017	Bcl-2-like protein 13	Bcl2l13
P61967	AP-1 complex subunit sigma-1A	Ap1s1
P61971	Nuclear transport factor 2	Nutf2
P63147	Ubiquitin-conjugating enzyme E2 B	Ube2b
P70279	Surfeit locus protein 6	Surf6
P70333	Heterogeneous nuclear ribonucleoprotein H2	Hnrnph2
P70388	DNA repair protein RAD50	Rad50
P81117	Nucleobindin-2	Nucb2
Q6P4T3	Eyes absent homolog 3	Eya3
P97481	Endothelial PAS domain-containing protein 1	Epas1
Q0VBL3	RNA-binding protein 15	Rbm15
Q14AX6	Cyclin-dependent kinase 12	Cdk12
Q14CH7	Alanine--tRNA ligase, mitochondrial	Aars2
Q32KG4	Retrotransposon gag domain-containing protein 1	Rgag1
Q3TC93	HCLS1-binding protein 3	Hs1bp3
H9H9T1	Protein FAM107B	Fam107b
Q3TMP1	General transcription factor IIIC, polypeptide 3	Gtf3c3
Q3TTY0	Phospholipase B1, membrane-associated	Plb1
Q3TZR9	Cyclic AMP-dependent transcription factor ATF-7	Atf7
Q3U186	Probable arginine--tRNA ligase, mitochondrial	Rars2
Q3UHI4	Protein TMED8	Tmed8
Q6PDG5	SWI/SNF complex subunit SMARCC2	Smarcc2
Q3UM18	Large subunit GTPase 1 homolog	Lsg1
Q3UMR5	Calcium uniporter protein, mitochondrial	Mcu
Q3UMU9	Hepatoma-derived growth factor-related protein 2	Hdgfrp2
Q3USJ8	FCH and double SH3 domains protein 2	Fchsd2
Q64458	Cytochrome P450 2C29	Cyp2c29
Q3UWX6	RIKEN cDNA E330034G19 gene	E330034G19Rik
Q561M1	Acp1 protein	Acp1
Q68FF6	ARF GTPase-activating protein GIT1	Git1
Q5ND29	Rab-interacting lysosomal protein	Rilp
Q8BFY7	Protein FAM64A	Fam64a
Q5RJG1	Nucleolar protein 10	Nol10
Q99N89	39S ribosomal protein L43, mitochondrial	Mrpl43
Q5SSW2	Proteasome activator complex subunit 4	Psme4
Q7TNE3	Sperm-associated antigen 7	Spag7
Q60596	DNA repair protein XRCC1	Xrcc1

Q60778	NF-kappa-B inhibitor beta	Nfkbib
Q60886	Olfactory receptor 147	Olfr147
Q61025	Intraflagellar transport protein 20 homolog	Ift20
Q61048	WW domain-binding protein 4	Wbp4
Q61136	Serine/threonine-protein kinase PRP4 homolog	Prpf4b
Q61838	Alpha-2-macroglobulin	A2m
Q63886	UDP-glucuronosyltransferase 1-1	Ugt1a1
Q641P0	Actin-related protein 3B	Actr3b
Q64676	2-hydroxyacylsphingosine 1-beta-galactosyltransferase	Ugt8
Q6A037	NEDD4-binding protein 1	N4bp1
Q6A152	Cytochrome P450 4X1	Cyp4x1
Q6DID3	Protein SCAF8	Scaf8
Q6NV83	U2 snRNP-associated SURP motif-containing protein	U2surp
Q6NXJ0	Protein WWC2	Wwc2
Q6NZR5	Superkiller viralicidic activity 2-like (S. cerevisiae)	Skiv2l
Q6P1C6	Leucine-rich repeats and immunoglobulin-like domains protein 3	Lrig3
Q6P5E6	ADP-ribosylation factor-binding protein GGA2	Gga2
Q6P9J9	Anoctamin-6	Ano6
Q6PGC1	ATP-dependent RNA helicase Dhx29	Dhx29
Q6V4S5	Protein sidekick-2	Sdk2
Q6ZQ73	Cullin-associated NEDD8-dissociated protein 2	Cand2
Q7TMM9	Tubulin beta-2A chain	Tubb2a
Q7TPM6	Fibronectin type III and SPRY domain-containing protein 1	Fsd1
Q7TQA6	Taste receptor type 2 member 38	Tas2r38
Q7TQT7	Olfactory receptor	Olfr1371
Q7TQZ0	Olfactory receptor	Olfr32
Q7TR71	Olfactory receptor	Olfr1062
Q7TRI9	Olfactory receptor	Olfr129
Q80X59	Transmembrane and coiled-coil domain-containing protein 5B	Tmco5b
Q80X71	Transmembrane protein 106B	Tmem106b
Q80X98	DEAH (Asp-Glu-Ala-His) box polypeptide 38	Dhx38
Q80ZX2	Zfp790 protein	Zfp790
Q8BFQ4	WD repeat-containing protein 82	Wdr82
Q8BGD6	Putative sodium-coupled neutral amino acid transporter 9	Slc38a9
Q8BGR9	Ubiquitin-like domain-containing CTD phosphatase 1	Ublcp1
Q9EQ28	DNA polymerase delta subunit 3	Pold3
Q8BH79	Anoctamin-10	Ano10
Q8BHF7	CDP-diacylglycerol--glycerol-3-phosphate 3-phosphatidyltransferase, mitochondrial	Pgs1
Q8BJ03	Cytochrome c oxidase assembly protein COX15 homolog	Cox15
Q8BP48	Methionine aminopeptidase 1	Metap1
Q9CTN4	Rho-related BTB domain-containing protein 3	Rhobtb3
Q8BVG4	Dipeptidyl peptidase 9	Dpp9
Q8BYL4	Tyrosine--tRNA ligase, mitochondrial	Yars2
Q8C052	Microtubule-associated protein 1S	Map1s
Q8C0L8	Conserved oligomeric Golgi complex subunit 5	Cog5
Q8C263	Spindle and kinetochore-associated protein 3	Ska3

Q8C3Y4	Kinetochore-associated protein 1	Kntc1
Q8C9W3	A disintegrin and metalloproteinase with thrombospondin motifs 2	Adamts2
Q8CD10	EF-hand domain-containing family member A1	Efha1
Q8CD92	Tetratricopeptide repeat protein 27	Ttc27
Q8CDA1	Phosphatidylinositide phosphatase SAC2	Inpp5f
Q8CE46	Pseudouridylate synthase 7 homolog-like protein	Pus7l
Q8CEC6	Peptidylprolyl isomerase domain and WD repeat-containing protein 1	Ppwd1
Q8CI03	FLYWCH-type zinc finger-containing protein 1	Flywch1
Q8CI61	BAG family molecular chaperone regulator 4	Bag4
Q8CIL4	Uncharacterized protein C1orf131 homolog	
Q8CJ27	Abnormal spindle-like microcephaly-associated protein homolog	Aspm
Q8CJG0	Protein argonaute-2	Eif2c2
Q8K202	DNA-directed RNA polymerase I subunit RPA49	Polr1e
Q8K248	4-hydroxyphenylpyruvate dioxygenase-like protein	Hpdl
Q8K4P0	pre-mRNA 3 end processing protein WDR33	Wdr33
Q8R000	Organic solute transporter subunit alpha	Osta
Q8R080	G2 and S phase-expressed protein 1	Gtse1
Q8R0A0	General transcription factor IIF subunit 2	Gtf2f2
Q8R293	Vomeronasal type-1 receptor	Vmn1r73
Q8R322	Nucleoporin GLE1	Gle1
Q8R3H7	Heparan sulfate 2-O-sulfotransferase 1	Hs2st1
Q8R3K3	Pentatricopeptide repeat-containing protein 2	Ptcd2
Q8R3N6	THO complex subunit 1	Thoc1
Q8R480	Nuclear pore complex protein Nup85	Nup85
Q8R4H4	Carboxypeptidase A5	Cpa5
Q8R5A6	TBC1 domain family member 22A	Tbc1d22a
Q8VCV2	Protein NDRG3	Ndrg3
Q8VDK1	Nitrilase homolog 1	Nit1
Q8VED5	Keratin, type II cytoskeletal 79	Krt79
Q8VGW6	Olfactory receptor	Olfr124
Q8VHZ7	U3 small nucleolar ribonucleoprotein protein IMP4	Imp4
Q8VI47	Canalicular multispecific organic anion transporter 1	Abcc2
Q8VIH1	Homeobox protein NOBOX	Nobox
Q91UZ5	Inositol monophosphatase 2	Impa2
Q91WG2	Rab GTPase-binding effector protein 2	Rabep2
Q91XL3	UDP-glucuronic acid decarboxylase 1	Uxs1
Q920G5	Olfactory receptor	Olfr713
Q99J10	Cytoplasmic tRNA 2-thiolation protein 1	Ctu1
Q99L85	Dermal papilla-derived protein 6 homolog	Derp6
Q99LB2	Dehydrogenase/reductase SDR family member 4	Dhrs4
Q99NI3	General transcription factor II-I repeat domain-containing protein 2	Gtf2ird2
Q99P31	Hsp70-binding protein 1	Hspbp1
Q99PL6	UBX domain-containing protein 6	Ubxn6
Q9CQA6	Coiled-coil-helix-coiled-coil-helix domain-containing protein 1	Chchd1
Q9CQT7	Desumoylating isopeptidase 1	Pppde2
Q9CWE0	Protein FAM54B	Fam54b

Q9CZH7	Matrix-remodeling-associated protein 7	Mxra7
Q9D0N7	Chromatin assembly factor 1 subunit B	Chaf1b
Q9D1M4	Eukaryotic translation elongation factor 1 epsilon-1	Eef1e1
Q9D2F1	PRAME family member 12	Pramef12
Q9D2H8	Fibronectin type III domain-containing protein 8	Fndc8
Q9D2R8	28S ribosomal protein S33, mitochondrial	Mrps33
Q9D6X6	Serine protease 23	Prss23
Q9D771	Transmembrane protein 206	Tmem206
Q9D7A8	Armadillo repeat-containing protein 1	Armc1
Q9D9S2	Transmembrane protein 225	Tmem225
Q9DC33	High mobility group protein 20A	Hmg20a
Q9DC70	NADH dehydrogenase [ubiquinone] iron-sulfur protein 7, mitochondrial	Ndufs7
Q9DCC4	Pyrroline-5-carboxylate reductase 3	Pycrl
Q9EP97	Sentrin-specific protease 3	Senp3
Q9EPQ8	Transcription factor 20	Tcf20
Q9EQG9	Collagen type IV alpha-3-binding protein	Col4a3bp
Q9ER38	Torsin-3A	Tor3a
Q9ER81	Torsin-1A-interacting protein 2, isoform IFRG15	Tor1aip2
Q9ESN1	Double C2-like domain-containing protein gamma	Doc2g
Q9JKS4	LIM domain-binding protein 3	Ldb3
Q9JL35	High mobility group nucleosome-binding domain-containing protein 5	Hmgn5
Q9QWV9	Cyclin-T1	Ccnt1
Q9QXV1	Chromobox protein homolog 8	Cbx8
Q9QXW0	F-box/LRR-repeat protein 6	Fbxl6
Q9QYC1	Pecanex-like protein 1	Pcnx
Q9QYX7	Protein piccolo	Pclo
Q9QZI8	Serine incorporator 1	Serinc1
Q9WTP7	GTP:AMP phosphotransferase, mitochondrial	Ak3
Q9WUK4	Replication factor C subunit 2	Rfc2
Q9WUN2	Serine/threonine-protein kinase TBK1	Tbk1
Q9WVL0	Maleylacetoacetate isomerase	Gstz1
Q9Z2U2	Zinc finger protein 292	Zfp292
S4R1D6	H-2 class I histocompatibility antigen, TLA(B) alpha chain	H2-T3
Z4YKJ7	Excitatory amino acid transporter 5	Slc1a7

Table 4 List of the proteins expressed only in OligoGM1 cells in the comparison OligoGM1 vs CONTROL N2a cells

Majority protein IDs	Protein names	Gene names
A0A075B607	T cell receptor alpha variable 14-3	Trav14d-2
A0A075B6D5	Immunoglobulin kappa chain variable 19-93	Igkv19-93
A0A087WQ44	Snf2-related CREBBP activator protein	Srcap
Q5DTW7	Uncharacterized protein C12orf35 homolog	Kiaa1551
A0A087WR36	Vomeronasal type-1 receptor	Vmn1r90
A0A1L1SQU7	FAT atypical cadherin 1	Fat1
A0A0A0MQA5	Tubulin alpha-4A chain	Tuba4a
A0A0A0MQD1	Tudor domain-containing protein 7	Tdrd7
P09925	Surfeit locus protein 1	Surf1
Q3TRR0	Microtubule-associated protein 9	Map9
A0A0A6YVV8	Muscleblind-like protein 1	Mbnl1
Q8VBV3	Exosome complex component RRP4	Exosc2
Q99PJ1	Protocadherin-15	Pcdh15
A0A0A6YX01	Protocadherin beta-6	Pcdhb6
A0A0A6YY47	Neural cell adhesion molecule 1	Ncam1
A0A0B4J1I7	Immunoglobulin kappa variable 4-68	Igkv4-68
A0A0G2JDF6	RIKEN cDNA I830077J02 gene	I830077J02Rik
A0A0G2JDW9	Immunoglobulin kappa variable 4-62	Igkv4-62
A0A0G2JE49	Paired immunoglobulin-like type 2 receptor alpha	Pilra
A0A0G2JEK2	Cysteine-rich protein 1	Crip1
A0A0G2JEY5	Immunoglobulin kappa variable 4-81	
Q920L5	Elongation of very long chain fatty acids protein 6	Elovl6
A0A0G2JFV8	Polypyrimidine tract-binding protein 2	Ptbp2
Q5DW34	Histone-lysine N-methyltransferase EHMT1	Ehmt1
A0A0J9YUP9	Transcription factor 4	Tcf4
Q91YP3	Putative deoxyribose-phosphate aldolase	Dera
A0A1N9MDH9	Probable G-protein coupled receptor 19	Gpr19
B2RPV6	Multimerin-1	Mmrn1
Q91WI7	Integrin-alpha FG-GAP repeat-containing protein 2	Itfg2
F6V2U0	Type I inositol 3,4-bisphosphate 4-phosphatase	Inpp4a
A0A0R4J0U3	Period circadian protein homolog 2	Per2
A0A0R4J187	X-ray repair cross-complementing protein 6	Xrcc6
A0A0R4J1N7	Ankyrin-1	Ank1
Q8R2Q6	Tectonic-3	Tctn3
A0A0U1RPA0	Pleckstrin homology domain-containing family A member 7	Plekha7
Q8BMB0	Protein EMSY	Emsy
A0A0U1RQ37	Ubiquitin-conjugating enzyme E2 S	Ube2s
Q9Z179	SHC SH2 domain-binding protein 1	Shcbp1
E9QPQ8	39S ribosomal protein L48, mitochondrial	Mrpl48

Q571B6	WASP homolog-associated protein with actin, membranes and microtubules	Whamm
Q9CQG6	Transmembrane protein 147	Tmem147
A0A140LIT2	7-dehydrocholesterol reductase	Dhcr7
A0A140LIW7	Ankyrin-repeat and fibronectin type III domain-containing 1	Ankfn1
Q8CG73	Protein fantom	Rpgrip1l
Q9D6T0	Nitric oxide synthase-interacting protein	Nosip
Q8JZK6	MCG22896, isoform CRA_b	Trim61
A0A1D5RLF0	F-box and WD-40 domain protein 27	Fbxw27
A0A1D5RLL4	Transformation/transcription domain-associated protein	Trrap
F8WI85	Leucine-rich repeat-containing protein 36	Lrrc36
A0A1L1SRQ8	Olfactory receptor	Olfr251
Q91XE8	Transmembrane protein 205	Tmem205
Q9DCU6	39S ribosomal protein L4, mitochondrial	Mrpl4
A0A1L1SSZ5	Olfactory receptor 1248	Olfr1248
Q9D083	Kinetochore protein Spc24	Spc24
A0A1W2P7F9	MCG50764, isoform CRA_a	Btg1
Q9CWV7	Zinc finger SWIM domain-containing protein 1	Zswim1
Q3TB48	Transmembrane protein 104	Tmem104
Q9D7S1	Transmembrane protein 54	Tmem54
A2A9L3	Serine/threonine-protein kinase PDIK1L	Pdik1l
E9Q0J2	Ral GTPase-activating protein subunit beta	Ralgapb
A2ACM0	Regulatory-associated protein of mTOR	Rptor
Q9ER67	Maged2 protein	Maged2
A2AI92	Predicted gene 9112	Gm9112
Q6P2L7	Protein CASC4	Casc4
A2AT37	UPF2 regulator of nonsense transcripts homolog (Yeast)	Upf2
Q80YN3	Breast carcinoma-amplified sequence 1 homolog	Bcas1
A2AX52	Collagen alpha-4(VI) chain	Col6a4
A4QPD3	Proto-oncogene c-Rel	Rel
A6PWV5	AT-rich interactive domain-containing protein 3C	Arid3c
A7TZG3	Selection and upkeep of intraepithelial T-cells protein 9	Skint9
B2RQS1	Striatin-3	Strn3
B2RXC1	Trafficking protein particle complex subunit 11	Trappc11
Q8BXQ2	GPI transamidase component PIG-T	Pigt
J3QQ27	Coiled-coil domain-containing 191	2610015P09Rik
B8QI34	Liprin-alpha-2	Ppfia2
D3YU71	3 beta-hydroxysteroid dehydrogenase type 7	Hsd3b7
D3YUK0	Predicted gene 3259	Gm3259
D3YUP1	Histone-arginine methyltransferase CARM1	Carm1
Q3TQR0	Post-GPI attachment to proteins factor 2	Pgap2
Q99LG0	Ubiquitin carboxyl-terminal hydrolase 16	Usp16
P30285	Cyclin-dependent kinase 4	Cdk4
Q9JIY5	Serine protease HTRA2, mitochondrial	Htra2
D3YYL7	40S ribosomal protein S29	Gm10126
D3YZP5	Ras-related protein Rab-3A	Rab3a
D3Z0X5	Pleckstrin homology-like domain family B member 1	Phldb1

Q9DCL8	Protein phosphatase inhibitor 2	Ppp1r2
D3Z3G0	Uncharacterized protein C12orf56 homolog	D930020B18Rik
D3Z3S5	Predicted gene 4744	Gm4744
Q9CXK9	RNA-binding protein 33	Rbm33
D3Z6C4	Carbonyl reductase family member 4	Cbr4
Q9D8N6	Protein lin-37 homolog	Lin37
Q9Z120	tRNA (guanine-N(7)-)-methyltransferase	Mettl1
D6RFB0	Adhesion G protein-coupled receptor L3	Lphn3
E9Q2M9	WD repeat and FYVE domain-containing 4	Wdfy4
E9PXJ8	Vomeronasal 2, receptor 90	Vmn2r90
Q8C2B3	Histone deacetylase 7	Hdac7
Q9CQJ6	Density-regulated protein	Denr
E9Q0J5	Kinesin-like protein KIF21A	Kif21a
E9Q0N0	Intersectin-1	Itsn1
E9Q163	X-ray repair cross-complementing protein 6	Xrcc6
E9Q1P2	Olfactory receptor	Olfr288
A7RDN6	Renalase	Rnls
Q9QVP9	Protein-tyrosine kinase 2-beta	Ptk2b
Q8BMQ2	General transcription factor 3C polypeptide 4	Gtf3c4
E9Q5A3	Histone-lysine N-methyltransferase EHMT1	Ehmt1
E9Q622	Protocadherin 11 X-linked	Pcdh11x
Q6ZQE4	Transmembrane protein 194A	Tmem194a
E9Q7Q3	Tropomyosin alpha-3 chain	Tpm3
E9Q876	ATP-binding cassette, sub-family A (ABC1), member 12	Abca12
E9Q912	RAP1, GTP-GDP dissociation stimulator 1	Rap1gds1
E9Q9M1	Cytosolic purine 5-nucleotidase	Nt5c2
E9QAN2	Poly(A) polymerase alpha	Papola
Q6RT24	Centromere-associated protein E	Cenpe
E9QKK4	Glucocorticoid-induced transcript 1 protein	Glcci1
Q70KF4	Cardiomyopathy-associated protein 5	Cmya5
Q8VEH3	ADP-ribosylation factor-like protein 8A	Arl8a
Q3UQN2	FCH domain only protein 2	Fcho2
F6UK53	MCG62900	4933403O08Rik
P10493	Nidogen-1	Nid1
F6VWU8	Zinc finger protein 946	Zfp946
Q8BND4	Protein DDX26B	Ddx26b
Q8K3A9	7SK snRNA methylphosphate capping enzyme	Mepce
F8VPP8	Zinc finger CCCH type-containing 7B	Zc3h7b
F8WIN2	AT-rich interactive domain-containing protein 3B	Arid3b
V9GX74	Zinc finger transcription factor Trps1	Trps1
Q9QUS9	Reg III delta	Reg3d
Q3UW64	Bifunctional UDP-N-acetylglucosamine 2-epimerase/N-acetylmannosamine kinase	Gne
H3BJU3	Mitoguardin 2	Fam73b
Q4VGL6	Roquin	Rc3h1
Q549C9	Cellular tumor antigen p53	Trp53
Q9D572	UBX domain-containing protein 11	Ubxn11

J3QMK1	Shugoshin 2B	Sgo2b
J3QNW4	UPF0533 protein C5orf44 homolog	Trappc13
K3W4Q5	Protein FAM186A	FAM186A
O55057	Retinal rod rhodopsin-sensitive cGMP 3,5-cyclic phosphodiesterase subunit delta	Pde6d
O08643	Granzyme M	Gzmm
O35257	Prolactin-6A1	Prl6a1
O35615	Zinc finger protein ZFPM1	Zfpm1
O35654	DNA polymerase delta subunit 2	Pold2
O35943	Frataxin, mitochondrial	Fxn
O54786	DNA fragmentation factor subunit alpha	Dffa
O54988	STE20-like serine/threonine-protein kinase	Slk
O55142	60S ribosomal protein L35a	Rpl35a
O55183	Stanniocalcin-1	Stc1
O88495	Melatonin-related receptor	Gpr50
O88574	Histone deacetylase complex subunit SAP30	Sap30
O88630	Golgi SNAP receptor complex member 1	Gosr1
O89001	Carboxypeptidase D	Cpd
P01325	Insulin-1	Ins1
P01639	Ig kappa chain V-V region MOPC 41	Gm5571
P08508	Low affinity immunoglobulin gamma Fc region receptor III	Fcgr3
P11438	Lysosome-associated membrane glycoprotein 1	Lamp1
P11930	Nucleoside diphosphate-linked moiety X motif 19, mitochondrial	Nudt19
P12367	cAMP-dependent protein kinase type II-alpha regulatory subunit	Prkar2a
P16330	2,3-cyclic-nucleotide 3-phosphodiesterase	Cnp
P16382	Interleukin-4 receptor subunit alpha	Il4r
P19137	Laminin subunit alpha-1	Lama1
P22339	Growth arrest and DNA damage-inducible protein GADD45 beta	Gadd45b
P30549	Substance-K receptor	Tacr2
P34152	Focal adhesion kinase 1	Ptk2
P35546	Proto-oncogene tyrosine-protein kinase receptor Ret	Ret
P45952	Medium-chain specific acyl-CoA dehydrogenase, mitochondrial	Acadm
P46414	Cyclin-dependent kinase inhibitor 1B	Cdkn1b
P48455	Serine/threonine-protein phosphatase 2B catalytic subunit gamma isoform	Ppp3cc
P48542	G protein-activated inward rectifier potassium channel 2	Kcnj6
P54726	UV excision repair protein RAD23 homolog A	Rad23a
P61027	Ras-related protein Rab-10	Rab10
P61458	Pterin-4-alpha-carbinolamine dehydratase	Pcbd1
P61957	Small ubiquitin-related modifier 2	Sumo2
P62071	Ras-related protein R-Ras2	Rras2
P62911	60S ribosomal protein L32	Rpl32
P63166	Small ubiquitin-related modifier 1	Sumo1
P63328	Serine/threonine-protein phosphatase 2B catalytic subunit alpha isoform	Ppp3ca
P70213	Friend virus susceptibility protein 1	Fv1
P70298	Homeobox protein cut-like 2	Cux2
P97489	Transcription factor GATA-5	Gata5
P97496	SWI/SNF complex subunit SMARCC1	Smarcc1

Q02614	SAP30-binding protein	Sap30bp
Q03402	Cysteine-rich secretory protein 3	Crisp3
Q04447	Creatine kinase B-type	Ckb
Q07563	Collagen alpha-1(XVII) chain	Col17a1
Q0V8T7	Contactin-associated protein like 5-3	Cntnap5c
Q0VAV1	Muc6 protein	Muc6
Q8BZH4	Pogo transposable element with ZNF domain	Pogz
Q3TCU5	Tapasin	Tapbp
Q3TDD9	Protein phosphatase 1 regulatory subunit 21	Ppp1r21
Q80W82	Mitogen-activated protein kinase 10	Mapk10
Q3TSN9	BTB/POZ domain-containing protein 3	Btbd3
Q3UDW8	Heparan-alpha-glucosaminide N-acetyltransferase	Hgsnat
Q3UQ17	MCG3834	Zbtb16
Q3UVL4	Protein fat-free homolog	Ffr
Q3UY93	Melanin-concentrating hormone receptor 1	Mchr1
Q3V3G9	Nardilysin, N-arginine dibasic convertase, NRD convertase 1	Nrd1
Q3V3Q4	Pyrin domain-containing protein 3	Pydc3
Q4ZGD9	Nuclear RNA export factor 3	Nxf3
Q569L8	Centromere protein J	Cenpj
Q91YI4	Beta-arrestin-2	Arrb2
A2AH25	Rho GTPase-activating protein 1	Arhgap1
Q5I043	Ubiquitin carboxyl-terminal hydrolase 28	Usp28
Q5SSE9	ATP-binding cassette sub-family A member 13	Abca13
E9Q284	Coilin	Coil
Q5SXG7	Vitelline membrane outer layer protein 1 homolog	Vmo1
Q60707	T-box transcription factor TBX2	Tbx2
Q61687	Transcriptional regulator ATRX	Atrx
Q61781	Keratin, type I cytoskeletal 14	Krt14
Q62048	Astrocytic phosphoprotein PEA-15	Pea15
Q62095	ATP-dependent RNA helicase DDX3Y	Ddx3y
Q62172	RalA-binding protein 1	Ralbp1
Q640M1	U3 small nucleolar RNA-associated protein 14 homolog A	Utp14a
Q64505	Cholesterol 7-alpha-monooxygenase	Cyp7a1
Q6DFV1	Condensin-2 complex subunit G2	Ncapg2
Q9WV80	Sorting nexin-1	Snx1
Q6P1G0	HEAT repeat-containing protein 6	Heatr6
Q6P539	Uncharacterized protein C17orf63 homolog	Fam222b
Q6P6J9	Thioredoxin domain-containing protein 15	Txndc15
Q6P8K3	Predicted gene 7978	BC061212
Q6P9R1	ATP-dependent RNA helicase DDX51	Ddx51
Q6PGF7	Exocyst complex component 8	Exoc8
Q6PR54	Telomere-associated protein RIF1	Rif1
Q6UJY2	Sodium/hydrogen exchanger 10	Slc9c1
Q6ZPY5	Zinc finger protein 507	Znf507
Q704Y3	Transient receptor potential cation channel subfamily V member 1	Trpv1
Q7M721	Taste receptor type 2 member 120	Tas2r120

Q7TS04	Olfactory receptor 301	Olfr301
Q80UW8	DNA-directed RNA polymerases I, II, and III subunit RPABC1	Polr2e
Q80WQ2	Protein VAC14 homolog	Vac14
Q8BHE0	Proline-rich protein 11	Prr11
Q8BHG9	CGG triplet repeat-binding protein 1	Cggbp1
Q8BLY2	Probable threonine--tRNA ligase 2, cytoplasmic	Tarsl2
Q8BNY6	Neuronal calcium sensor 1	Ncs1
Q8R2L5	28S ribosomal protein S18c, mitochondrial	Mrps18c
Q8BU03	Periodic tryptophan protein 2 homolog	Pwp2
Q8BUJ9	Low-density lipoprotein receptor-related protein 12	Lrp12
Q8BVT7	RIKEN cDNA 4921511C20 gene	4921511C20Rik
Q8BXZ1	Protein disulfide-isomerase TMX3	Tmx3
Q8BZR0	Probable G-protein coupled receptor 82	Gpr82
Q8C2E4	Pentatricopeptide repeat-containing protein 1	Ptcd1
Q8C5R8	Ribose-phosphate pyrophosphokinase	Prps1l1
Q8C754	Vacuolar protein sorting-associated protein 52 homolog	Vps52
Q8C845	EF-hand domain-containing protein D2	Efhd2
Q8CBF3	Ephrin type-B receptor 1	Ephb1
Q8CCX5	Keratin-like protein KRT222	Krt222
Q8CDK2	Cytosolic carboxypeptidase 2	Agbl2
Q8CF66	UPF0539 protein C7orf59 homolog	Lamtor4
Q8CH09	SURP and G-patch domain-containing protein 2	Sugp2
Q8CIV2	Membralin	ORF61
Q8JZM8	Mucin-4	Muc4
Q8JZR0	Long-chain-fatty-acid--CoA ligase 5	Acsl5
Q8K0Z7	Translational activator of cytochrome c oxidase 1	Taco1
Q8K394	Inactive phospholipase C-like protein 2	Plcl2
Q8K3H0	DCC-interacting protein 13-alpha	Appl1
Q8K3V4	Protein-arginine deiminase type-6	Padi6
Q8N7N5	DDB1- and CUL4-associated factor 8	Dcaf8
Q8R054	Sushi repeat-containing protein SRPX2	Srpx2
Q8R105	Vacuolar protein sorting-associated protein 37C	Vps37c
Q8R2E3	Vomeronasal type-1 receptor	Vmn1r36
Q8R2P1	Ectoderm-neural cortex protein 2	Klhl25
Q8R3F5	Malonyl-CoA-acyl carrier protein transacylase, mitochondrial	Mcat
Q8R420	ATP-binding cassette sub-family A member 3	Abca3
Q8R4Y8	Rotatin	Rttn
Q8VDV8	MIT domain-containing protein 1	Mitd1
Q8VFJ7	Olfactory receptor	Olfr1012
Q8VFV9	Olfactory receptor	Olfr1459
Q8VFZ3	Olfactory receptor	Olfr513
Q8VG32	Olfactory receptor	Olfr1408
Q8VGE3	Olfactory receptor	Olfr160
Q8VGL3	Olfactory receptor	Olfr535
F8WJ23	Hornerin	Hrnr
Q8VHP6	Cadherin-related family member 1	Cdhr1

Q8VHY0	Chondroitin sulfate proteoglycan 4	Cspg4
Q91XC9	Peroxisomal membrane protein PEX16	Pex16
Q91YP0	L-2-hydroxyglutarate dehydrogenase, mitochondrial	L2hgdh
Q91ZP4	MCG3105, isoform CRA_a	Slc5a4b
Q91ZZ3	Beta-synuclein	Sncb
Q921Y2	U3 small nucleolar ribonucleoprotein protein IMP3	Imp3
Q922B1	O-acetyl-ADP-ribose deacetylase MACROD1	Macrod1
Q99L04	Dehydrogenase/reductase SDR family member 1	Dhrs1
Q99LI5	Zinc finger protein 281	Zfp281
Q99LJ0	CTTNBP2 N-terminal-like protein	Cttnbp2nl
Q99MR1	PERQ amino acid-rich with GYF domain-containing protein 1	Gigyf1
Q99MZ3	Carbohydrate-responsive element-binding protein	Mlxipl
Q99N05	Membrane-spanning 4-domains subfamily A member 4D	Ms4a4d
Q99N96	39S ribosomal protein L1, mitochondrial	Mrpl1
Q9CPN9	RIKEN cDNA 2210010C04 gene	2210010C04Rik
Q9CQ54	NADH dehydrogenase [ubiquinone] 1 subunit C2	Ndufc2
Q9CQQ7	ATP synthase subunit b, mitochondrial	Atp5f1
E9PW43	Protein transport protein Sec61 subunit beta	Gm10320
Q9CR02	Translation machinery-associated protein 16	Tma16
Q9CXR1	Dehydrogenase/reductase SDR family member 7	Dhrs7
Q9CY97	RNA polymerase II subunit A C-terminal domain phosphatase SSU72	Ssu72
Q9CZN8	Glutamyl-tRNA(Gln) amidotransferase subunit A, mitochondrial	Qrsl1
Q9CZX5	PIN2/TERF1-interacting telomerase inhibitor 1	Pinx1
Q9D0M5	Dynein light chain 2, cytoplasmic	Dynll2
Q9D1C8	Vacuolar protein sorting-associated protein 28 homolog	Vps28
Q9D1H8	39S ribosomal protein L53, mitochondrial	Mrpl53
Q9D1N9	39S ribosomal protein L21, mitochondrial	Mrpl21
Q9D1Z3	Protein FAM173B	Fam173b
Q9D267	Epididymal-specific lipocalin-9	Lcn9
Q9D3Z8	RIKEN cDNA 4933425L06	4933425L06Rik
Q9D411	Testis-specific serine/threonine-protein kinase 4	Tssk4
Q9D9V3	Ethylmalonyl-CoA decarboxylase	Echdc1
Q9DAT2	MRG-binding protein	Mrgbp
Q9DBE0	Cysteine sulfinic acid decarboxylase	Csad
Q9DBG1	Sterol 26-hydroxylase, mitochondrial	Cyp27a1
Q9DBJ3	Brain-specific angiogenesis inhibitor 1-associated protein 2-like protein 1	Baiap2l1
Q9DCA5	Ribosome biogenesis protein BRX1 homolog	Brix1
Q9DCF9	Translocon-associated protein subunit gamma	Ssr3
Q9DD18	D-tyrosyl-tRNA(Tyr) deacylase 1	Dtd1
Q9EQ06	Estradiol 17-beta-dehydrogenase 11	Hsd17b11
Q9ERN0	Secretory carrier-associated membrane protein 2	Scamp2
Q9ES83	Blood vessel epicardial substance	Bves
Q9JIK9	28S ribosomal protein S34, mitochondrial	Mrps34
Q9JIX0	Enhancer of yellow 2 transcription factor homolog	Eny2
Q9JJ28	Protein flightless-1 homolog	Flii
Q9JJ78	Lymphokine-activated killer T-cell-originated protein kinase	Pbk

Q9JJ94	Sjoegren syndrome nuclear autoantigen 1 homolog	Ssna1
Q9JJT0	RNA 3-terminal phosphate cyclase-like protein	Rcl1
Q9R0H0	Peroxisomal acyl-coenzyme A oxidase 1	Acox1
Q9R0K2	Olfactory receptor	Olfr1264
Q9WTR1	Transient receptor potential cation channel subfamily V member 2	Trpv2
Q9WV54	Acid ceramidase	Asah1
Q9Z262	Claudin-6	Cldn6
Q9Z2X2	26S proteasome non-ATPase regulatory subunit 10	Psmd10
V9GXI9	Striatin-4	Strn4

Table 5 Bioinformatic analysis by David of the proteins exclusively expressed in OligoGM1 cells in the comparison OligoGM1 vs CONTROL N2a cells

DAVID analysis p-value ≤ 0.05 counts ≥ 2

	Category	Term	Count	p-value	Genes
Endosome/endocytic trafficking					
	Annotation Cluster 1	*Enrichment Score: 1.9283871903046559*			
	UP_KEYWORDS	Endosome	14	7,27E-03	RET, SCAMP2, VAC14, VPS52, SNX1, VPS37C, MITD1, APPL1, EPHB1, LAMP1, CDKN1B, ARL8A, VPS28, RAB10
	GOTERM_CC_DIRECT	GO:0010008~endosome membrane	7	8,49E-03	LAMP1, RET, VAC14, VPS52, SNX1, VPS28, APPL1
	GOTERM_CC_DIRECT	GO:0005768~endosome	15	2,66E-02	RAB3A, RET, SCAMP2, VAC14, VPS52, SNX1, VPS37C, MITD1, APPL1, EPHB1, LAMP1, CDKN1B, ARL8A, RAB10, VPS28
	Annotation Cluster 5	*Enrichment Score: 1.2682691071296288*			
	SMART	SM00282: LamG	4	1,77E-02	LAMA1, FAT1, CSPG4, CNTNAP5C
	INTERPRO	IPR001791: Laminin G domain	4	4,92E-02	LAMA1, FAT1, CSPG4, CNTNAP5C
	Annotation Cluster 8	*Enrichment Score: 1.0091254512435084*			
	UP_KEYWORDS	Coated pit	4	2,82E-02	ARRB2, LRP12, ITSN1, FCHO2
Ribosome biogenesis and					

regulation of transcription					
	Annotation Cluster 2	*Enrichment Score: 1.5686242450542756*			
	GOTERM_CC_DIRECT	GO:0005840~ribosome	10	1,65E-03	MRPL53, MRPL1, RPL35A, MRPS34, MRPL4, MRPL21, MRPS18C, RPL32, TMA16, DENR
	UP_KEYWORDS	Ribosomal protein	9	6,36E-03	MRPL53, MRPL1, RPL35A, MRPS34, MRPL4, MRPL21, MRPS18C, RPL32, MRPL48
	UP_KEYWORDS	Ribonucleoprotein	10	2,42E-02	MRPL53, MRPL1, RPL35A, IMP3, MRPS34, MRPL4, MRPL21, MRPS18C, RPL32, MRPL48
	GOTERM_CC_DIRECT	GO:0030529~intracellular ribonucleoprotein complex	10	4,28E-02	MRPL53, MRPL1, RPL35A, IMP3, MRPS34, MRPL4, MRPL21, MRPS18C, RPL32, TDRD7
	Annotation Cluster 3	*Enrichment Score: 1.561905533986465*			
	UP_KEYWORDS	Ribosome biogenesis	5	8,66E-03	RCL1, IMP3, BRIX1, UTP14A, DDX51
	GOTERM_BP_DIRECT	GO:0006364~rRNA processing	6	3,71E-02	RCL1, RPL35A, IMP3, EXOSC2, UTP14A, DDX51
	GOTERM_BP_DIRECT	GO:0042254~ribosome biogenesis	5	4,09E-02	RCL1, IMP3, BRIX1, UTP14A, DDX51
	KEGG_PATHWAY	mmu03008: Ribosome biogenesis in eukaryotes	5	4,31E-02	RCL1, IMP3, NXF3, UTP14A, PWP2
	Annotation Cluster 24	*Enrichment Score: 0.586830761089792*			

	GOTERM_MF_DIRECT	GO:0001085~RNA polymerase II transcription factor binding	4	4,51E-02	TRP53, GATA5, TRPS1, ZFPM1
	Annotation Cluster 28	*Enrichment Score: 0.547197473552621*			
	GOTERM_BP_DIRECT	GO:0000122~negative regulation of transcription from RNA polymerase II promoter	19	2,07E-02	TRP53, EHMT1, TBX2, TRPV1, MLXIPL, ZBTB16, MAPK10, SAP30, REL, CGGBP1, PSMD10, TRPS1, PER2, ZFP281, CUX2, ZFPM1, TCF4, MEPCE, …
Cell cycle					
	Annotation Cluster 9	*Enrichment Score: 0.9624582129177877*			
	GOTERM_BP_DIRECT	GO:0051301~cell division	11	4,77E-02	SPC24, POGZ, NCAPG2, ARL8A, CENPE, MITD1, MAP9, USP16, CDK4, CENPJ, UBE2S
	Annotation Cluster 11	*Enrichment Score: 0.8865229236222075*			
	GOTERM_BP_DIRECT	GO:0051726~regulation of cell cycle	6	2,39E-02	TRP53, PRR11, PER2, USP16, CDK4, GADD45B
Mitochondrion, fatty acid metabolism					
	Annotation Cluster 4	*Enrichment Score: 1.2776717793217818*			
	UP_KEYWORDS	Mitochondrion	23	2,91E-02	TRP53, MRPL53, MRPL1, MRPS34, MRPL4, ACADM, MCAT, ATP5F1, NDUFC2, CBR4, MAPK10, TACO1, QRSL1, MRPL21, MRPS18C, HTRA2
	Annotation Cluster 6	*Enrichment Score: 1.0521935305885302*			

	KEGG_PATHWAY	mmu01212: Fatty acid metabolism	5	8,61E-03	ACOX1, ACADM, MCAT, ELOVL6, ACSL5
	UP_KEYWORDS	Fatty acid metabolism	6	2,63E-02	ACOX1, ACADM, MCAT, CBR4, ELOVL6, ACSL5
	GOTERM_BP_DIRECT	GO:0006631~fatty acid metabolic process	7	2,67E-02	ACOX1, ACADM, MCAT, PER2, CBR4, ELOVL6, ACSL5
	KEGG_PATHWAY	mmu03320: PPAR signaling pathway	5	3,84E-02	ACOX1, ACADM, CYP27A1, CYP7A1, ACSL5
	Annotation Cluster 12	*Enrichment Score: 0.8062496294708845*			
	INTERPRO	IPR026082:ABC transporter A, ABCA	3	2,11E-02	ABCA3, ABCA13, ABCA12
Cell adhesion					
	Annotation Cluster 7	*Enrichment Score: 1.0256913451821696*			
	INTERPRO	IPR002126: Cadherin	6	3,29E-02	RET, PCDHB6, PCDH11X, FAT1, CDHR1, PCDH15
	INTERPRO	IPR015919: Cadherin-like	6	3,48E-02	RET, PCDHB6, PCDH11X, FAT1, CDHR1, PCDH15
	Annotation Cluster 21	*Enrichment Score: 0.6276318581765036*			
	GOTERM_BP_DIRECT	GO:0030155~regulation of cell adhesion	4	2,30E-02	LAMA1, RET, PTK2, PTK2B
Various					
	Annotation Cluster 18	*Enrichment Score: 0.6872907708951744*			
	UP_KEYWORDS	Nucleotide-binding	36	1,25E-02	RAB3A, GNE, TRPV1, XRCC6, ABCA3, EPHB1, CKB, QRSL1, PRKAR2A, PTK2, SLK, PTK2B, NT5C2, DDX3Y, 4933425L06RIK, KIF21A, …

UP_SEQ_FEATURE	active site:Proton acceptor	19	1,51E-02	HSD17B11, ACOX1, RET, ACADM, HSD3B7, NRD1, CNP, CBR4, PBK, MAPK10, CDK4, EPHB1, DHRS7, DHRS1, PDIK1L, PTK2, SLK, PTK2B, TSSK4
UP_KEYWORDS	ATP-binding	27	4,62E-02	TRPV1, GNE, XRCC6, ABCA3, EPHB1, CKB, QRSL1, PTK2, SLK, PTK2B, DDX3Y, KIF21A, TARSL2, ABCA13, ABCA12, ACSL5, RET, ATRX, …
GOTERM_MF_DIRECT	GO:0000166~nucleotide binding	38	4,64E-02	RAB3A, RBM33, GNE, TRPV1, XRCC6, ABCA3, EPHB1, CKB, QRSL1, PRKAR2A, PTK2, SLK, PTK2B, NT5C2, DDX3Y, 4933425L06RIK, PTBP2, …
Annotation Cluster 25	*Enrichment Score: 0.5793190221422585*			
UP_SEQ_FEATURE	binding site:S-adenosyl-L-methionine; via carbonyl oxygen	3	4,30E-02	METTL1, CARM1, MEPCE

Appendix II

Glycoconjugate Journal
https://doi.org/10.1007/s10719-020-09963-7

ORIGINAL ARTICLE

Modulation of calcium signaling depends on the oligosaccharide of GM1 in Neuro2a mouse neuroblastoma cells

Giulia Lunghi[1] · Maria Fazzari[1] · Erika Di Biase[1] · Laura Mauri[1] · Sandro Sonnino[1] · Elena Chiricozzi[1]

Received: 10 September 2020 / Revised: 2 November 2020 / Accepted: 9 November 2020

Abstract

Recently, we demonstrated that the oligosaccharide portion of ganglioside GM1 is responsible, via direct interaction and activation of the TrkA pathway, for the ability of GM1 to promote neuritogenesis and to confer neuroprotection in Neuro2a mouse neuroblastoma cells. Recalling the knowledge that ganglioside GM1 modulates calcium channels activity, thus regulating the cytosolic calcium concentration necessary for neuronal functions, we investigated if the GM1-oligosaccharide would be able to overlap the GM1 properties in the regulation of calcium signaling, excluding a specific role played by the ceramide moiety inserted into the external layer of plasma membrane. We observed, by calcium imaging, that GM1-oligosaccharide administration to undifferentiated Neuro2a cells resulted in an increased calcium influx, which turned out to be mediated by the activation of TrkA receptor. The biochemical analysis demonstrated that PLCγ and PKC activation follows the TrkA stimulation by GM1-oligosaccharide, leading to the opening of calcium channels both on the plasma membrane and on intracellular storages, as confirmed by calcium imaging experiments performed with IP3 receptor inhibitor. Subsequently, we found that neurite elongation in Neuro2a cells was blocked by subtoxic administration of extracellular and intracellular calcium chelators, suggesting that the increase of intracellular calcium is responsible of GM1-oligosaccharide mediated differentiation. These results suggest that GM1-oligosaccharide is responsible for the regulation of calcium signaling and homeostasis at the base of the neuronal functions mediated by plasma membrane GM1.

Keywords GM1 ganglioside · GM1-oligosaccharide · TrkA neurotrophin receptor · Calcium signaling · Plasma membrane signaling · Neurodifferentiation

Abbreviations

A.U.	arbitrary units
BAPTA-AM	1,2-bis(o-aminophenoxy)ethane-N,N,N′,N′-tetraacetic acid (acetoxymethyl ester)
BSA	bovine serum albumin
Ca^{2+}	calcium
CTRL	control
DMEM HG	Dulbecco's modified Eagle's high glucose medium
DRM	Detergent-resistant membrane
DTT	1,4-Dithiothreitol
EDTA	ethylenediamine tetraacetic acid
EGTA	ethylene glycol tetraacetic acid
ERK1/2	extracellular signal-regulated protein kinases 1 and 2
FBS	fetal bovine serum
F	fluorescence
GM1	$II^3Neu5Ac\text{-}Gg_4Cer$, β-Gal-(1–3)-β-GalNAc-(1–4)-[α-Neu5Ac-(2–3)]-β-Gal-(1–4)-β-Glc-Cer
$HBSS^+$	Hank's Balanced Salt Solution containing calcium and magnesium
HPTLC	High-performance thin-layer chromatography
IP_3	inositol trisphosphate
N2a	Neuro2a cells
NS	no significant

Ganglioside nomenclature is in accordance with IUPAC-IUBB recommendations [56].

✉ Giulia Lunghi

✉ Elena Chiricozzi

[1] Department of Medical Biotechnology and Translational Medicine, University of Milano, Segrate, Milano, Italy

Published online: 17 November 2020

OligoGM1	GM1-oligosaccharide, $II^3Neu5Ac\text{-}Gg_4$
PBS	phosphate-buffered saline
P-ERK1/2	phosphorylated ERK1/2
PKC	Protein kinase C
PLCγ	Phospholipase C γ
PNS	post nuclear supernatant
P-TrkA	phosphorylated TrkA
PM	plasma membrane
PVDF	polyvinylidene difluoride
RRID	Research Resource Identifiers
TBS	Tris-buffered saline
TLC	thin-layer chromatography
Trk	neurotrophin tyrosine kinase receptor
Tyr490	tyrosine 490

Introduction

Among gangliosides, a particular class of sialic acid-containing glycosphingolipids enriched in neuronal membranes, particular attention is given to GM1, β-Gal-(1–3)-β-GalNAc-(1–4)-[α-Neu5Ac-(2–3)]-β-Gal-(1–4)-β-Glc-(1–1)-Cer ($II^3Neu5Ac\text{-}Gg_4Cer$) by virtue of its relevant implication in neuronal differentiation and in neuronal recovery and protection [1–6]. Component of all mammalian brains, GM1 is inserted into the outer layer of the plasma membrane (PM) with the hydrophobic moiety, the ceramide, while the saccharide portion protrudes into the extracellular milieu interacting with a wide range of membrane-associated proteins, including receptors and enzymes [1–6]. It has been extensively studied how GM1 induction of neurite outgrowth and neuroprotective phenomena are accomplished through GM1 specific interaction with neurotrophin tyrosine kinase receptors (Trk) and via its ability to modulate cellular calcium (Ca^{2+}) levels, acting on Ca^{2+} influx channels, Ca^{2+} exchangers, and various Ca^{2+}-utilizing enzymes [3, 7, 8]. Elevation of endogenous PM GM1 or exogenous applied GM1 in mouse neuroblastoma cells Neuro2a (N2a) and in other neuroblastoma cells leads to the increase of intracellular Ca^{2+}, which is accompanied by neurite outgrowth and extension [7, 9, 10]. Additionally, cultured neurons from the B*4galnt1* knock out mouse, characterized by deficiency of GM1 and its oligosialo derivatives, showed impaired Ca^{2+} regulatory capability, which translates in significantly retarded outgrowth [11, 12] and in increased vulnerability to KCl and glutamate excitotoxicity, which is rescued after GM1 application [12].

Although the numerous properties of GM1 have been extensively studied over the years, its mechanism of action is still being explored. It has been proved that GM1-oligosaccharide, β-Gal-(1–3)-β-GalNAc-(1–4)-[α-Neu5Ac-(2–3)]-β-Gal-(1–4)-Glc (OligoGM1; $II^3Neu5Ac\text{-}Gg_4$), exogenously added to the culture medium of N2a neuroblastoma cells, was able alone to induce the neuritogenesis process by directly interacting with nerve growth factor (NGF)-specific receptor TrkA at the PM, reserving to the ceramide an exclusively anchor and structural role [13]. Subsequently we found that OligoGM1 administered to cerebellar granule neurons enhanced neuron clustering, neurite sprouting and networking, thus confirming the specific role of the oligosaccharide chain in the processes of neuronal differentiation and maturation, known to be regulated by the entire GM1 [14]. Additionally, the OligoGM1 was found to mediate also the neuroprotective phenomena attributed to ganglioside GM1, being able to induce protection from 1-methyl-4-phenyl-1,2,3,6-tetrahydropyridine hydrochloride (MPTP) neurotoxicity in N2a neuroblastoma cells [15] acting on mitochondria [16], and to rescue the physical and biochemical defects due to the partial lack of GM1 content in a mouse model of Parkinson's disease [17].

The present work aims to further investigate the mechanism of action of OligoGM1, as the bioactive component of ganglioside GM1, focusing on its ability to modulate the cell Ca^{2+} flow, mechanism at the base of GM1-mediated neuronal differentiation. We describe that the addition of OligoGM1 to the culture medium of N2a cells is able to activate the TrkA-phospholipase C gamma (PLCγ) pathway at the cell surface, leading to an increase of cytosolic Ca^{2+} necessary for OligoGM1-induced cell differentiation. These data contribute to explain the molecular mechanism underlying the neurotrophic action of OligoGM1, shedding new light on the mechanism of action of ganglioside GM1.

Methods

Materials

Commercial chemicals were of the highest purity available, common solvents were distilled before use and water was doubly distilled in a glass apparatus.

Phosphate buffered saline (PBS), sodium orthovanadate (Na_3VO_4), phenylmethanesulfonyl fluoride (PMSF), aprotinin, protease inhibitor cocktail (IP), ethylenediamine tetraacetic acid (EDTA), bovine serum albumin (BSA), Xestspongin C, calcium ionophore A23187, mouse anti-alpha-tubulin (RRID: AB_477579) antibody and mouse neuroblastoma N2a cells (RRID: CVCL_0470) were from Sigma-Aldrich (St. Louis, MO, USA). TrkA-inhibitor (CAS 388626-12-8) was from Merk Millipore (Billerica, MA, USA). Fluo-4 acetoxymethyl (AM), 1,2-bis(o-aminophenoxy)ethane-N,N,N′,N′-tetraacetic acid AM (BAPTA-AM), Hank's Balanced Salt Solution containing calcium and magnesium ($HBSS^+$) and Sodium pyruvate were from Thermo Fisher Scientific (Waltham, MA, USA). Rabbit anti-TrkA (RRID: AB_10695253), rabbit anti-phospho-TrkA (Tyr 490) (RRID: AB_10235585), rabbit anti-flotillin-1 (RRID: AB_2773040),

and goat anti-rabbit IgG (RRID: AB_2099233) antibodies were from Cell Signaling Technology (Danvers, MA, USA). Mouse anti-PLCγ1 (RRID: AB_628119), anti-phospho-PLCγ1 (Tyr 783) (RRID: AB_2163561), Protein kinase C (PKC) (RRID: AB_628139), anti-phospho-PKCα (Ser 657) (RRID not found) antibodies were from Santa Cruz Biotechnology (Dallas, TX, USA). Mouse anti-calnexin (RRID: AB_397884) antibody was from BD Biosciences. Chemiluminescent kit for western blot was from Cyanagen (Bologna, Italy). 4 − 20% Mini-PROTEAN® TGX™ Precast Protein Gels, Turbo Polyvinylidene difluoride (PVDF) Mini -Midi membrane and DC™ protein assay kit were from BioRad (Hercules, CA, USA). Triton X -100 were from Merk Millipore (Frankfurten, Germany). Cell culture flasks, dishes, and plates were purchased from Corning (Corning, NY, USA). Dulbecco's modified Eagle's high glucose medium (DMEM HG), fetal bovine serum (FBS), L-glutamine (L-Glut), Penicillin/streptomycin (10.000 Units/ml) (10.000 U/mL), Streptomycin (10 mg/mL), and acrylamide were purchased from EuroClone (Paignton, UK).

GM1-oligosaccharide preparation

GM1 ganglioside was purified from the total ganglioside mixture extracted from fresh pig brains collected at the slaughterhouse of the Galbani Company (Melzo, Italy), according to the procedure developed previously [18]. Briefly, high amount of GM1 was obtained by the sialidase treatment of the total pig brain ganglioside mixture. This simplified the purification process as the major part of polysialogangliosides were transformed into GM1 [19]. The ganglioside mixture, 5 g as sialic acid, was dissolved in pre-warmed (36 °C) 500 mL of 0.05 M sodium acetate, 1 mM $CaCl_2$ buffer pH 5.5. *Vibrio cholerae* sialidase (1 unit) was added to the solution every 12 h. Incubation at 36 °C and magnetic stirring was maintained for two days, and the solution dialyzed at 23 °C for 4 days against 10 L of water changed 5 times a day. The sialidase treated ganglioside mixture was subjected to 150 cm x 2 cm silica gel 100 column chromatography equilibrated and eluted with chloroform/methanol/water, 60:35:5 by vol. The fractions containing GM1, identified by TLC, were pooled, dried and submitted to a further column chromatographic purification using the above experimental conditions. Fractions containing pure GM1 were collected and dried. The residue was dissolved in chloroform/methanol (2:1 v/v) and precipitated by adding 4 volumes of cold acetone. After centrifugation (15,000 *x* g) the GM1 pellet was separated from the acetone, dried, dissolved in 50 mL of deionized water and lyophilized giving 1,350 mg of white powder which was stored at -20 °C.

The OligoGM1 was prepared by ozonolysis of GM1 followed by alkaline degradation [20] (Supplementary Fig. S1). Briefly, GM1 was dissolved in methanol and slowly saturated with ozone at 23 °C. Triethylamine / water (5:1) was added to the mixture bringing the pH to 10.5–11.0 and the reaction continued for three days. Then, solvent was evaporated and OligoGM1 was purified by flash chromatography using chloroform/methanol/2-propanol/water 60:35:5:5 by vol as eluent. The oligosaccharide was dissolved in methanol and stored at 4 °C.

The NMR spectrum showed a correct ratio between the main peaks and contained no unclear signals, mass spectrometry indicated the correct molecular mass, and HPTLC analyzes performed showed a single band. Overall, and considering that the OligoGM1 was prepared from homogeneous GM1, these results suggest homogeneity for the prepared oligosaccharide (Supplementary Figure S2).

N2a cell cultures

Murine neuroblastoma cells N2a were cultured and propagated as monolayer on 75 cm^2 flasks in DMEM HG medium supplemented with 10% heat inactivated FBS, 1% L-glutamine, 1% Penicillin/Streptomycin and 1 mM sodium pyruvate, at 37 °C in a humidified atmosphere of 95% air / 5% CO_2. Cells were sub-cultured to a fresh culture when growth reached the 80–90% confluence (i.e. every 3–4 days). In subcultures passages cells were washed once with PBS and detached by 0.02% EDTA − 0.6% glucose in PBS (w/v).

Cell treatments

N2a cells were plated at 5×10^3 / cm^2 on 6-well plates in complete DMEM HG medium for 24 h to allow cells attachment and recovery in complete medium before treatments.

OligoGM1 treatment

24 h after plating, growth medium was removed and N2a cells were pre-incubated in pre-warmed (37 °C) DMEM HG medium containing 2% FBS, 1% L-glutamine, and 1% penicillin/streptomycin, for 30 min at 37 °C.

Subsequently, OligoGM1 was solubilized in water at 2 mM concentration by vortex agitation and sonication in water bath 3 times for 30 sec. Solubilized OligoGM1 was administered to cells at the final concentration of 50 μM. This dose condition has been previously found to promote neurodifferentiation and neuroprotection in N2a cells via TrkA-ERK1/2 signaling pathway activation [13, 15]. Control cells were incubated under the same experimental conditions but omitting any addition of OligoGM1.

Inhibition of TrkA receptor

To block TrkA activity in N2a cells, TrkA inhibitor (120 nM) was added to the incubation medium 1 h before the addition of OligoGM1 [13, 21].

EGTA and BAPTA-AM treatment

To chelate Ca^{2+} ions in N2a cells, the extracellular Ca^{2+} chelating agent EGTA (100 μM) or the intracellular Ca^{2+} chelating agent BAPTA-AM (1 μM) were added to the incubation medium together with OligoGM1 or alone as control condition [22].

Morphological analysis and neurite outgrowth evaluation

N2a cells untreated (control) or treated with 50 μM OligoGM1 in presence or absence of EGTA/BAPTA-AM for 24 h were observed by phase contrast microscopy (Olympus BX50 microscope; Olympus, Tokyo, Japan).

The neurite-like processes length was measured after treatment with OligoGM1 on bidimensional images acquired with 200X magnification with phase contrast microscopy and expressed as the ratio between neurite length and cell body diameter [13, 23, 24]. Five random fields were examined from each well, giving a total cell count of at least 200 cells per well.

Isolation of detergent-resistant membrane (DRM) fractions

N2a cells were incubated in the absence (control) or in the presence of 50 μM OligoGM1 for 3 h at 37 °C. Detergent-resistant membrane (DRM) were prepared by ultracentrifugation on discontinuous sucrose gradient of cells subjected to homogenization with 1% Triton X-100, as previously described [25, 26]. Briefly, cells were mechanically harvested in PBS 1X and centrifuged at 270 *x* g for 10 min at 4 °C. Cell pellet was lysed in 1.2 mL of 1% Triton X-100 in TNEV buffer (10 mM TrisHCl pH 10, 150 mM NaCl, 5 mM EDTA pH 7.5) in the presence of 1 mM Na_3VO_4, 1 mM PMSF, and 75 mU/mL aprotinin and homogenized for 11-folds with tight Dounce. Cell lysate (2 mg of cell protein/mL) was centrifuged for 5 min at 1,300 *x* g at 4 °C to remove nuclei and cellular debris and obtain a post nuclear supernatant (PNS). A volume of 1 mL of PNS was mixed with an equal volume of 85% sucrose (w/v) in TNEV buffer containing 1 mM Na_3VO_4, placed at the bottom of a discontinuous sucrose gradient (30–5%), and centrifuged for 17 h at 200,000 *x* g at 4 °C. After ultracentrifugation, 12 fractions were collected starting from the top of the tube. The light scattering band, corresponding to the DRM fraction, was located at the interface between 5 and 30% sucrose corresponding to fractions 4–6. The entire procedure was performed at 0–4° C on ice immersion. Equal amounts from each fraction were diluted with Laemmli sample buffer (0.15 M DTT, 94 mM Tris-HCl, 3% SDS w/v, 0.015% blue bromophenol, v/v) without glycerol and used for protein analysis as reported below.

Protein determination

Protein concentration of samples was assessed using a DC™ protein assay kit according to manufacturer's instructions, using BSA as standard.

Protein analysis

N2a cells were washed with cold PBS containing 1 mM Na_3VO_4 and lysed by hot Laemmli sample buffer (0.15 M DTT, 94 mM Tris-HCl, 15% glycerol, v/v, 3% SDS w/v, 0.015% blue bromophenol, v/v). After the probe sonication (50 W, 30 kHz Vibra-Cell™ Ultrasonic VXC130) and the boiling of the lysed samples for 5 min at 99 °C, equal amounts of denatured proteins derived from OligoGM1 treated and untreated cells were separated on 4–20% precast polyacrylamide gels, and transferred to PVDF membranes using the Trans -Blot® Turbo™ Transfer System (Bio -Rad).

PVDF membranes were blocked with 5% milk (w/v) in TBS-0.1% tween-20 (v/v) at 23 °C for 1 h under gentle shaking. The presence of TrkA and p-TrkA was determined by using specific rabbit primary antibodies, both diluted 1:1,000 in 5% BSA (w/v) in TBS-0.1% tween-20. PLCγ1, P-PLCγ1, PKCα, P-PKCα were detected by the specific mouse primary antibodies diluted 1:500 in 5% milk (w/v) in TBS-0.1% tween-20 (v/v). Flotillin was detected by the specific rabbit primary antibody diluted 1:1,000 in 5% milk (w/v) in TBS-0.1% tween-20 (v/v). Calnexin, used as loading controls, weas detected by the specific mouse primary antibodies diluted 1:40,000 in 5% milk (w/v) in TBS-0.1% tween-20 (v/v) and 1:1,000 in 5% BSA (w/v) in TBS-0.1% tween-20, respectively. The incubation was performed overnight (i.e. 16 h) at 4 °C under gentle shaking. Following, PVDF membranes were washed three times with TBS-0.1% tween-20. The reaction with secondary horseradish peroxidase-conjugated antibodies was following performed at 23 °C 1 h in gentle agitation. The data acquisition and analysis were performed using Alliance Uvitec (Cleaver Scientific Ltd, UK).

Calcium-imaging

N2a cells were plated at 7.5×10^3 / cm^2 on a 24 mm coverglass in complete DMEM HG medium. 48 h after plating medium was removed and cells were rinsed three times with HBSS containing calcium and magnesium ($HBSS^+$). After washing, cells were incubated with 2.5 μM Fluo-4

AM (494/506 nm) in $HBSS^+$ for 30 min at 23 °C in the dark. Subsequently cells were washed three times with $HBSS^+$ to remove any dye that is not specifically associated with the cell surface and then incubated in $HBSS^+$. Fluorescent emission was examined by live cell analysis using Axio Observer (Zeiss Axio Observer.Z1 with Hamamatsu EMCCD 9100–02) with 400X magnification. The frames were acquired every 5 sec for 20 min (Supplementary Fig. S3). After 3 min of acquisition, 50 μM OligoGM1 solubilized in $HBSS^+$ was administered to the cells and after 15 min the Ca^{2+} ionophore A23187 (2 μM) in $HBSS^+$ was added to the cells. Control cells were subjected to the same experimental conditions but $HBSS^+$ alone without OligoGM1 was administered. Only ionophore responsive cells were analysed. At least 6 cells for field were quantified. The fluorescence for each acquisition (F) was related to the basal fluorescence (Fmin) according to the following formula:

$$\frac{F - Fmin}{Fmin}$$

To evaluate the involvement of TrkA receptor in the induction of Ca^{2+} influx by the OligoGM1, the TrkA inhibitor (120 nM) was added to the growth medium 30 min before the incubation with Fluo-4. After 30 min, cells were washed three times with $HBSS^+$ and then incubated with Fluo-4 AM in $HBSS^+$ containing 120 nM TrkA inhibitor for 30 min at 23 °C in the dark. Subsequently, cells were washed three times with $HBSS^+$ and incubated in $HBSS^+$ with 120 nM TrkA inhibitor.

To inhibit the inositol trisphosphate (IP_3)-receptors, the selective membrane-permeable inhibitor of IP_3 receptor Xestospongin C (2.5 μM) [27, 28] was administered together with Fluo-4 for 30 min. After washing with $HBSS^+$, Xestospongin C was added again to the working solution and left for the entire duration of the experiment.

Statistical analysis

Data are expressed as mean ± SEM. The analysis was performed with Prism software (GraphPad Software, Inc. La Jolla, CA, USA). The normality distribution was verified using Kolmogorov–Smirnov, D' Agostino & Pearson and Shapiro-Wilk tests; in case of a non-Gaussian distribution of data, non-parametric tests were used as indicated in the legend of the figures. A p-value < 0.05 was considered significant.

Other analytical methods

NMR spectra were recorded with a Bruker AVANCE-500 spectrometer at a sample temperature of 298 K. NMR spectra were recorded in CDCl3 or CD3OD and calibrate using the TMS signal as internal reference. Mass spectrometric analysis were performed in positive or negative ESI-MS. Mass spectra were recorded on a Thermo Quest Finningan LCQTM DECA ion trap mass spectrometer, equipped with a Finnigan ESI interface; data were processed by Finnigan Xcalibur software system. All reactions were monitored by TLC on silica gel 60 plates (Merck).

Results

OligoGM1 neuritogenic effect depends on calcium levels modulation

Exogenously administered GM1, or its endogenous increase, induces the differentiation of murine neuroblastoma cells as well as the maturation state of primary neurons [3, 29]. Importantly, the GM1 mediated neurite outgrowth is known to be strictly dependent on Ca^{2+} influx [30–32].

It has recently been observed that the administration of the GM1-oligosaccharide component alone induces the same neuritogenic action in N2a cells, demonstrating that GM1 pentasaccharide is responsible for this effect [13, 14].

Additionally, proteomic analysis of N2a cells exposed to OligoGM1 identified the *ex-novo* expression of several proteins [15] involved in the regulation of Ca^{2+} homeostasis and in Ca^{2+}-dependent differentiative and neuroprotective pathways (Table 1), suggesting a possible modulation of Ca^{2+} signaling by OligoGM1.

Thus, to study the influence of Ca^{2+} on OligoGM1 enhanced neuritogenesis, 50 μM OligoGM1 was administered to N2a cells in the presence or absence of subtoxic concentrations of extracellular (EGTA, 100 μM) or intracellular (BAPTA-AM, 1 μM) Ca^{2+} chelators for 24 h. None EGTA or BAPTA-AM at indicated concentration affected the N2a cells morphology in our experimental conditions with respect to control N2a cells (Fig. 1).

As highlighted in the images reported in Fig. 1a, the presence of both extracellular and intracellular Ca^{2+} chelators abolished the neurite sprouting induced by OligoGM1 after 24 h. As it emerges from the graph in Fig. 1b, the length of the neuritogenesis in cells incubated with OligoGM1 resulted at least two-fold higher compared to the control cells but equalized the control condition when Ca^{2+} chelators were administered in combination with OligoGM1. This result suggests that, as already reported for GM1 [3], the increase of cytoplasmic Ca^{2+} is fundamental for OligoGM1-mediated neuronal differentiation.

OligoGM1 modulates intracellular calcium levels

To study the OligoGM1 ability to modulate Ca^{2+} flux required for the neuritogenesis process, we performed calcium-imaging experiments on N2a cells using the non-ratiometric

Table 1 List of the Ca^{2+}-related proteins statistically differentially expressed in OligoGM1-treated N2a cells with respect to control cells

Majority protein IDs	Protein names	Gene names
P35546	Proto-oncogene tyrosine-protein kinase receptor Ret	Ret
A0A0A6YX01	Protocadherin beta-6	Pcdhb6
E9Q622	Protocadherin 11 X-linked	Pcdh11x
A0A1L1SQU7	FAT atypical cadherin 1	Fat1
Q8VHP6	Cadherin-related family member 1	Cdhr1
Q99PJ1	Protocadherin-15	Pcdh15
F8WJ23	Hornerin	Hrnr
Q91ZZ3	Beta-synuclein	Sncb
Q8BNY6	Neuronal calcium sensor 1	Ncs1
P10493	Nidogen-1	Nid1
E9Q0N0	Intersectin-1	Itsn1
B2RPV6	Multimerin-1	Mmrn1
Q8C845	EF-hand domain-containing protein D2	Efhd2
Q8K3V4	Protein-arginine deiminase type-6	Padi6
Q704Y3	Transient receptor potential cation channel subfamily V member 1	Trpv1
Q9WTR1	Transient receptor potential cation channel subfamily V member 2	Trpv2
B2RQS1	Striatin-3	Strn3
V9GXI9	Striatin-4	Strn4
P48455	Serine/threonine-protein phosphatase 2B catalytic subunit gamma isoform	Ppp3cc
P63328	Serine/threonine-protein phosphatase 2B catalytic subunit alpha isoform	Ppp3ca
A0A087WQ44	Snf2-related CREBBP activator protein	Srcap
Q9QVP9	Protein-tyrosine kinase 2-beta	Ptk2b

Proteins were selected from the full list reported by Chiricozzi et al. [15] and obtained from three biological replicates of OligoGM1-treated versus control N2a cells. For statistical analysis, a p-value ≤ 0.01 by Student's t-test was considered significant

calcium-sensitive Fluo-4 probe. The binding of Fluo-4 to Ca^{2+} results in increased fluorescence excitation at 488 nm and consequently higher fluorescence signal levels.

We find out that the administration of OligoGM1 to undifferentiated N2a cells induces a significant Ca^{2+} influx, starting from about 5 min after OligoGM1 administration as shown in Fig. 2. On the contrary, no increase in fluorescence is observed in control cells. This result proved a direct modulation of intracellular Ca^{2+} flux by the exogenous administration of OligoGM1.

OligoGM1-mediated calcium modulation depends on TrkA activation

In N2a neuroblastoma cell line, as well as in primary neurons, the OligoGM1 is not internalized by the cells, and its effects are due to a direct interaction with TrkA receptor at the PM level [13, 14]. Thus, taking into account the reported effect prompted by GM1 on TrkA mediated neuronal differentiation [33–38] and considering the recent result where OligoGM1 was found to increase TrkA phosphorylation [13, 14], we investigated if also Ca^{2+} flow modulation could be a molecular event downstream of TrkA activation induced by OligoGM1.

To evaluate the involvement of TrkA receptor, calcium-imaging experiments were performed in the presence of a cell-permeable and highly selective TrkA inhibitor [13, 21]. First, we confirmed that the co-administration of TrkA inhibitor is able to prevent the specific TrkA receptor activation induced by OligoGM1 after 5–30 min from its addition to cell culture medium. (Fig. 3a). Following, we repeated the calcium-imaging experiment in the presence of TrkA inhibitor. As shown in Fig. 3b and Supplementary Figure S3, there is no significant increase of the fluorescence signal in the presence of TrkA inhibitor, suggesting that the opening of the cell Ca^{2+} channels and the Ca^{2+} influx following OligoGM1 administration is mediated by the activation of TrkA receptor.

Identification of the cellular pathways involved in OligoGM1-mediated calcium influx

To biochemically characterize the effect of OligoGM1 on Ca^{2+} flux in N2a cells following TrkA activation, we investigated the involvement of TrkA downstream effectors known

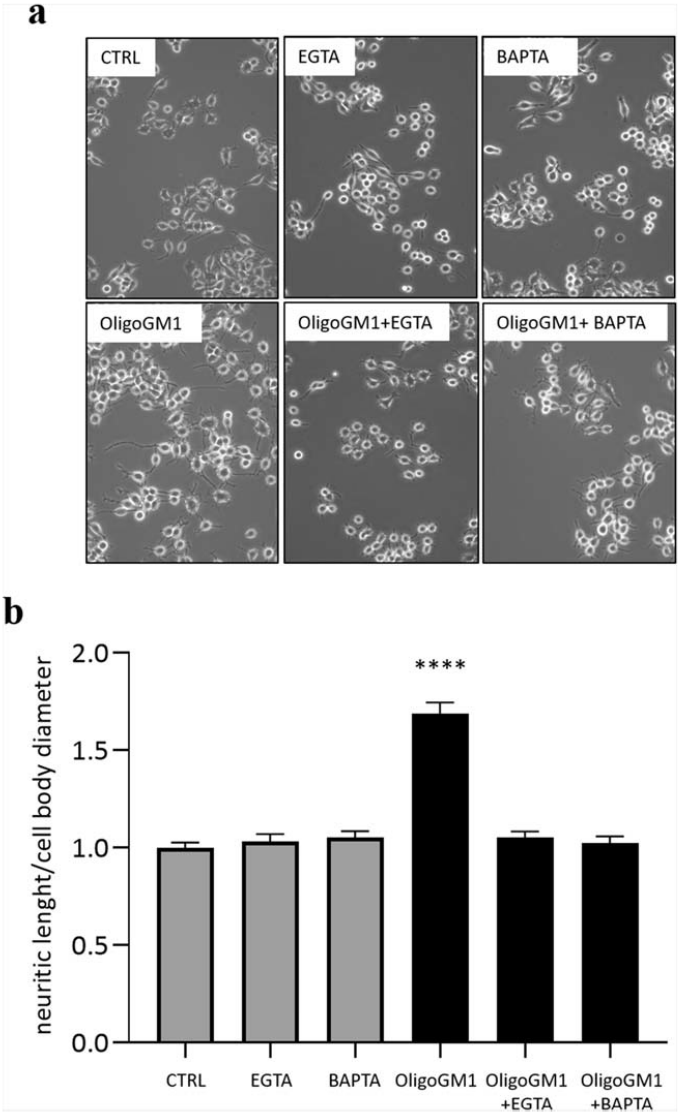

Fig. 1 Morphological outcomes of N2a cells treated with 50 μM OligoGM1 in presence or absence of 100 μM EGTA or 1 μM BAPTA-AM for 24 h. **a** Cells were observed by phase contrast microscopy with 200X magnification. Images are representative of three independent experiments ($n = 3$); **b** Evaluation of neurite sprouting and elongation in N2a cells. Neurite extensions were evaluated as the ratio between process length and cell body diameter. The bars show the mean values ± SEM from three different experiments ($n = 3$, OligoGM1 ****$p < 0.0001$ vs. CTRL, OligoGM1 + EGTA, OligoGM1 + BAPTA, non-parametric one-way ANOVA)

to modulate of Ca^{2+} signaling such as the phospholipase C gamma (PLCγ) and the protein kinase C (PKC) [39].

To unveil if OligoGM1 administration could lead to the increase of intracellular Ca^{2+} through this cellular pathway, an immunoblotting analysis evaluating the phosphorylation status of the TrkA receptor, PLCγ1 and PKCα on N2a cells after 5, 30 and 60 min following OligoGM1 administration was performed.

As shown in Fig. 4 we found that 5 min after OligoGM1 administration there is an activation of TrkA receptor, confirming previous results [13]. Moreover, we observed an enhanced activation of PLCγ1 starting from 5 min from OligoGM1 administration followed, after 1 h, by a hyperphosphorylation of PKCα1, which is a priming event that enables its catalytic activation.

Although the phosphorylation is a key event for the catalytic activity of PKC, it is known that its activation depends on its translocation to the PM [40, 41]. Thus, to verify whether the administration of OligoGM1 was followed by an enrichment of PKC in lipid rafts, 3 h after treating N2a cells with OligoGM1, lipid rafts were isolated as the DRM, according to the procedure described in "Methods" Section.

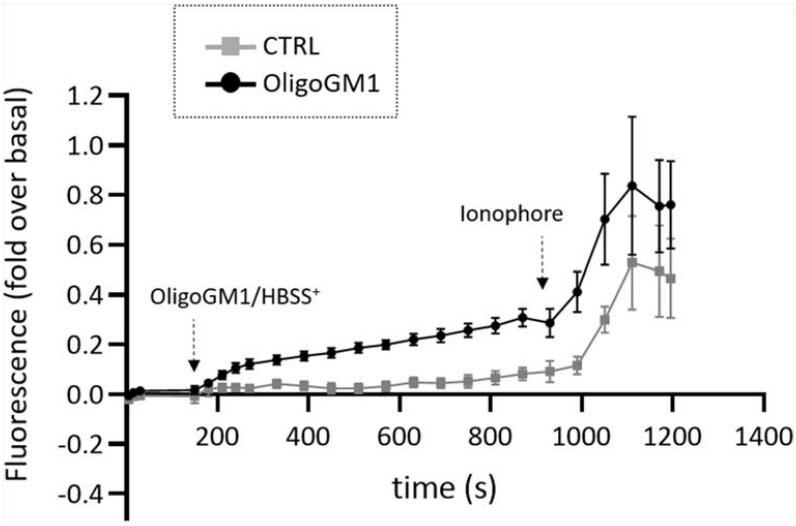

Fig. 2 OligoGM1 modulation of intracellular Ca^{2+} level. Intracellular Ca^{2+} level of N2a cells treated with 50 μM OligoGM1 was analysed measuring the green fluorescent emission of 2.5 μM Fluo-4. The frames were acquired every 5 sec for 20 min with Widefields Zeiss Axio Observer.Z1 with a 400X magnification. After 3 min of basal acquisition, OligoGM1 was administered to the cells and after 15 min the calcium ionophore A23187 (2 μM) was added. Control cells were loaded with $HBSS^+$ alone. Only ionophore responsive cells were analyzed. The fluorescence (F) of each frame (Fx) was related to the fluorescence of the basal condition (F0) (Fx-F0/F0). Results are expressed as the mean ± SEM of fluorescence intensity of at least three independent experiments (OligoGM1 $*p < 0.05$ vs. basal, one-way ANOVA, $n = 11$; OligoGM1 $**p < 0.01$ vs. CTRL, two-way ANOVA; CTRL no significant (NS) vs. basal, one-way ANOVA, $n = 5$)

Western blotting analysis revealed a PKCα enrichment in DRM fractions in OligoGM1 treated cells, while in control cells PKCα is present in the fluid membrane fraction, solubilized by the detergent (Fig. 5).

These events could be responsible for the opening of Ca^{2+} channels on both PM and intracellular storages (i.e. endoplasmic reticulum), resulting in an increase of intracellular Ca^{2+}.

To disclose if the cytoplasmic Ca^{2+} increase after OligoGM1 administration derives from the extracellular environment through the PM Ca^{2+} channels or from the intracellular storages, the calcium-imaging experiment was performed in the presence of Xestospongin C, a selective, reversible and potent inhibitor of IP_3 receptors on endoplasmic reticulum [28]. The calcium-imaging representative frames (Supplementary Fig. S3) and the relative graph shown in Fig. 6 demonstrate that in the presence of the IP_3 receptors inhibitor, the Ca^{2+} influx following OligoGM1 administration is reduced but is not completely abolished, suggesting that both PM and intracellular channels may be modulated by OligoGM1 administration.

Discussion

For several years ganglioside GM1 has been widely studied for its essential role in neuronal differentiation, protection and restoration [3, 5, 6, 29], accomplished through the cooperation with several players expressed on the PM.

In particular, the GM1 enrichment in PM allows the dimerization and activation of neurotrophins' receptors belonging to Trk family [3, 42, 43] and modulates Ca^{2+} influx channels and Ca^{2+} exchange proteins causing changes in cellular Ca^{2+} levels [3, 7, 8]. The increase of cytosolic Ca^{2+} is essential for the morphological changes accompanying the neurodifferentiative properties prompted by GM1, triggering specific signaling cascades resulting in actin depolymerization, axon protrusion, and elongation [7, 44 49].

Despite the long-standing research on the GM1, the fine molecular mechanism at the basis of its functions remained obscure until recent years when in a murine neuroblastoma cell line it has been observed that, within the entire molecule, the oligosaccharide chain (OligoGM1) represents, alone, the bioactive component of GM1 ganglioside [13]. Following its isolation from parental compound, the GM1-oligosaccharide added to the culture medium of N2a neuroblastoma cells was observed to induce the neuritogenesis process as equimolar concentration of GM1 did, acting at the PM level by enhancing the phosphorylation of the TrkA receptor followed by the increase in ERK1/2 phosphorylation [13].

This finding was supported by the revelation that, in N2a cells, TrkA and GM1 belong to separate membrane domains. In fact TrkA does not belong to lipid rafts where GM1 is located, suggesting that its interaction with GM1 and the

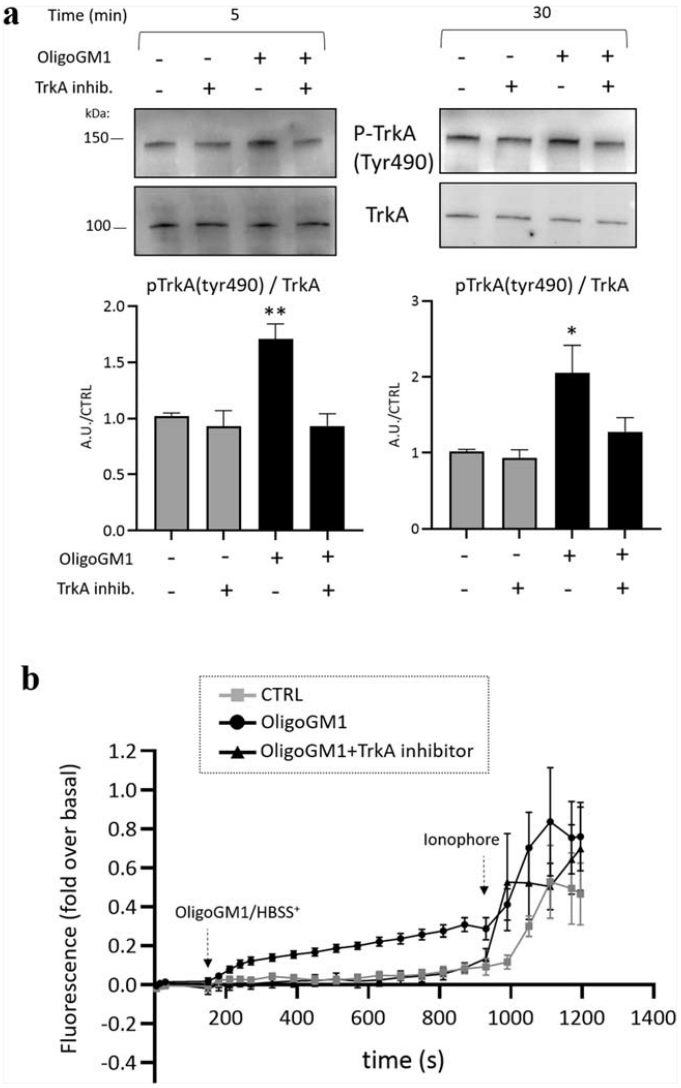

Fig. 3 OligoGM1-mediated Ca^{2+} modulation depends on TrkA activation. **a** The TrkA receptor inhibitor (120 nM) was added to the N2a cells 1 h before the administration of 50 μM OligoGM1. Expression of TrkA and p-TrkA (tyrosine 490, Tyr490) was evaluated 5 and 30 min after OligoGM1 treatment by western blot using specific antibodies and revealed by enhanced chemiluminescence. Top: immunoblotting images are shown. Bottom: semiquantitative analysis of p-TrkA related to total level of TrkA. Data are expressed as fold increase over control of the mean ± SEM from three different experiments (*$p < 0.05$, **$p < 0.01$, two-way ANOVA, $n = 3$); **b** Intracellular Ca^{2+} level of N2a cells treated with OligoGM1 was analyzed measuring the green fluorescent emission of 2.5 μM Fluo-4. The frames were acquired every 5 sec for 20 min with Widefields Zeiss Axio Observer.Z1 with a 400X magnification. The TrkA inhibitor (120 nM) was added to the culture medium for 30 min before Fluo-4 administration and left for the duration of the experiment. After 3 min of basal acquisition, 50 μM OligoGM1 was administered to the cells and after 15 min the calcium ionophore A23187 (2 μM) was added. Control cells were loaded with $HBSS^+$ alone. Only ionophore responsive cells were analyzed. The fluorescence of each frame (Fx) was related to the fluorescence of the basal condition (F0) (Fx-F0/F0). Results are expressed as the mean ± SEM of fluorescence intensity of at least three independent experiments (OligoGM1 * $p < 0.05$ vs. basal, one-way ANOVA, $n = 11$; OligoGM1 **$p < 0.01$ vs. CTRL, two-way ANOVA; OligoGM1 + TrkA inhibitor NS vs. basal, one-way ANOVA, $n = 5$; OligoGM1 + TrkA inhibitor NS vs. CTRL, two-way ANOVA)

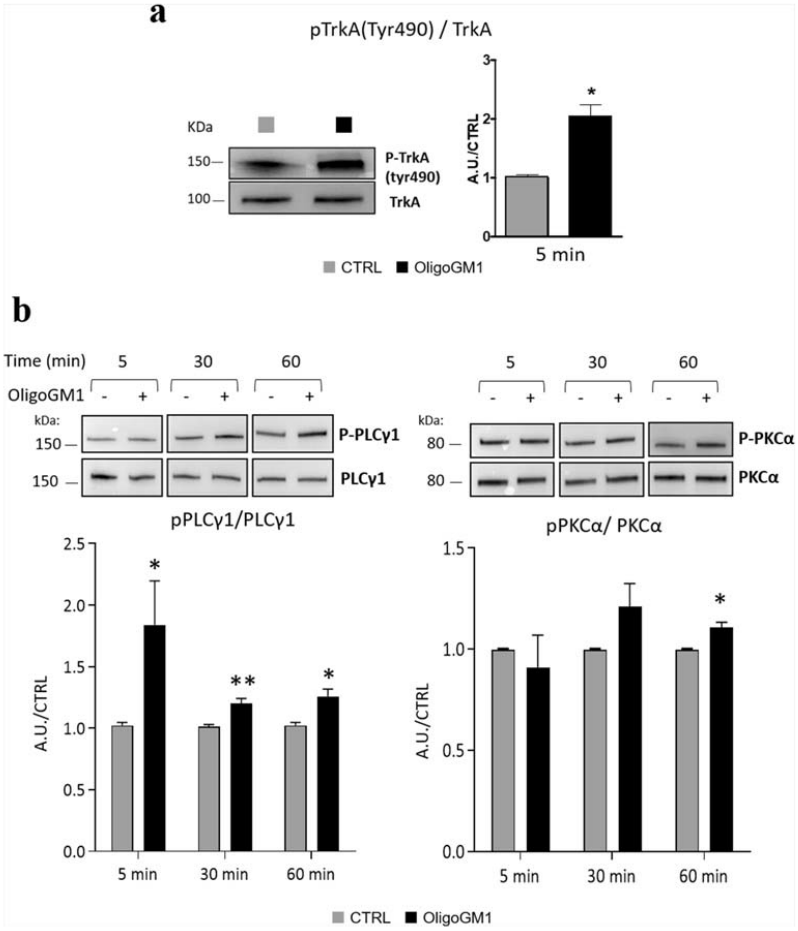

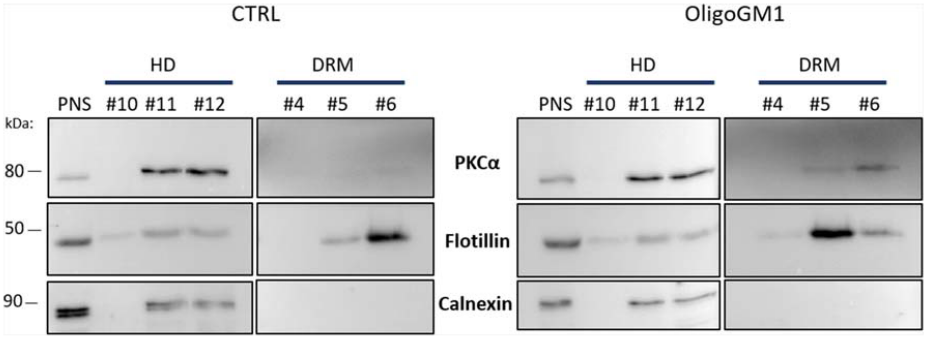

Fig. 4 OligoGM1 effect on TrkA-PLCγ1-PKCα pathway. N2a cells were culture in the absence (CTRL) or in the presence of 50 μM OligoGM1. Expression of TrkA, p-TrkA (tyr490), PLCγ1, p-PLCγ1, PKCα and p-PKCα was evaluated 5 min, 30 min and 1 h after OligoGM1 treatment by using specific antibodies and revealed by enhanced chemiluminescence. Top: representative immunoblotting images. Bottom: semi-quantitative analysis of signals of phosphorylated TrkA, PLCγ1 and PKCα related to signals of total TrkA, PLCγ1 and PKCα, respectively. Data are expressed as mean ± SEM of the fold increase over control from at least three experiments (*$p < 0.05$, **$p < 0.01$, Student's t-test)

Fig. 5 PKCα translocation in lipid rafts microdomains. N2a cells were incubated in the absence (CTRL), or in the presence of 50 μM OligoGM1 for 3 h at 37 °C. Cells were subsequently subjected to sucrose gradient ultracentrifugation to prepare PM microdomains. Twelve fractions were collected from the top of the tube, with fractions 4–6 corresponding to the detergent resistant membrane (DRM) fractions and fractions 10–12 corresponding to high density (HD) fractions. Expression of PKCα, Flotillin (DRM marker) and Calnexin (HD marker) was evaluated by western blot using specific antibodies and revealed by enhanced chemiluminescence. Images are representative of three independent cell culture preparations ($n = 3$)

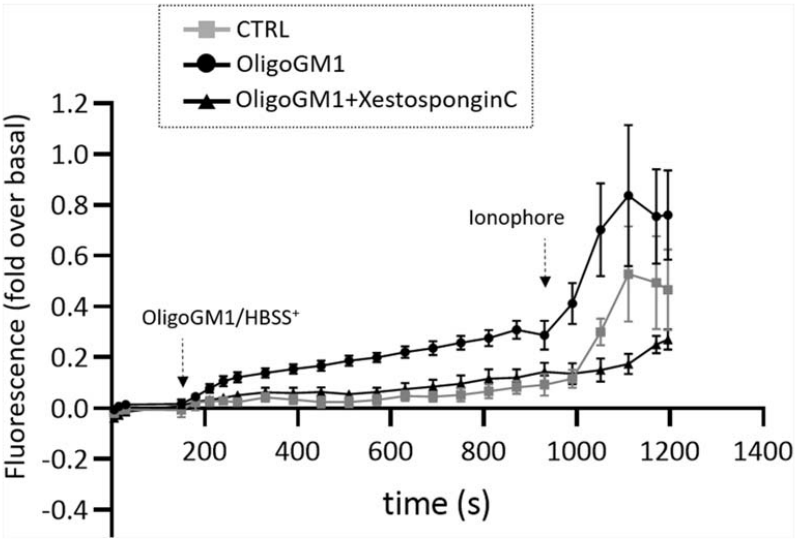

Fig. 6 OligoGM1-modulated Ca^{2+} derives from both the extracellular environment and the intracellular storages. Intracellular Ca^{2+} level of N2a cells treated with OligoGM1 was analysed measuring the green fluorescent emission of Fluo-4 (2.5 μM). The frames were acquired every 5 sec for 20 min with Widefields Zeiss Axio Observer.Z1 with a 400X magnification. The IP3 receptor inhibitor, Xestospongin C (2.5 μM) was added to the cells together with Fluo-4 for 30 min before starting the acquisitions and left for the entire duration of the experiment. After 3 min of basal acquisition, OligoGM1 (50 μM) was administered to the cells and after 15 min the calcium ionophore A23187 (2 μM) was added. Control cells were loaded with $HBSS^+$ alone. Only ionophore responsive cells were analysed. The fluorescence of each frame (Fx) was related to the fluorescence of the basal condition (F0) (Fx-F0/F0). Results are expressed as the mean ± SEM of fluorescence intensity of at least three independent experiments (OligoGM1 $*p < 0.05$ vs. basal, one-way ANOVA, $n = 11$; OligoGM1 $**p < 0.01$ vs. CTRL, two-way ANOVA; OligoGM1 + Xestospongin C $*p < 0.05$ vs. basal, one-way ANOVA, $n = 5$; OligoGM1 + Xestospongin C NS vs. CTRL, two-way ANOVA)

following stabilization which leads to its autophosphorylation involves only the GM1-oligosaccharide chain and the extracellular portion of TrkA, that may flop down on the PM approaching the GM1 saccharide [50]. These results were subsequently translated in a more physiological context by using primary cultures of murine granule cerebellar neurons [14]. According to this study, OligoGM1 administered to primary neurons enhanced cell clustering, neurite sprouting and networking, thus confirming the specific role of the OligoGM1 in the processes of neuronal differentiation and maturation, known to be regulated by the entire GM1.

Here, to further clarify the mechanism of action of OligoGM1, as the bioactive portion of GM1, we examined its ability to modulate the cellular Ca^{2+} flow, at the basis of the neuritogenic properties induced by GM1, using mouse neuroblastoma cells N2a as experimental model.

As shown by calcium-imaging experiments, the administration of 50 μM OligoGM1 to undifferentiated N2a is capable of inducing a significant Ca^{2+} intake starting from 5 min after OligoGM1 application (Fig. 2). This latency time suggests that the entry of Ca^{2+} is not due to the direct interaction of OligoGM1 with Ca^{2+} channels on the PM neither with intracellular channels, since it was demonstrated [13, 14] that the OligoGM1 is not internalized by the cells but rather it could be a result of the activation of PM receptors and downstream signaling pathways.

Since OligoGM1 carries out its neurotrophic and neuroprotective activities interacting with the TrkA receptor on PM, we verified a direct participation of TrkA in the OligoGM1-mediated Ca^{2+} modulation, performing the calcium-imaging experiment in the presence of the TrkA inhibitor. In this case, no Ca^{2+} influx was observed following OligoGM1 administration, indicating that TrkA receptor activation is the upstream event modulating Ca^{2+} flux upon OligoGM1 addition (Fig. 3b).

Subsequently, we studied in more detail the involvement of signaling proteins downstream of TrkA receptor, known to be responsible for cellular Ca^{2+} mobilization, such as PLCγ.

PLCγ is a membrane-associated enzyme that cleaves PIP_2 into DAG and IP_3 [51]. The two products of the PLC catalysed reaction, DAG and IP_3, are important second messengers that propagate and regulate cellular signaling via Ca^{2+} mobilization and activation of protein kinases, such as PKC, and ion channels [51]. When PIP_2 is cleaved, DAG remains bound to the membrane, whereas IP_3 is released as a soluble molecule into the cytosol, binding IP_3-sensitive intracellular Ca^{2+} channels predominately located in the membrane of the endoplasmic reticulum, regulating the Ca^{2+} flux from

intracellular stores to the cytosol [52]. The other product, DAG, triggers Ca^{2+} influx from extracellular environment independently from IP_3 activity by directing plasma membrane TRP channels [53] and activating PKC [54]. The function of the PKC is regulated by two mechanisms: its phosphorylation allows the correct alignment of the residues necessary for the catalysis, while the increase in the intracellular Ca^{2+} concentration triggers the membrane translocation of PKC and its association with DAG at the PM microdomains, stimulating the enzyme activity [40, 41, 54]. Additionally, PKC phosphorylates other molecules, modulating several cellular events: the activation of PKC in the nervous system has been involved in the regulation of ion channels activity, neurotransmitter release, growth, differentiation, and neural plasticity [54].

By immunoblotting analysis we found a hyperphosphorylation of PLCγ occurring 5 min upon OligoGM1 administration (Fig. 4), followed by a hyperphosphorylation of PKC 1 h after OligoGM1 was supplemented to the medium and by its enrichment in lipid rafts, confirming its activation (Fig. 5).

The involvement of IP_3 in mobilizing Ca^{2+} from the intracellular stores was confirmed by calcium-imaging experiments performed by administering OligoGM1 together with the selective IP_3 inhibitor, Xestospongin C [27, 28]. Interestingly, while a lower increase in intracellular Ca^{2+} level was recorded (Fig. 6), the Ca^{2+} influx was not completely abolished, suggesting the possible involvement of Ca^{2+} channels of both the intracellular and plasma membranes in the modulation of the cytoplasmic Ca^{2+} levels, which could be activated by IP_3 and DAG respectively.

Thus, we finally proved that GM1 neuritogenic effect is mediated by an increase in intracellular Ca^{2+} following the OligoGM1-TrkA interaction at the PM level, leading to the recruitment and activation of multiple intracellular players eventually promoting neurite sprouting (Fig. 7). In fact, we observed that OligoGM1 is not able to induce neurite emission in N2a cells if Ca^{2+} ions, both intracellular and extracellular, are chelated (Fig. 1), suggesting that the modulation of cytosolic Ca^{2+} levels by OligoGM1 is fundamental for the execution of its neurodifferentiative properties.

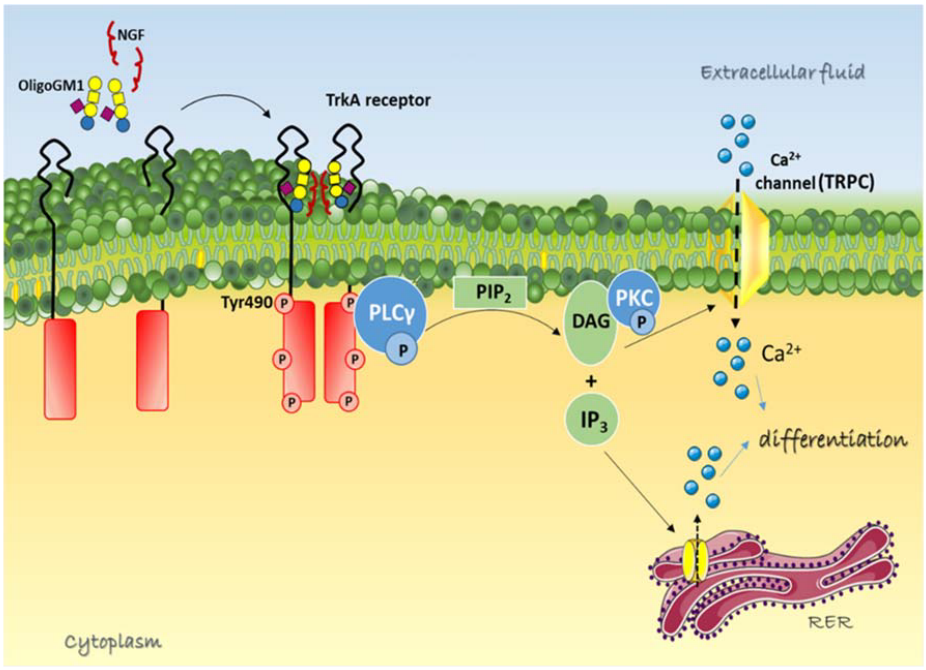

Fig. 7 Schematic representation of molecular mechanism underling OligoGM1 neurotrophic function. OligoGM1 enhances the activation of TrkA signaling pathway, which could be associated to an increased activation of PLCγ1, leading to the formation of second messengers DAG and IP3. These events bring to the opening of Ca^{2+} channels on the PM and on endoplasmic reticulum, leading to an increase of cytosolic Ca^{2+} responsible for N2a differentiation. TrkA, neurotrophin tyrosine kinase receptor A; NGF, nerve growth factor; PLCγ, phospholipase C gamma; PIP2, phosphatidylinositol 4,5-bisphosphate; DAG, diacylglycerol; IP3, inositol 1,4,5-trisphosphate; PKC, protein kinase C; TRPC, transient receptor potential channel; RER, rough endoplasmic reticulum. GM1 sugar code is according to Varki et al. 2015 [55]. This image is updated from Chiricozzi et al. [13]

Although here the identity of Ca^{2+} channels modulated by OligoGM1 has not been identified and will be investigate in a later study, the present work demonstrates that the GM1-oligosaccharide is responsible on its own also for the GM1 modulation of Ca^{2+} homeostasis and that the regulation of Ca^{2+} signaling is a fundamental mechanism at the base of OligoGM1 neurogenic action, partially revealing the mechanism of action of the oligosaccharide chain of ganglioside GM1.

Supplementary Information The online version contains supplementary material available at https://doi.org/10.1007/s10719-020-09963-7.

Acknowledgements This work was supported by University of Milano departmental funds RV_TAR16SSONN_M to SS and by Mizutani Foundation for Glycoscience funds to EC. The authors acknowledge Euro-BioImaging (www.eurobioimaging.eu) for providing access to imaging technologies and services via the Italian Node (ALEMBIC, Milano, Italy).

Funding Open access funding provided by Università degli Studi di Milano within the CRUI-CARE Agreement.

Compliance with ethical standards

Conflict of interest The authors declare that they have no conflicts of interest.

Ethical approval This article does not contain any studies with human participants or animals performed by any of the authors.

References

1. Schengrund, C.L., Ringler, N.J.: Binding of Vibrio cholera toxin and the heat-labile enterotoxin of Escherichia coli to GM1, derivatives of GM1, and nonlipid oligosaccharide polyvalent ligands. J. Biol. Chem. **264**, 13233–13237 (1989)
2. Schengrund, C.L., Mummert, C.M.: Exogenous gangliosides. How do they cross the blood-brain barrier and how do they inhibit cell proliferation. Ann N Y Acad Sci. **845**, 278–284 (1998)
3. Ledeen, R.W., Wu, G.: The multi-tasked life of GM1 ganglioside, a true factotum of nature. Trends Biochem. Sci. **40**, 407–418 (2015)
4. Zhai, H.W., Gong, Z.K., Sun, J., Chen, W., Zhang, M., Zhou, J.J., Zheng, B.: Ganglioside with nerve growth factor for the recovery of extremity function following spinal cord injury and somatosensory evoked potential. Eur. Rev. Med. Pharmacol. Sci. **19**, 2282–2286 (2015)
5. Aureli, M., Mauri, L., Ciampa, M.G., Prinetti, A., Toffano, G., Secchieri, C., Sonnino, S.: GM1 ganglioside: past studies and future potential. Mol. Neurobiol. **53**, 1824–1842 (2016)
6. Chiricozzi, E., Lunghi, G., Di Biase, E., Fazzari, M., Sonnino, S., Mauri, L.: GM1 Ganglioside is a key factor in maintaining the mammalian neuronal functions avoiding neurodegeneration. Int. J. Mol. Sci. **21**, 868 (2020)
7. Wu, G., Fang, Y., Lu, Z.H., Ledeen, R.W.: Induction of axon-like and dendrite-like processes in neuroblastoma cells. J. Neurocytol. **27**, 1–14 (1998)
8. Wu, G., Xie, X., Lu, Z.H., Ledeen, R.W.: Sodium-calcium exchanger complexed with GM1 ganglioside in nuclear membrane transfers calcium from nucleoplasm to endoplasmic reticulum. Proc. Natl. Acad. Sci. U. S. A. **106**, 10829–10834 (2009)
9. Wu, G., Ledeen, R.W.: Stimulation of neurite outgrowth in neuroblastoma cells by neuraminidase: putative role of GM1 ganglioside in differentiation. J. Neurochem. **56**, 95–104 (1991)
10. Wu, G., Lu, Z.H., Obukhov, A.G., Nowycky, M.C., Ledeen, R.W.: Induction of calcium influx through TRPC5 channels by cross-linking of GM1 ganglioside associated with alpha5beta1 integrin initiates neurite outgrowth. J. Neurosci. **27**, 7447–7458 (2007)
11. Wu, G., Lu, Z.H., Xie, X., Ledeen, R.W.: Susceptibility of cerebellar granule neurons from GM2/GD2 synthase-null mice to apoptosis induced by glutamate excitotoxicity and elevated KCl: rescue by GM1 and LIGA20. Glycoconj. J. **21**, 305–313 (2004)
12. Wu, G., Xie, X., Lu, Z.H., Ledeen, R.W.: Cerebellar neurons lacking complex gangliosides degenerate in the presence of depolarizing levels of potassium. Proc. Natl. Acad. Sci. U. S. A. **98**, 307–312 (2001)
13. Chiricozzi, E., Pome, D.Y., Maggioni, M., Di Biase, E., Parravicini, C., Palazzolo, L., Loberto, N., Eberini, I., Sonnino, S.: Role of the GM1 ganglioside oligosaccharide portion in the TrkA-dependent neurite sprouting in neuroblastoma cells. J. Neurochem. **143**, 645–659 (2017)
14. Di Biase, E., Lunghi, G., Fazzari, M., Maggioni, M., Pome, D.Y., Valsecchi, M., Samarani, M., Fato, P., Ciampa, M.G., Prioni, S., Mauri, L., Sonnino, S., Chiricozzi, E.: Gangliosides in the differentiation process of primary neurons: the specific role of GM1-oligosaccharide. Glycoconj. J. **37**, 329–343 (2020)
15. Chiricozzi, E., Maggioni, M., di Biase, E., Lunghi, G., Fazzari, M., Loberto, N., Elisa, M., Scalvini, F.G., Tedeschi, G., Sonnino, S.: The neuroprotective role of the GM1 oligosaccharide, II(3)Neu5Ac-Gg4, in neuroblastoma cells. Mol. Neurobiol. **56**, 6673–6702 (2019)
16. Fazzari, M., Audano, M., Lunghi, G., Di Biase, E., Loberto, N., Mauri, L., Mitro, N., Sonnino, S., Chiricozzi, E.: The oligosaccharide portion of ganglioside GM1 regulates mitochondrial function in neuroblastoma cells. Glycoconj. J. **37**(3), 293–306 (2020)
17. Chiricozzi, E., Mauri, L., Lunghi, G., Di Biase, E., Fazzari, M., Maggioni, M., Valsecchi, M., Prioni, S., Loberto, N., Pome, D.Y., Ciampa, M.G., Fato, P., Verlengia, G., Cattaneo, S., Assini, R., Wu, G., Alselehdar, S., Ledeen, R.W., Sonnino, S.: Parkinson's disease recovery by GM1 oligosaccharide treatment in the B4galnt1(+/-) mouse model. Sci. Rep. **9**, 19330 (2019)
18. Tettamanti, G., Bonali, F., Marchesini, S., Zambotti, V.: A new procedure for the extraction, purification and fractionation of brain gangliosides. Biochim. Biophys. Acta **296**, 160–170 (1973)
19. Acquotti, D., Poppe, L., Dabrowski, J., Von der Lieth, C.W., Sonnino, S., Tettamanti, G.: Three-dimensional structure of the

oligosaccharide chain of GM1 ganglioside revealed by a distance-mapping procedure: A rotating and laboratory frame nuclear Overhauser enhancement investigation of native glycolipid in dimethyl sulfoxide and in water-dodecylphosphocholine solutions. J. Am. Chem. Soc. **112**, 7772–7778 (1990)
20. Wiegandt, H., Bucking, H.W.: Carbohydrate components of extraneuronal gangliosides from bovine and human spleen, and bovine kidney. Eur. J. Biochem. **15**, 287–292 (1970)
21. Wood, E.R., Kuyper, L., Petrov, K.G., Hunter, R.N. III; Harris, P.A., Lackey, K.: Discovery and in vitro evaluation of potent TrkA kinase inhibitors: oxindole and aza-oxindoles. Bioorg. Med. Chem. Lett. **14**, 953–7 (2004)
22. Chiricozzi, E., Fernandez-Fernandez, S., Nardicchi, V., Almeida, A., Bolanos, J.P., Goracci, G.: Group IIA secretory phospholipase A2 (GIIA) mediates apoptotic death during NMDA receptor activation in rat primary cortical neurons. J. Neurochem. **112**, 1574–1583 (2010)
23. Schengrund, C.L., Prouty, C.: Oligosaccharide portion of GM1 enhances process formation by S20Y neuroblastoma cells. J. Neurochem. **51**, 277–282 (1988)
24. Sato, C., Matsuda, T., Kitajima, K.: Neuronal differentiation-dependent expression of the disialic acid epitope on CD166 and its involvement in neurite formation in Neuro2A cells. J. Biol. Chem. **277**, 45299–45305 (2002)
25. Chiricozzi, E., Ciampa, M.G., Brasile, G., Compostella, F., Prinetti, A., Nakayama, H., Ekyalongo, R.C., Iwabuchi, K., Sonnino, S., Mauri, L.: Direct interaction, instrumental for signaling processes, between LacCer and Lyn in the lipid rafts of neutrophil-like cells. J. Lipid Res. **56**, 129–141 (2015)
26. Schiumarini, D., Loberto, N., Mancini, G., Bassi, R., Giussani, P., Chiricozzi, E., Samarani, M., Munari, S., Tamanini, A., Cabrini, G., Lippi, G., Dechecchi, M.C., Sonnino, S., Aureli, M.: Evidence for the involvement of lipid rafts and plasma membrane sphingolipid hydrolases in pseudomonas aeruginosa infection of cystic fibrosis bronchial epithelial cells. Mediat. Inflamm. **2017**, 1730245 (2017)
27. Miyamoto, S., Izumi, M., Hori, M., Kobayashi, M., Ozaki, H., Karaki, H.: Xestospongin C, a selective and membrane-permeable inhibitor of IP(3) receptor, attenuates the positive inotropic effect of alpha-adrenergic stimulation in guinea-pig papillary muscle. Br. J. Pharmacol. **130**, 650–654 (2000)
28. Gafni, J., Munsch, J.A., Lam, T.H., Catlin, M.C., Costa, L.G., Molinski, T.F., Pessah, I.N.: Xestospongins: potent membrane permeable blockers of the inositol 1,4,5-trisphosphate receptor. Neuron. **19**, 723–33 (1997)
29. Schengrund, C.L.: Gangliosides: glycosphingolipids essential for normal neural development and function. Trends Biochem. Sci. **40**, 397–406 (2015)
30. Masco, D., Van de Walle, M., Spiegel, S.: Interaction of ganglioside GM1 with the B subunit of cholera toxin modulates growth and differentiation of neuroblastoma N18 cells. J. Neurosci. **11**, 2443–2452 (1991)
31. Wu, G., Ledeen, R.W.: Gangliosides as modulators of neuronal calcium. Prog. Brain Res. **101**, 101–112 (1994)
32. Fang, Y., Wu, G., Xie, X., Lu, Z.H., Ledeen, R.W.: Endogenous GM1 ganglioside of the plasma membrane promotes neuritogenesis by two mechanisms. Neurochem. Res. **25**, 931–940 (2000)
33. Farooqui, T., Franklin, T., Pearl, D.K., Yates, A.J.: Ganglioside GM1 enhances induction by nerve growth factor of a putative dimer of TrkA. J. Neurochem. **68**, 2348–2355 (1997)
34. Singleton, D.W., Lu, C.L., Colella, R., Roisen, F.J.: Promotion of neurite outgrowth by protein kinase inhibitors and ganglioside GM1 in neuroblastoma cells involves MAP kinase ERK1/2. Int. J. Dev. Neurosci. **18**, 797–805 (2000)
35. Duchemin, A.M., Ren, Q., Mo, L., Neff, N.H., Hadjiconstantinou, M.: GM1 ganglioside induces phosphorylation and activation of Trk and Erk in brain. J. Neurochem. **81**, 696–707 (2002)
36. Da Silva, J.S., Hasegawa, T., Miyagi, T., Dotti, C.G., Abad-Rodriguez, J.: Asymmetric membrane ganglioside sialidase activity specifies axonal fate. Nat. Neurosci. **8**, 606–615 (2005)
37. Mocchetti, I.: Exogenous gangliosides, neuronal plasticity and repair, and the neurotrophins. Cell. Mol. Life Sci. **62**, 2283–2294 (2005)
38. Zakharova, I.O., Sokolova, T.V., Vlasova, Y.A., Furaev, V.V., Rychkova, M.P., Avrova, N.F.: GM1 ganglioside activates ERK1/2 and Akt downstream of Trk tyrosine kinase and protects PC12 cells against hydrogen peroxide toxicity. Neurochem. Res. **39**, 2262–2275 (2014)
39. Huang, E.J., Reichardt, L.F.: Trk receptors: roles in neuronal signal transduction. Annu. Rev. Biochem. **72**, 609–642 (2003)
40. Freeley, M., Kelleher, D., Long, A.: Regulation of Protein Kinase C function by phosphorylation on conserved and non-conserved sites. Cell. Signal **23**, 753–762 (2011)
41. Igumenova, T.I.: Dynamics and membrane interactions of Protein Kinase C. Biochemistry. **54**, 4953–68 (2015)
42. Mutoh, T., Tokuda, A., Miyadai, T., Hamaguchi, M., Fujiki, N.: Ganglioside GM1 binds to the Trk protein and regulates receptor function. Proc. Natl. Acad. Sci. U. S. A. **92**, 5087–5091 (1995)
43. Rabin, S.J., Mocchetti, I.: GM1 ganglioside activates the high-affinity nerve growth factor receptor trkA. J. Neurochem. **65**, 347–354 (1995)
44. Kappagantula, S., Andrews, M.R., Cheah, M., Abad-Rodriguez, J., Dotti, C.G., Fawcett, J.W.: Neu3 sialidase-mediated ganglioside conversion is necessary for axon regeneration and is blocked in CNS axons. J. Neurosci. **34**, 2477–2492 (2014)
45. Wu, G., Lu, Z.H., Nakamura, K., Spray, D.C., Ledeen, R.W.: Trophic effect of cholera toxin B subunit in cultured cerebellar granule neurons: modulation of intracellular calcium by GM1 ganglioside. J. Neurosci. Res. **44**, 243–54 (1996)
46. Milani, D., Minozzi, M.C., Petrelli, L., Guidolin, D., Skaper, S.D., Spoerri, P.E.: Interaction of ganglioside GM1 with the B subunit of cholera toxin modulates intracellular free calcium in sensory neurons. J. Neurosci. Res. **33**, 466–475 (1992)
47. Bachis, A., Rabin, S.J., Del Fiacco, M., Mocchetti, I.: Gangliosides prevent excitotoxicity through activation of TrkB receptor. Neurotox. Res. **4**, 225–234 (2002)
48. Sokolova, T.V., Rychkova, M.P., Avrova, N.F.: [Protective effect of GM1 ganglioside against toxic action of glutamate on cerebellar granule cells]. Zh. Evol. Biokhim. Fiziol. **50**, 399–401 (2014)
49. Park, D.H., Wang, L., Pittock, P., Lajoie, G., Whitehead, S.N.: Increased expression of GM1 detected by electrospray mass spectrometry in rat primary embryonic cortical neurons exposed to glutamate toxicity. Anal. Chem. **88**, 7844–7852 (2016)
50. Chiricozzi, E., Biase, E.D., Maggioni, M., Lunghi, G., Fazzari, M., Pome, D.Y., Casellato, R., Loberto, N., Mauri, L., Sonnino, S.: GM1 promotes TrkA-mediated neuroblastoma cell differentiation by occupying a plasma membrane domain different from TrkA. J. Neurochem. **149**, 231–241 (2019)
51. Fukami, K., Inanobe, S., Kanemaru, K., Nakamura, Y.: Phospholipase C is a key enzyme regulating intracellular calcium and modulating the phosphoinositide balance. Prog. Lipid Res. **49**, 429–437 (2010)
52. Alzayady, K.J., Wang, L., Chandrasekhar, R., Wagner, L.E. II, Van Petegem, F., Yule, D.I.: Defining the stoichiometry of inositol 1,4,5-trisphosphate binding required to initiate Ca2 + release. Sci. Signal. **9**, ra35 (2016)
53. Hofmann, T., Obukhov, A.G., Schaefer, M., Harteneck, C., Gudermann, T., Schultz, G.: Direct activation of human TRPC6 and TRPC3 channels by diacylglycerol. Nature. **397**, 259–263 (1999)
54. Huang, K.P.: The mechanism of protein kinase C activation. Trends Neurosci. **12**, 425–432 (1989)

55. Varki, A., Cummings, R.D., Aebi, M., Packer, N.H., Seeberger, P.H., Esko, J.D., Stanley, P., Hart, G., Darvill, A., Kinoshita, T., Prestegard, J.J., Schnaar, R.L., Freeze, H.H., Marth, J.D., Bertozzi, C.R., Etzler, M.E., Frank, M., Vliegenthart, J.F., Lutteke, T., Perez, S., Bolton, E., Rudd, P., Paulson, J., Kanehisa, M., Toukach, P., Aoki-Kinoshita, K.F., Dell, A., Narimatsu, H., York, W., Taniguchi, N., Kornfeld, S.: Symbol Nomenclature for graphical representations of glycans. Glycobiology. **25**, 1323–4 (2015)

56. Chester, M.A.: IUPAC-IUB Joint Commission on Biochemical Nomenclature (JCBN). Nomenclature of glycolipids–recommendations 1997. Eur. J. Biochem. **257**, 293–298 (1998)

References

Acquotti, D. , L. Poppe, J. Dabrowski, C. W. Von der Lieth, S. Sonnino, and G. Tettamanti. 1990. 'Three-dimensional structure of the oligosaccharide chain of GM1 ganglioside revealed by a distance-mapping procedure: A rotating and laboratory frame nuclear Overhauser enhancement investigation of native glycolipid in dimethyl sulfoxide and in water-dodecylphosphocholine solutions', *Journal of the American Chemical Society*, 112: 7772-78.

Alzayady, K. J., L. Wang, R. Chandrasekhar, L. E. Wagner, 2nd, F. Van Petegem, and D. I. Yule. 2016. 'Defining the stoichiometry of inositol 1,4,5-trisphosphate binding required to initiate Ca2+ release', *Sci Signal*, 9: ra35.

Audano, M., S. Pedretti, M. Crestani, D. Caruso, E. De Fabiani, and N. Mitro. 2019. 'Mitochondrial dysfunction increases fatty acid beta-oxidation and translates into impaired neuroblast maturation', *FEBS Lett*, 593: 3173-89.

Aureli, M., N. Loberto, P. Lanteri, V. Chigorno, A. Prinetti, and S. Sonnino. 2011. 'Cell surface sphingolipid glycohydrolases in neuronal differentiation and aging in culture', *J Neurochem*, 116: 891-9.

Aureli, M., L. Mauri, M. G. Ciampa, A. Prinetti, G. Toffano, C. Secchieri, and S. Sonnino. 2016. 'GM1 Ganglioside: Past Studies and Future Potential', *Mol Neurobiol*, 53: 1824-42.

Avrova, N. F., I. V. Victorov, V. A. Tyurin, I. O. Zakharova, T. V. Sokolova, N. A. Andreeva, E. V. Stelmaschuk, Y. Y. Tyurina, and V. S. Gonchar. 1998. 'Inhibition of glutamate-induced intensification of free radical reactions by gangliosides: possible role in their protective effect in rat cerebellar granule cells and brain synaptosomes', *Neurochem Res*, 23: 945-52.

Bachis, A., S. J. Rabin, M. Del Fiacco, and I. Mocchetti. 2002. 'Gangliosides prevent excitotoxicity through activation of TrkB receptor', *Neurotox Res*, 4: 225-34.

Bartels, T., N. C. Kim, E. S. Luth, and D. J. Selkoe. 2014. 'N-alpha-acetylation of alpha-synuclein increases its helical folding propensity, GM1 binding specificity and resistance to aggregation', *PLoS One*, 9: e103727.

Bertoli, E., M. Masserini, S. Sonnino, R. Ghidoni, B. Cestaro, and G. Tettamanti. 1981. 'Electron paramagnetic resonance studies on the fluidity and surface dynamics of egg phosphatidylcholine vesicles containing gangliosides', *Biochim Biophys Acta*, 647: 196-202.

Besnard, A., B. Galan-Rodriguez, P. Vanhoutte, and J. Caboche. 2011. 'Elk-1 a transcription factor with multiple facets in the brain', *Front Neurosci*, 5: 35.

Breiden, B., and K. Sandhoff. 2018. 'Ganglioside Metabolism and Its Inherited Diseases', *Methods Mol Biol*, 1804: 97-141.

Burette, A., J. M. Rockwood, E. E. Strehler, and R. J. Weinberg. 2003. 'Isoform-specific distribution of the plasma membrane Ca2+ ATPase in the rat brain', *J Comp Neurol*, 467: 464-76.

Cantu, L., M. Corti, S. Sonnino, and G. Tettamanti. 1986. 'Light scattering measurements on gangliosides: dependence of micellar properties on molecular structure and temperature', *Chem Phys Lipids*, 41: 315-28.

Carpenter, G., and Qs Ji. 1999. 'Phospholipase C-gamma as a signal-transducing element', *Exp Cell Res*, 253: 15-24.

Chen, C., Z. Shi, W. Zhang, M. Chen, F. He, Z. Zhang, Y. Wang, M. Feng, W. Wang, Y. Zhao, J. H. Brown, S. Jiao, and Z. Zhou. 2014. 'Striatins contain a noncanonical coiled coil that binds protein phosphatase 2A A subunit to form a 2:2 heterotetrameric core of striatin-interacting phosphatase and kinase (STRIPAK) complex', *J Biol Chem*, 289: 9651-61.

Chester, M. A. 1998. 'IUPAC-IUB Joint Commission on Biochemical Nomenclature (JCBN). Nomenclature of glycolipids--recommendations 1997', *Eur J Biochem*, 257: 293-8.

Chiricozzi, E., E. D. Biase, M. Maggioni, G. Lunghi, M. Fazzari, D. Y. Pome, R. Casellato, N. Loberto, L. Mauri, and S. Sonnino. 2019. 'GM1 promotes TrkA-mediated neuroblastoma cell differentiation by occupying a plasma membrane domain different from TrkA', *J Neurochem*, 149: 231-41.

Chiricozzi, E., M. G. Ciampa, G. Brasile, F. Compostella, A. Prinetti, H. Nakayama, R. C. Ekyalongo, K. Iwabuchi, S. Sonnino, and L. Mauri. 2015. 'Direct interaction, instrumental for signaling processes, between LacCer and Lyn in the lipid rafts of neutrophil-like cells', *J Lipid Res*, 56: 129-41.

Chiricozzi, E., S. Fernandez-Fernandez, V. Nardicchi, A. Almeida, J. P. Bolanos, and G. Goracci. 2010. 'Group IIA secretory phospholipase A2 (GIIA) mediates apoptotic death during NMDA receptor activation in rat primary cortical neurons', *J Neurochem*, 112: 1574-83.

Chiricozzi, E., G. Lunghi, E. Di Biase, M. Fazzari, S. Sonnino, and L. Mauri. 2020. 'GM1 Ganglioside Is A Key Factor in Maintaining the Mammalian Neuronal Functions Avoiding Neurodegeneration', *Int J Mol Sci*, 21.

Chiricozzi, E., M. Maggioni, E. di Biase, G. Lunghi, M. Fazzari, N. Loberto, M. Elisa, F. G. Scalvini, G. Tedeschi, and S. Sonnino. 2019. 'The Neuroprotective Role of the GM1 Oligosaccharide, II(3)Neu5Ac-Gg4, in Neuroblastoma Cells', *Mol Neurobiol*, 56: 6673-702.

Chiricozzi, E., L. Mauri, G. Lunghi, E. Di Biase, M. Fazzari, M. Maggioni, M. Valsecchi, S. Prioni, N. Loberto, D. Y. Pome, M. G. Ciampa, P. Fato, G. Verlengia, S. Cattaneo, R. Assini, G. Wu, S. Alselehdar, R. W. Ledeen, and S. Sonnino. 2019. 'Parkinson's disease recovery by GM1 oligosaccharide treatment in the B4galnt1(+/-) mouse model', *Sci Rep*, 9: 19330.

Chiricozzi, E., D. Y. Pome, M. Maggioni, E. Di Biase, C. Parravicini, L. Palazzolo, N. Loberto, I. Eberini, and S. Sonnino. 2017. 'Role of the GM1 ganglioside oligosaccharide portion in the TrkA-dependent neurite sprouting in neuroblastoma cells', *J Neurochem*, 143: 645-59.

Coccetti, P., F. Tripodi, G. Tedeschi, S. Nonnis, O. Marin, S. Fantinato, C. Cirulli, M. Vanoni, and L. Alberghina. 2008. 'The CK2 phosphorylation of catalytic domain of Cdc34 modulates its activity at the G1 to S transition in Saccharomyces cerevisiae', *Cell Cycle*, 7: 1391-401.

Corti, M., V. Degiorgio, R. Ghidoni, S. Sonnino, and G. Tettamanti. 1980. 'Laser-light scattering investigation of the micellar properties of gangliosides', *Chem Phys Lipids*, 26: 225-38.

Coskun, U., and K. Simons. 2011. 'Cell membranes: the lipid perspective', *Structure*, 19: 1543-8.

Costa, E., D. Armstrong, A. Guidotti, A. Kharlamov, L. Kiedrowski, and J. T. Wroblewski. 1993. 'Ganglioside GM1 and its semisynthetic lysogangliosides reduce glutamate neurotoxicity by a novel mechanism', *Adv Exp Med Biol*, 341: 129-41.

Da Silva, J. S., T. Hasegawa, T. Miyagi, C. G. Dotti, and J. Abad-Rodriguez. 2005. 'Asymmetric membrane ganglioside sialidase activity specifies axonal fate', *Nat Neurosci*, 8: 606-15.

Dell'Orco, M., P. Milani, L. Arrigoni, O. Pansarasa, V. Sardone, E. Maffioli, F. Polveraccio, M. Bordoni, L. Diamanti, M. Ceroni, F. A. Peverali, G. Tedeschi, and C. Cereda. 2016. 'Hydrogen peroxide-mediated induction of SOD1 gene transcription is independent from Nrf2 in a cellular model of neurodegeneration', *Biochim Biophys Acta*, 1859: 315-23.

Denham, D. A., D. T. Dennis, T. Ponnudurai, G. S. Nelson, and F. Guy. 1971. 'Comparison of a counting chamber and thick smear methods of counting microfilariae', *Trans R Soc Trop Med Hyg*, 65: 521-6.

Di Biase, E., G. Lunghi, M. Fazzari, M. Maggioni, D. Y. Pome, M. Valsecchi, M. Samarani, P. Fato, M. G. Ciampa, S. Prioni, L. Mauri, S. Sonnino, and E. Chiricozzi. 2020. 'Gangliosides in the differentiation process of primary neurons: the specific role of GM1-oligosaccharide', *Glycoconj J*.

Duchemin, A. M., Q. Ren, L. Mo, N. H. Neff, and M. Hadjiconstantinou. 2002. 'GM1 ganglioside induces phosphorylation and activation of Trk and Erk in brain', *J Neurochem*, 81: 696-707.

Facci, L., A. Leon, G. Toffano, S. Sonnino, R. Ghidoni, and G. Tettamanti. 1984. 'Promotion of neuritogenesis in mouse neuroblastoma cells by exogenous gangliosides. Relationship between the effect and the cell association of ganglioside GM1', *J Neurochem*, 42: 299-305.

Fang, Y., G. Wu, X. Xie, Z. H. Lu, and R. W. Ledeen. 2000. 'Endogenous GM1 ganglioside of the plasma membrane promotes neuritogenesis by two mechanisms', *Neurochem Res*, 25: 931-40.

Fantini, J., and Nouara Yahi. 2015. *Brain lipids in synaptic function and neurological disease : clues to innovative therapeutic strategies for brain disorders* (Elsevier/Academic Press: London).

Farooqui, T., T. Franklin, D. K. Pearl, and A. J. Yates. 1997. 'Ganglioside GM1 enhances induction by nerve growth factor of a putative dimer of TrkA', *J Neurochem*, 68: 2348-55.

Fazzari, M., M. Audano, G. Lunghi, E. Di Biase, N. Loberto, L. Mauri, N. Mitro, S. Sonnino, and E. Chiricozzi. 2020. 'The oligosaccharide portion of ganglioside GM1 regulates mitochondrial function in neuroblastoma cells', *Glycoconj J*.

Ferrari, G., B. L. Anderson, R. M. Stephens, D. R. Kaplan, and L. A. Greene. 1995. 'Prevention of apoptotic neuronal death by GM1 ganglioside. Involvement of Trk neurotrophin receptors', *J Biol Chem*, 270: 3074-80.

Freeley, M., D. Kelleher, and A. Long. 2011. 'Regulation of Protein Kinase C function by phosphorylation on conserved and non-conserved sites', *Cell Signal*, 23: 753-62.

Fukami, K., S. Inanobe, K. Kanemaru, and Y. Nakamura. 2010. 'Phospholipase C is a key enzyme regulating intracellular calcium and modulating the phosphoinositide balance', *Prog Lipid Res*, 49: 429-37.

Furukawa, K., Y. Ohmi, Y. Ohkawa, N. Tokuda, Y. Kondo, O. Tajima, and K. Furukawa. 2011. 'Regulatory mechanisms of nervous systems with glycosphingolipids', *Neurochem Res*, 36: 1578-86.

Gafni, J., J. A. Munsch, T. H. Lam, M. C. Catlin, L. G. Costa, T. F. Molinski, and I. N. Pessah. 1997. 'Xestospongins: potent membrane permeable blockers of the inositol 1,4,5-trisphosphate receptor', *Neuron*, 19: 723-33.

Hadaczek, P., G. Wu, N. Sharma, A. Ciesielska, K. Bankiewicz, A. L. Davidow, Z. H. Lu, J. Forsayeth, and R. W. Ledeen. 2015. 'GDNF signaling implemented by GM1 ganglioside; failure in Parkinson's disease and GM1-deficient murine model', *Exp Neurol*, 263: 177-89.

Hakomori, S., K. Handa, K. Iwabuchi, S. Yamamura, and A. Prinetti. 1998. 'New insights in glycosphingolipid function: "glycosignaling domain," a cell surface assembly of glycosphingolipids with signal transducer molecules,involved in cell adhesion coupled with signaling', *Glycobiology*, 8: xi-xix.

Hansson, H. A., J. Holmgren, and L. Svennerholm. 1977. 'Ultrastructural localization of cell membrane GM1 ganglioside by cholera toxin', *Proc Natl Acad Sci U S A*, 74: 3782-6.

Herrero-Garcia, E., and J. P. O'Bryan. 2017. 'Intersectin scaffold proteins and their role in cell signaling and endocytosis', *Biochim Biophys Acta Mol Cell Res*, 1864: 23-30.

Hofmann, T., A. G. Obukhov, M. Schaefer, C. Harteneck, T. Gudermann, and G. Schultz. 1999. 'Direct activation of human TRPC6 and TRPC3 channels by diacylglycerol', *Nature*, 397: 259-63.

Huang, E. J., and L. F. Reichardt. 2003. 'Trk receptors: roles in neuronal signal transduction', *Annu Rev Biochem*, 72: 609-42.

Huang, K. P. 1989. 'The mechanism of protein kinase C activation', *Trends Neurosci*, 12: 425-32.

Hui, K., G. H. Fei, B. J. Saab, J. Su, J. C. Roder, and Z. P. Feng. 2007. 'Neuronal calcium sensor-1 modulation of optimal calcium level for neurite outgrowth', *Development*, 134: 4479-89.

Igumenova, T. I. 2015. 'Dynamics and Membrane Interactions of Protein Kinase C', *Biochemistry*, 54: 4953-68.

Jakob, B., G. Kochlamazashvili, M. Japel, A. Gauhar, H. H. Bock, T. Maritzen, and V. Haucke. 2017. 'Intersectin 1 is a component of the Reelin pathway to regulate neuronal migration and synaptic plasticity in the hippocampus', *Proc Natl Acad Sci U S A*, 114: 5533-38.

Kan, R., P. Yurttas, B. Kim, M. Jin, L. Wo, B. Lee, R. Gosden, and S. A. Coonrod. 2011. 'Regulation of mouse oocyte microtubule and organelle dynamics by PADI6 and the cytoplasmic lattices', *Dev Biol*, 350: 311-22.

Kappagantula, S., M. R. Andrews, M. Cheah, J. Abad-Rodriguez, C. G. Dotti, and J. W. Fawcett. 2014. 'Neu3 sialidase-mediated ganglioside conversion is necessary for axon regeneration and is blocked in CNS axons', *J Neurosci*, 34: 2477-92.

Karlsson, K. A. 1970. 'On the chemistry and occurrence of sphingolipid long-chain bases', *Chem Phys Lipids*, 5: 6-43.

Kashyap, M. P., C. Roberts, M. Waseem, and P. Tyagi. 2018. 'Drug Targets in Neurotrophin Signaling in the Central and Peripheral Nervous System', *Mol Neurobiol*, 55: 6939-55.

Kilka, S., F. Erdmann, A. Migdoll, G. Fischer, and M. Weiwad. 2009. 'The proline-rich N-terminal sequence of calcineurin Abeta determines substrate binding', *Biochemistry*, 48: 1900-10.

Kolter, T. 2012. 'Ganglioside biochemistry', *ISRN Biochem*, 2012: 506160.

Ledeen, R. W., and G. Wu. 2015. 'The multi-tasked life of GM1 ganglioside, a true factotum of nature', *Trends Biochem Sci*, 40: 407-18.

———. 2018a. 'Gangliosides, alpha-Synuclein, and Parkinson's Disease', *Prog Mol Biol Transl Sci*, 156: 435-54.

Ledeen, R., and G. Wu. 2018b. 'Gangliosides of the Nervous System', *Methods Mol Biol*, 1804: 19-55.

Lee, H. K., I. A. Seo, D. J. Suh, and H. T. Park. 2009. 'Nidogen plays a role in the regenerative axon growth of adult sensory neurons through Schwann cells', *J Korean Med Sci*, 24: 654-9.

Lunghi, G., M. Fazzari, E. Di Biase, L. Mauri, S. Sonnino, and E. Chiricozzi. 2020. 'Modulation of calcium signaling depends on the oligosaccharide of GM1 in Neuro2a mouse neuroblastoma cells', *Glycoconj J*.

Magistretti, P. J., F. H. Geisler, J. S. Schneider, P. A. Li, H. Fiumelli, and S. Sipione. 2019. 'Gangliosides: Treatment Avenues in Neurodegenerative Disease', *Front Neurol*, 10: 859.

Martinez, Z., M. Zhu, S. Han, and A. L. Fink. 2007. 'GM1 specifically interacts with alpha-synuclein and inhibits fibrillation', *Biochemistry*, 46: 1868-77.

Masco, D., M. Van de Walle, and S. Spiegel. 1991. 'Interaction of ganglioside GM1 with the B subunit of cholera toxin modulates growth and differentiation of neuroblastoma N18 cells', *J Neurosci*, 11: 2443-52.

Mauri, L., S. Prioni, N. Loberto, V. Chigorno, A. Prinetti, and S. Sonnino. 2004. 'Synthesis of radioactive and photoactivable ganglioside derivatives for the study of ganglioside-protein interactions', *Glycoconj J*, 20: 11-23.

Milani, D., M. C. Minozzi, L. Petrelli, D. Guidolin, S. D. Skaper, and P. E. Spoerri. 1992. 'Interaction of ganglioside GM1 with the B subunit of cholera toxin modulates intracellular free calcium in sensory neurons', *J Neurosci Res*, 33: 466-75.

Miyagi, T., and K. Yamaguchi. 2012. 'Mammalian sialidases: physiological and pathological roles in cellular functions', *Glycobiology*, 22: 880-96.

Mocchetti, I. 2005. 'Exogenous gangliosides, neuronal plasticity and repair, and the neurotrophins', *Cell Mol Life Sci*, 62: 2283-94.

Moisoi, N., K. Klupsch, V. Fedele, P. East, S. Sharma, A. Renton, H. Plun-Favreau, R. E. Edwards, P. Teismann, M. D. Esposti, A. D. Morrison, N. W. Wood, J. Downward, and L. M. Martins. 2009. 'Mitochondrial dysfunction triggered by loss of HtrA2 results in the activation of a brain-specific transcriptional stress response', *Cell Death Differ*, 16: 449-64.

Monroy, M. A., D. D. Ruhl, X. Xu, D. K. Granner, P. Yaciuk, and J. C. Chrivia. 2001. 'Regulation of cAMP-responsive element-binding protein-mediated transcription by the SNF2/SWI-related protein, SRCAP', *J Biol Chem*, 276: 40721-6.

Mutoh, T., T. Hamano, S. Yano, H. Koga, H. Yamamoto, K. Furukawa, and R. W. Ledeen. 2002. 'Stable transfection of GM1 synthase gene into GM1-deficient NG108-15 cells, CR-72 cells, rescues the responsiveness of Trk-neurotrophin receptor to its ligand, NGF', *Neurochem Res*, 27: 801-6.

Mutoh, T., A. Tokuda, T. Miyadai, M. Hamaguchi, and N. Fujiki. 1995. 'Ganglioside GM1 binds to the Trk protein and regulates receptor function', *Proc Natl Acad Sci U S A*, 92: 5087-91.

Nakamura, K., G. Wu, and R. W. Ledeen. 1992. 'Protection of neuro-2a cells against calcium ionophore cytotoxicity by gangliosides', *J Neurosci Res*, 31: 245-53.

Ngamukote, S., M. Yanagisawa, T. Ariga, S. Ando, and R. K. Yu. 2007. 'Developmental changes of glycosphingolipids and expression of glycogenes in mouse brains', *J Neurochem*, 103: 2327-41.

Nguyen, T., and S. Di Giovanni. 2008. 'NFAT signaling in neural development and axon growth', *Int J Dev Neurosci*, 26: 141-5.

O'Hanlon, G. M., T. R. Hirst, and H. J. Willison. 2003. 'Ganglioside GM1 binding toxins and human neuropathy-associated IgM antibodies differentially promote neuritogenesis in a PC12 assay', *Neurosci Res*, 47: 383-90.

Ohmi, Y., Y. Ohkawa, Y. Yamauchi, O. Tajima, K. Furukawa, and K. Furukawa. 2012. 'Essential roles of gangliosides in the formation and maintenance of membrane microdomains in brain tissues', *Neurochem Res*, 37: 1185-91.

Osellame, L. D., T. S. Blacker, and M. R. Duchen. 2012. 'Cellular and molecular mechanisms of mitochondrial function', *Best Pract Res Clin Endocrinol Metab*, 26: 711-23.

Park, D. H., L. Wang, P. Pittock, G. Lajoie, and S. N. Whitehead. 2016. 'Increased Expression of GM1 Detected by Electrospray Mass Spectrometry in Rat Primary Embryonic Cortical Neurons Exposed to Glutamate Toxicity', *Anal Chem*, 88: 7844-52.

Petta, I., N. Bougarne, J. Vandewalle, L. Dejager, S. Vandevyver, M. Ballegeer, S. Desmet, J. Thommis, L. De Cauwer, S. Lievens, C. Libert, J. Tavernier, and K. De Bosscher. 2017. 'Glucocorticoid Receptor-mediated transactivation is hampered by Striatin-3, a novel interaction partner of the receptor', *Sci Rep*, 7: 8941.

Piccinini, M., F. Scandroglio, S. Prioni, B. Buccinna, N. Loberto, M. Aureli, V. Chigorno, E. Lupino, G. DeMarco, A. Lomartire, M. T. Rinaudo, S. Sonnino, and A. Prinetti. 2010. 'Deregulated sphingolipid metabolism and membrane organization in neurodegenerative disorders', *Mol Neurobiol*, 41: 314-40.

Pitto, M., T. Mutoh, M. Kuriyama, A. Ferraretto, P. Palestini, and M. Masserini. 1998. 'Influence of endogenous GM1 ganglioside on TrkB activity, in cultured neurons', *FEBS Lett*, 439: 93-6.

Polo, A., G. Kirschner, A. Guidotti, and E. Costa. 1994. 'Brain content of glycosphingolipids after oral administration of monosialogangliosides GM1 and LIGA20 to rats', *Mol Chem Neuropathol*, 21: 41-53.

Rabin, S. J., and I. Mocchetti. 1995. 'GM1 ganglioside activates the high-affinity nerve growth factor receptor trkA', *J Neurochem*, 65: 347-54.

Ragg, E. M., V. Galbusera, A. Scarafoni, A. Negri, G. Tedeschi, A. Consonni, F. Sessa, and M. Duranti. 2006. 'Inhibitory properties and solution structure of a potent Bowman-Birk protease inhibitor from lentil (Lens culinaris, L) seeds', *FEBS J*, 273: 4024-39.

Rodriguez, J. A., E. Piddini, T. Hasegawa, T. Miyagi, and C. G. Dotti. 2001. 'Plasma membrane ganglioside sialidase regulates axonal growth and regeneration in hippocampal neurons in culture', *J Neurosci*, 21: 8387-95.

Saqr, H. E., D. K. Pearl, and A. J. Yates. 1993. 'A review and predictive models of ganglioside uptake by biological membranes', *J Neurochem*, 61: 395-411.

Sato, C., T. Matsuda, and K. Kitajima. 2002. 'Neuronal differentiation-dependent expression of the disialic acid epitope on CD166 and its involvement in neurite formation in Neuro2A cells', *J Biol Chem*, 277: 45299-305.

Schengrund, C. L. 2015. 'Gangliosides: glycosphingolipids essential for normal neural development and function', *Trends Biochem Sci*, 40: 397-406.

Schengrund, C. L., and C. M. Mummert. 1998. 'Exogenous gangliosides. How do they cross the blood-brain barrier and how do they inhibit cell proliferation', *Ann N Y Acad Sci*, 845: 278-84.

Schengrund, C. L., and C. Prouty. 1988. 'Oligosaccharide portion of GM1 enhances process formation by S20Y neuroblastoma cells', *J Neurochem*, 51: 277-82.

Schengrund, C. L., and N. J. Ringler. 1989. 'Binding of Vibrio cholera toxin and the heat-labile enterotoxin of Escherichia coli to GM1, derivatives of GM1, and nonlipid oligosaccharide polyvalent ligands', *J Biol Chem*, 264: 13233-7.

Schiumarini, D., N. Loberto, G. Mancini, R. Bassi, P. Giussani, E. Chiricozzi, M. Samarani, S. Munari, A. Tamanini, G. Cabrini, G. Lippi, M. C. Dechecchi, S. Sonnino, and M. Aureli. 2017. 'Evidence for the Involvement of Lipid Rafts and Plasma Membrane Sphingolipid Hydrolases in Pseudomonas aeruginosa Infection of Cystic Fibrosis Bronchial Epithelial Cells', *Mediators Inflamm*, 2017: 1730245.

Schneider, J. S. 2018. 'Altered expression of genes involved in ganglioside biosynthesis in substantia nigra neurons in Parkinson's disease', *PLoS One*, 13: e0199189.

Schneider, J. S., R. Aras, C. K. Williams, J. B. Koprich, J. M. Brotchie, and V. Singh. 2019. 'GM1 Ganglioside Modifies alpha-Synuclein Toxicity and is Neuroprotective in a Rat alpha-Synuclein Model of Parkinson's Disease', *Sci Rep*, 9: 8362.

Schneider, J. S., F. Cambi, S. M. Gollomp, H. Kuwabara, J. R. Brasic, B. Leiby, S. Sendek, and D. F. Wong. 2015. 'GM1 ganglioside in Parkinson's disease: Pilot study of effects on dopamine transporter binding', *J Neurol Sci*, 356: 118-23.

Schneider, J. S., S. M. Gollomp, S. Sendek, A. Colcher, F. Cambi, and W. Du. 2013. 'A randomized, controlled, delayed start trial of GM1 ganglioside in treated Parkinson's disease patients', *J Neurol Sci*, 324: 140-8.

Schneider, J. S., A. Pope, K. Simpson, J. Taggart, M. G. Smith, and L. DiStefano. 1992. 'Recovery from experimental parkinsonism in primates with GM1 ganglioside treatment', *Science*, 256: 843-6.

Schneider, J. S., D. P. Roeltgen, D. S. Rothblat, J. Chapas-Crilly, L. Seraydarian, and J. Rao. 1995. 'GM1 ganglioside treatment of Parkinson's disease: an open pilot study of safety and efficacy', *Neurology*, 45: 1149-54.

Schneider, J. S., S. Sendek, C. Daskalakis, and F. Cambi. 2010. 'GM1 ganglioside in Parkinson's disease: Results of a five year open study', *J Neurol Sci*, 292: 45-51.

Schneider, J. S., T. N. Seyfried, H. S. Choi, and S. K. Kidd. 2015. 'Intraventricular Sialidase Administration Enhances GM1 Ganglioside Expression and Is Partially Neuroprotective in a Mouse Model of Parkinson's Disease', *PLoS One*, 10: e0143351.

Senn, H. J., M. Orth, E. Fitzke, H. Wieland, and W. Gerok. 1989. 'Gangliosides in normal human serum. Concentration, pattern and transport by lipoproteins', *Eur J Biochem*, 181: 657-62.

Seong, E., L. Yuan, and J. Arikkath. 2015. 'Cadherins and catenins in dendrite and synapse morphogenesis', *Cell Adh Migr*, 9: 202-13.

Simons, K., and J. L. Sampaio. 2011. 'Membrane organization and lipid rafts', *Cold Spring Harb Perspect Biol*, 3: a004697.

Singleton, D. W., C. L. Lu, R. Colella, and F. J. Roisen. 2000. 'Promotion of neurite outgrowth by protein kinase inhibitors and ganglioside GM1 in neuroblastoma cells involves MAP kinase ERK1/2', *Int J Dev Neurosci*, 18: 797-805.

Sokolova, T. V., M. P. Rychkova, and N. F. Avrova. 2014. '[Protective effect of GM1 ganglioside against toxic action of glutamate on cerebellar granule cells]', *Zh Evol Biokhim Fiziol*, 50: 399-401.

Sonnino, S., L. Cantu, M. Corti, D. Acquotti, and B. Venerando. 1994. 'Aggregative properties of gangliosides in solution', *Chem Phys Lipids*, 71: 21-45.

Sonnino, S., and V. Chigorno. 2000. 'Ganglioside molecular species containing C18- and C20-sphingosine in mammalian nervous tissues and neuronal cell cultures', *Biochim Biophys Acta*, 1469: 63-77.

Sonnino, S., V. Chigorno, M. Aureli, A. P. Masilamani, M. Valsecchi, N. Loberto, S. Prioni, L. Mauri, and A. Prinetti. 2011. 'Role of gangliosides and plasma membrane-associated sialidase in the process of cell membrane organization', *Adv Exp Med Biol*, 705: 297-316.

Sonnino, S., L. Mauri, V. Chigorno, and A. Prinetti. 2007. 'Gangliosides as components of lipid membrane domains', *Glycobiology*, 17: 1R-13R.

Spoerri, P. E., A. K. Dozier, and F. J. Roisen. 1990. 'Calcium regulation of neuronal differentiation: the role of calcium in GM1-mediated neuritogenesis', *Brain Res Dev Brain Res*, 56: 177-88.

Strauss, K. M., L. M. Martins, H. Plun-Favreau, F. P. Marx, S. Kautzmann, D. Berg, T. Gasser, Z. Wszolek, T. Muller, A. Bornemann, H. Wolburg, J. Downward, O. Riess, J. B. Schulz, and R. Kruger. 2005. 'Loss of function mutations in the gene encoding Omi/HtrA2 in Parkinson's disease', *Hum Mol Genet*, 14: 2099-111.

Suzuki, S. C., and M. Takeichi. 2008. 'Cadherins in neuronal morphogenesis and function', *Dev Growth Differ*, 50 Suppl 1: S119-30.

Svennerholm, L. 1964. 'The Gangliosides', *J Lipid Res*, 5: 145-55.

Svennerholm, L., K. Bostrom, B. Jungbjer, and L. Olsson. 1994. 'Membrane lipids of adult human brain: lipid composition of frontal and temporal lobe in subjects of age 20 to 100 years', *J Neurochem*, 63: 1802-11.

Tettamanti, G., F. Bonali, S. Marchesini, and V. Zambotti. 1973. 'A new procedure for the extraction, purification and fractionation of brain gangliosides', *Biochim Biophys Acta*, 296: 160-70.

Tomasi, M., L. G. Roda, C. Ausiello, G. D'Agnolo, B. Venerando, R. Ghidoni, S. Sonnino, and G. Tettamanti. 1980. 'Interaction of GMI ganglioside with bovine serum albumin: formation and isolation of multiple complexes', *Eur J Biochem*, 111: 315-24.

Toth, A. B., A. K. Shum, and M. Prakriya. 2016. 'Regulation of neurogenesis by calcium signaling', *Cell Calcium*, 59: 124-34.

Ulrich-Bott, B., and H. Wiegandt. 1984. 'Micellar properties of glycosphingolipids in aqueous media', *J Lipid Res*, 25: 1233-45.

Valaperta, R., M. Valsecchi, F. Rocchetta, M. Aureli, S. Prioni, A. Prinetti, V. Chigorno, and S. Sonnino. 2007. 'Induction of axonal differentiation by silencing plasma membrane-associated sialidase Neu3 in neuroblastoma cells', *J Neurochem*, 100: 708-19.

Valsecchi, M., V. Chigorno, S. Sonnino, and G. Tettamanti. 1992. 'Rat cerebellar granule cells in culture associate and metabolize differently exogenous GM1 ganglioside molecular species containing a C18 or C20 long chain base', *Chem Phys Lipids*, 60: 247-52.

Varki, A., R. D. Cummings, J. D. Esko, H. H. Freeze, P. Stanley, J. D. Marth, C. R. Bertozzi, G. W. Hart, and M. E. Etzler. 2009. 'Symbol nomenclature for glycan representation', *Proteomics*, 9: 5398-9.

Venerando, B., G. C. Goi, A. Preti, A. Fiorilli, A. Lombardo, and G. Tettamanti. 1982. 'Cytosolic sialidase in developing rat forebrain', *Neurochem Int*, 4: 313-20.

Wie, M. B., J. Y. Koh, M. H. Won, J. C. Lee, T. K. Shin, C. J. Moon, H. J. Ha, S. M. Park, and H. C. Kim. 2001. 'BAPTA/AM, an intracellular calcium chelator, induces delayed necrosis by lipoxygenase-mediated free radicals in mouse cortical cultures', *Prog Neuropsychopharmacol Biol Psychiatry*, 25: 1641-59.

Wiegandt, H., and H. W. Bucking. 1970. 'Carbohydrate components of extraneuronal gangliosides from bovine and human spleen, and bovine kidney', *Eur J Biochem*, 15: 287-92.

Winklhofer, K. F., and C. Haass. 2010. 'Mitochondrial dysfunction in Parkinson's disease', *Biochim Biophys Acta*, 1802: 29-44.

Wood, E. R., L. Kuyper, K. G. Petrov, R. N. Hunter, 3rd, P. A. Harris, and K. Lackey. 2004. 'Discovery and in vitro evaluation of potent TrkA kinase inhibitors: oxindole and aza-oxindoles', *Bioorg Med Chem Lett*, 14: 953-7.

Wu, G., Y. Fang, Z. H. Lu, and R. W. Ledeen. 1998. 'Induction of axon-like and dendrite-like processes in neuroblastoma cells', *J Neurocytol*, 27: 1-14.

Wu, G., and R. W. Ledeen. 1991. 'Stimulation of neurite outgrowth in neuroblastoma cells by neuraminidase: putative role of GM1 ganglioside in differentiation', *J Neurochem*, 56: 95-104.

———. 1994. 'Gangliosides as modulators of neuronal calcium', *Prog Brain Res*, 101: 101-12.

Wu, G., Z. H. Lu, N. Kulkarni, R. Amin, and R. W. Ledeen. 2011. 'Mice lacking major brain gangliosides develop parkinsonism', *Neurochem Res*, 36: 1706-14.

Wu, G., Z. H. Lu, N. Kulkarni, and R. W. Ledeen. 2012. 'Deficiency of ganglioside GM1 correlates with Parkinson's disease in mice and humans', *J Neurosci Res*, 90: 1997-2008.

Wu, G., Z. H. Lu, and R. W. Ledeen. 1995. 'Induced and spontaneous neuritogenesis are associated with enhanced expression of ganglioside GM1 in the nuclear membrane', *J Neurosci*, 15: 3739-46.

Wu, G., Z. H. Lu, K. Nakamura, D. C. Spray, and R. W. Ledeen. 1996. 'Trophic effect of cholera toxin B subunit in cultured cerebellar granule neurons: modulation of intracellular calcium by GM1 ganglioside', *J Neurosci Res*, 44: 243-54.

Wu, G., Z. H. Lu, A. G. Obukhov, M. C. Nowycky, and R. W. Ledeen. 2007. 'Induction of calcium influx through TRPC5 channels by cross-linking of GM1 ganglioside associated with alpha5beta1 integrin initiates neurite outgrowth', *J Neurosci*, 27: 7447-58.

Wu, G., Z. H. Lu, X. Xie, and R. W. Ledeen. 2004. 'Susceptibility of cerebellar granule neurons from GM2/GD2 synthase-null mice to apoptosis induced by glutamate excitotoxicity and elevated KCl: rescue by GM1 and LIGA20', *Glycoconj J*, 21: 305-13.

Wu, G., X. Xie, Z. H. Lu, and R. W. Ledeen. 2001. 'Cerebellar neurons lacking complex gangliosides degenerate in the presence of depolarizing levels of potassium', *Proc Natl Acad Sci U S A*, 98: 307-12.

———. 2009. 'Sodium-calcium exchanger complexed with GM1 ganglioside in nuclear membrane transfers calcium from nucleoplasm to endoplasmic reticulum', *Proc Natl Acad Sci U S A*, 106: 10829-34.

Xie, X., G. Wu, Z. H. Lu, and R. W. Ledeen. 2002. 'Potentiation of a sodium-calcium exchanger in the nuclear envelope by nuclear GM1 ganglioside', *J Neurochem*, 81: 1185-95.

Yu, R. K., Y. Nakatani, and M. Yanagisawa. 2009. 'The role of glycosphingolipid metabolism in the developing brain', *J Lipid Res*, 50 Suppl: S440-5.

Zakharova, I. O., T. V. Sokolova, Y. A. Vlasova, V. V. Furaev, M. P. Rychkova, and N. F. Avrova. 2014. 'GM1 ganglioside activates ERK1/2 and Akt downstream of Trk tyrosine kinase and protects PC12 cells against hydrogen peroxide toxicity', *Neurochem Res*, 39: 2262-75.

Zhao, Y., X. Fan, F. Yang, and X. Zhang. 2004. 'Gangliosides modulate the activity of the plasma membrane Ca(2+)-ATPase from porcine brain synaptosomes', *Arch Biochem Biophys*, 427: 204-12.